Fiber-Optic Fabry-Perot High-Temperature Strain Measurement System Feasibility Study

TR-107212
3876-06

Final Report, January 1997

Prepared by
Mechanical Technology Incorporated
968 Albany-Shaker Road
Latham, New York 12110

Principal Investigator
N. Narandran

Prepared for
Electric Power Research Institute
3412 Hillview Avenue
Palo Alto, California 94304

EPRI Project Manager
J. Weiss
Generation Group

DISCLAIMER OF WARRANTIES AND LIMITATION OF LIABILITIES

ORGANIZATION(S) THAT PREPARED THIS REPORT

MECHANICAL TECHNOLOGY INCORPORATED

ORDERING INFORMATION

Requests for copies of this report should be directed to the EPRI Distribution Center, 207 Coggins Drive, P.O. Box 23205, Pleasant Hill, CA 94523, (510) 934-4212

REPORT SUMMARY

Conventional strain gages have shortcomings when used in high temperature power plant applications. Fiber-optic Fabry-Perot sensors have shown promising results for highly localized strain measurements in laboratory environments and some specialized field tests.

Background
Foil and wire strain gages have been widely used for the past four decades to make reliable strain measurements. They work well at room temperature and moderate temperatures up to 500° F (260°C) with a fair amount of care. The problem arises once the working temperature exceeds 500° F (260°C). One major problem at high temperature is the availability of adhesives to attach strain gages, and a second problem is the reliability of the measured strain values. Structural components used in power plants would be a major beneficiary of a reliable, accurate high-temperature strain sensor. Recently, white-light interferometers have shown promise for making absolute strain measurements.

Objective
To develop a prototype optical strain gage sensor and evaluate its feasibility in high temperature power plant applications.

Approach
The research team developed a prototype fiber optic sensor, and tested it in the laboratory at varying conditions including room temperature, moderate temperature, and low-frequency dynamic loading. The team developed packaging and attachment methods for the sensor for high temperature applications. Field testing was performed on one of the steam lines at Tennessee Valley Authority's Kingston Power Plant to evaluate the feasibility of the system.

Results
This project demonstrated that Fabry-Perot fiber-optic strain sensors can withstand temperatures up to 1000°F (538°C). Sensor demodulation based on white-light

interferometric technique appears to have the necessary qualities to produce a viable fiber-optic sensor system for long term monitoring of structural health. Since the extrinsic Fabry-Perot strain gages are sensitive only to axial strain, data interpretation is straight forward. The thermal and mechanical strain on a structure can be separated. Further, these sensors can be easily attached to structures and can also be multiplexed using off-the-shelf fiber-optic switches. At the beginning of the study, the laser-welded joints in the earlier configurations of the extrinsic Fabry-Perot gages failed at higher strains and temperatures. This weakness was overcome when the gage supplier modified the gages with a decoupled configuration that relieved the strain on the lead-in fiber. Gage calibration is an area that needs improvement. Almost all the fiber-optic gages used in the study needed calibration because the gage length supplied by the manufacturer was inaccurate. Once initial calibration is performed, additional field calibration is not required.

EPRI Perspective

Fiber optic sensors have the capability for monitoring many parameters such as strain, temperature, vibration, and pressure. Further work is required to increase the capability of the existing sensing technology for measuring parameters in addition to temperature and strain. This program showed the feasibility of using fiber-optic strain gages at high temperatures. However, the gages were not used to estimate structural stress. It is expected that the end user will be interested in using these sensors to estimate structural stresses, creep, and fatigue. Consequently, further work needs to be done to correlate strain sensor data with theoretical predictions and incorporate the data into programs such as EPRI's Creep Fatigue Pro (EPRI report TR-100907 and EPRI technical review AP-101840-V2P18).

TR-107301

Interest Categories

Fossil steam plant performance optimization
Fossil steam plant O&M cost reduction

Key Words

Fiber-optics
Fabry-Perot
Strain gage

ABSTRACT

A comprehensive experimental study was conducted to investigate the applicability of fiber-optic strain and temperature sensors to monitor power plant structures. A superheated steam pipe operating at 1000°F (538°C) at the Tennessee Valley Authority (TVA) power plant in Kingston, Tennessee was chosen as the target structure. The potential applications of these fiber-optic sensors include health monitoring of high-temperature structures such as boilers, tube headers, and steam pipes, as well as many other power plant structures exposed to less severe environments. The sensor selected for this application is based on a white-light interferometric technique. The key features of this sensor include its ability for absolute measurements that are not affected by light loss along the fiber cable due to, for example, microbending effects and coupler loss, its compatibility with off-the-shelf fiber-optic components, and its low cost. The glass fiber-optic strain sensors were packaged in a rugged metal housing and were spot welded to the high-temperature steam pipe. Laboratory testing and power plant data results are encouraging and the details are presented in this report.

CONTENTS

LIST OF FIGURES

LIST OF TABLES

1

INTRODUCTION

This final report documents the work conducted under Contract RP 3876-06, entitled "Fiber-Optic Fabry-Perot High-Temperature Strain Measurement System Feasibility Study." The project was performed by Mechanical Technology Incorporated (MTI) for the Electric Power Research Institute (EPRI) from October 1993 to November 1995. Dr. N. Narandran served as principal investigator and Mr. J. Weiss was the EPRI project manager.

The objective of this project was to evaluate the feasibility of using fiber-optic sensors as strain gages in high temperature power plant applications. Fiber-optic Fabry-Perot sensors have shown promising results for highly localized strain measurements in laboratory environments and some specialized field tests. However, several technical issues needed investigation in order to make these sensors rugged and usable on high-temperature structures. MTI conducted an experimental study to address these issues and expand the base of knowledge on the use of fiber-optic sensors for high-temperature applications. Work under the project involved evaluation of a single-point strain sensor, temperature compensation and temperature measurements, and investigation of sensor packaging and attachment methods for a high-temperature environment (see Section 2). Sensors were subjected to high-temperature testing in the laboratory and in the field at a host utility (see Section 3). Proof-of-concept testing for multiplexed sensors was also performed (see Section 4).

For additional information on fiber-optic Fabry-Perot sensors, refer to EPRI final report "Fiber-Optic Thermowell Sensor," which documents the work conducted under Contract WO3462-01.

2

FIBER-OPTIC STRAIN SENSOR EVALUATION

The experimental study documented in this report was conducted to evaluate the feasibility of using fiber-optic strain sensors to measure strain at high temperatures. In this study, the temperature was limited to 1000°F (538°C), since the target application was strain measurements of super-heated steam pipes. However, these sensors have the potential to be used at even higher temperatures, up to 1500°F (815°C) with the same fibers and up to 3000°F (1650°C) with sapphire fibers.

Foil and wire strain gages have been widely used for the past four decades to make reliable strain measurements. They work well at room temperature and moderate temperatures (up to 500°F [260°C]) with a fair amount of care. The problem arises once the working temperature exceeds 500°F (260°C). One major problem at high temperature is the availability of adhesives to attach strain gages, and the second problem is the reliability of the measured strain values. A review article on high-temperature strain measurement covers some of the available techniques and their limitations [1]. Structural components used in power plants would be a major beneficiary of a reliable, accurate high-temperature strain sensor. This project also complements the analytical work in component life cycle fatigue calculations that until now were compelled to utilize design rather than actual strain data input.

Fiber-optic sensor development first started in the mid-seventies and has grown rapidly ever since. In recent years, the technology has matured to the state where these sensors are commercially available. Numerous sensing techniques based on intensity modulation and phase modulation or frequency (or wavelength) modulation have been reported for strain measurement [2-11]. Each of these techniques have their own strengths and weaknesses. Most intensity-modulated sensors are simple to construct and low cost. The major drawback of such sensors is light intensity loss due to couplers, microbending, and other attenuation factors. Such effects directly impact the accuracy and reliability of the measured signal. Phase-modulated sensors (or interferometric sensors) have shown high sensitivity, larger bandwidth, and also are not affected by light intensity fluctuations. However, these sensors are useful for measuring relative strain and not absolute strain. In addition, these devices require sophisticated optical components and phase demodulation electronics that make system cost high.

Recently, two sensors, namely Bragg grating and white-light interferometers, have shown promise for making absolute strain measurements while being insensitive to light intensity loss factors [9,10,11]. Bragg grating sensors have been evaluated by others for similar applications [9]. Previous EPRI work [10] identified temperature limitations with Bragg gratings (approximately 800°F [430°C]). Consequently, the sensor selected for study during the subject project is based on a white-light interferometric technique, which is a potential low-cost sensor for high-temperature strain measurement. This sensor utilizes a halogen lamp as the light source and multimode optical fibers for sensing and light transmission. Another key feature is its ability to make highly localized strain measurements due small gage lengths (0.5 to 10 mm). Details of the white-light interferometer and Fabry-Perot strain gage construction are explained below.

White-light Interferometric Sensor

A schematic diagram of a white-light interferometer (WFS-100, manufactured by National Optics Institute/FISO Technologies, Canada) is shown in Figure 2-1 [11]. Light from a halogen lamp is coupled into a multimode fiber (52.5/125 μm) coupler/splitter (2 X 1). The beam travels down the fiber and enters into a high fines extrinsic fiber-optic Fabry-Perot sensor. Depending on the length of the air gap, a particular wavelength component of the optical beam is strongly reflected back. A suitable spectrum analyzer placed at the output end can detect the wavelength of the reflected component, which represents a unique air gap length. Straining the Fabry-Perot sensor changes the air gap length, which is detected by the spectrum analyzer.

The spectrum analyzer portion of the WFS100 is an optical wedge (a Fizeau analyzer), which has a varying interference cavity length as a function of position along its length. The light intensity reflected from a Fabry-Perot sensor is maximally transmitted through the optical wedge at a position where the optical path length matches the optical path length of the Fabry-Perot cavity. A strain applied to the Fabry-Perot strain sensor changes the cavity length, resulting in a shift in the position of the maximum light intensity transmitted through the optical wedge. A linear photodiode array placed at the back of the optical wedge detects the transmitted beam, and a simple peak detection algorithm determines the location of the peak of the transmitted signal.

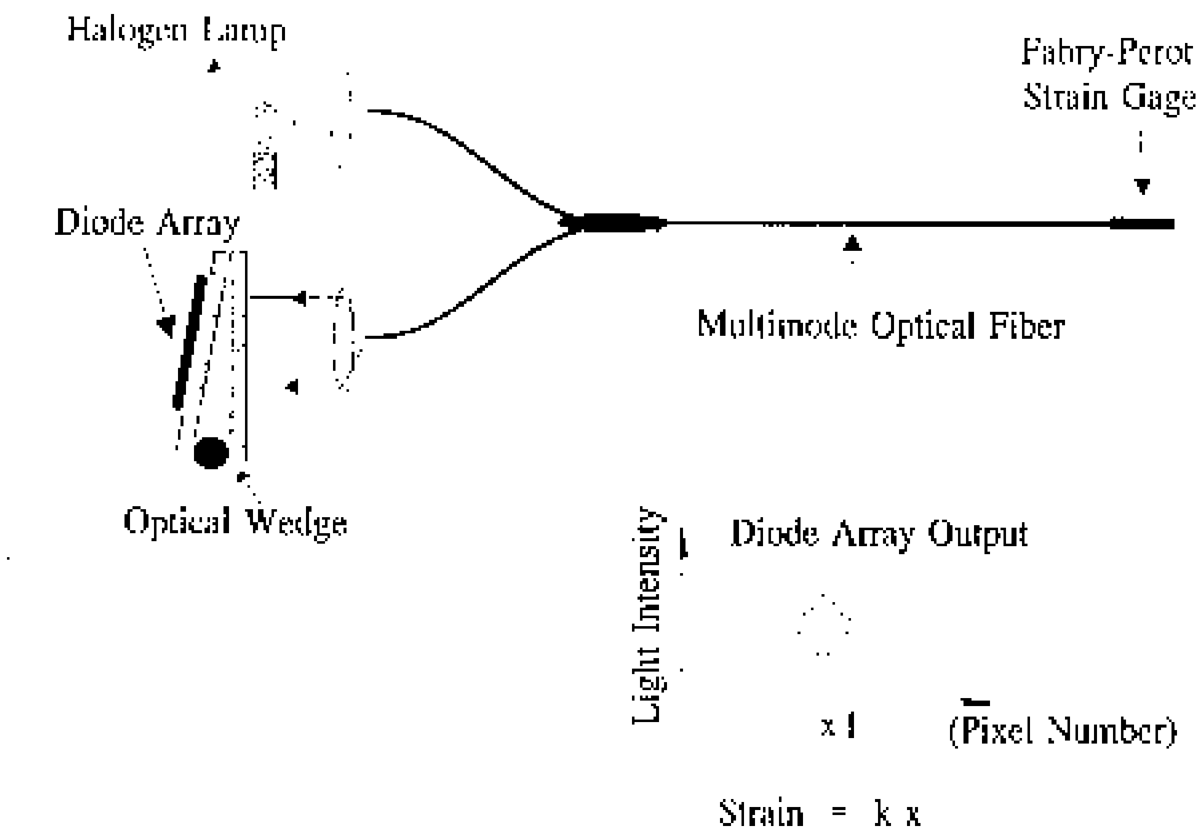

Figure 2-1 Schematic of White-Light Interferometer

The detector (optical wedge/Fizeau) interferometer portion of the system has a varying optical path length and provides a method to scan over a certain range to match with the sensing interferometer. This range determines the measurement range of the strain sensor. The light intensity at the linear diode array can be written as [9]

$$I(x) = 1 + 1/2 \exp \{[- [ø(x) - ø_s]/{}^1L_c]^2\} \cos [ø(x) - ø_s] \qquad (1)$$

where $ø(x)$ and $ø_s$ are the phase in the detector interferometer and the sensing interferometer, respectively, and L_c is the coherence length of the light source. The intensity, I, and the phase, ø, in the detector are both functions of x, which is the position on the linear diode array. Figure 2-2(a) illustrates the theoretical fringe pattern of this white-light interferometer generated using Eq. (2.1). The parameters chosen to generate this plot are arbitrary. Figure 2.2(b) illustrates a typical oscilloscope trace of intensity signal detected by the linear diode array.

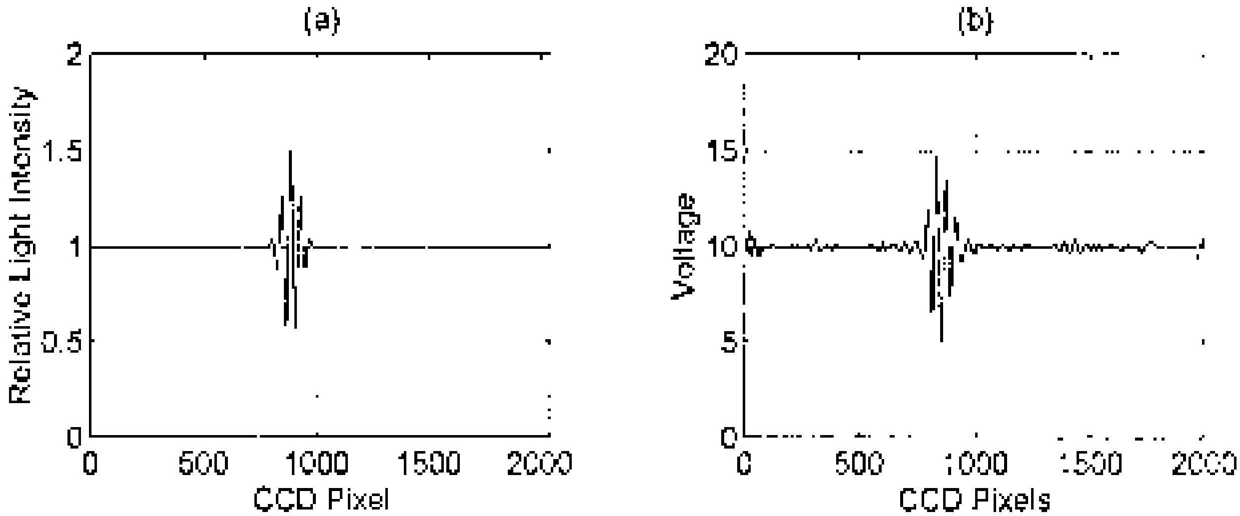

Figure 2-2 a) Theoretical Plot of the White-Light Interferometer Output Signal
b) Corresponding Experimental Output Signal

The position of the peak light intensity (when $ø(x) = ø_s$) on the linear array uniquely determines the cavity length of the Fabry-Perot strain sensor which is related to the strain sensed by the gage. The simple optical wedge analyzer and the linear array replaces expensive spectrum analyzer and sophisticated signal analysis needed to demodulate the reflected optical signal. The linear array in the demodulator used in this study has 512 pixels and the peak of the transmitted signal is detected to the accuracy of one-eighth of a pixel. Thus, the resolution of this system is 0.025% of full range, which implies that a strain sensor with a measurement range of 10,000 με can resolve strain levels as small as 2.5 με. This demodulator has now been upgraded with a 2048 pixel array to read strain levels smaller than 1 με.

Gage Description

There are two types of fiber-optic Fabry-Perot sensors: intrinsic and extrinsic. The intrinsic Fabry-Perot sensor is constructed by introducing two reflective surfaces into an optical fiber [7,12]. The sensor used in this EPRI study is an extrinsic type, and a schematic of an extrinsic Fabry-Perot sensor is shown in Figure 2-3 [6,11]. The extrinsic Fabry-Perot interferometer has low thermal apparent strain and no transverse strain sensitivity, and is not prone to the effects of polarization-signal fading commonly associated with intrinsic all-fiber interferometers since the air-cavity does not induce differential changes in the polarization recombination of the two optical paths. The fiber-optic Fabry-Perot strain sensor construction method is same for both laser interferometers and white-light interferometers. The main difference lies in the type of optical fiber used and the amount of reflectivity applied to the cavity surfaces. The laser sensors use single-mode optical fibers and the reflectivity of the transmit/receive fiber front surface, which forms one of the two parallel surfaces of the Fabry-Perot interferometer, is usually less than 10%, so that a low fines Fabry-Perot interferometer is formed [6]. White-light interferometers use multimode optical fibers and higher reflective (30%) surfaces for constructing a high fines Fabry-Perot interferometer [11].

As shown in Figure 2-3, two optical fibers are inserted into a hollow glass tube from both ends. The outer diameter of the fiber is same as the inner diameter of the hollow tube. The fiber end faces are cut square, a partial reflective coating is applied to the transmit/receive fiber, and the target fiber is coated with a multilayer dielectric mirror to produce higher reflectance. The fibers are fused to the glass tube as shown in Figure 2-3. The distance between the points where the fibers are attached to the glass tube is defined as the gage length. The target fiber could be a metal fiber with its end face polished to reflect the light.

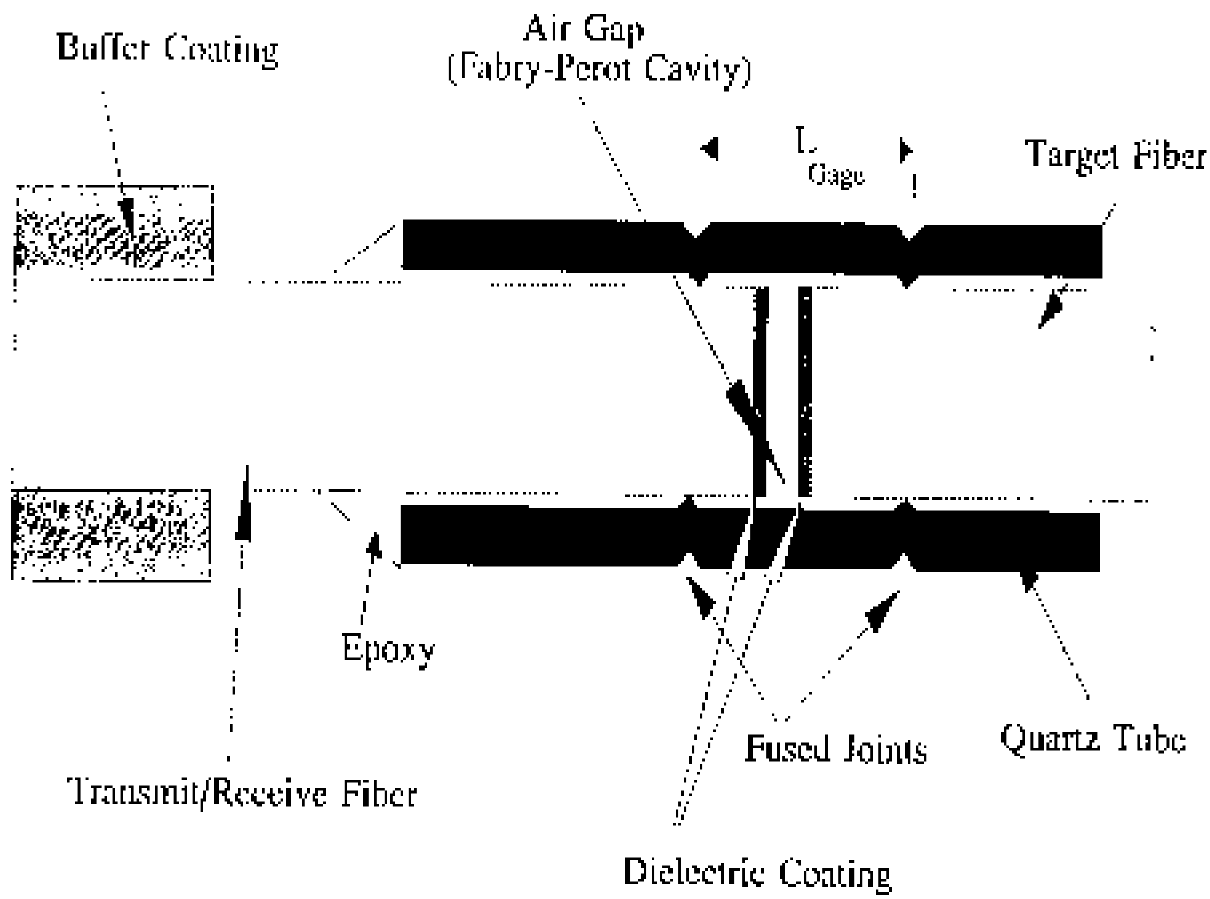

Figure 2-3 Extrinsic Fabry-Perot Strain Sensor

Part of the optical beam entering the Fabry-Perot cavity strongly reflects a particular wavelength of light created by the high fines interferometer. The reflected beam travels back along the same fiber and is detected at a spectrum analyzer after splitting off the (2 X 1) coupler/splitter. The temperature-compensated Fabry-Perot strain sensor is constructed by replacing the target optical fiber by a metallic fiber made from the same material as the structure to which the gage is bonded. Also, the transmit-receive fiber is attached to the glass tube very close to its end face as shown in Figure 2-4. Since the thermal growth of the metal rod is equal and opposite to the growth of the structure, the thermal strain will be compensated. This same gage could be used for measuring temperature.

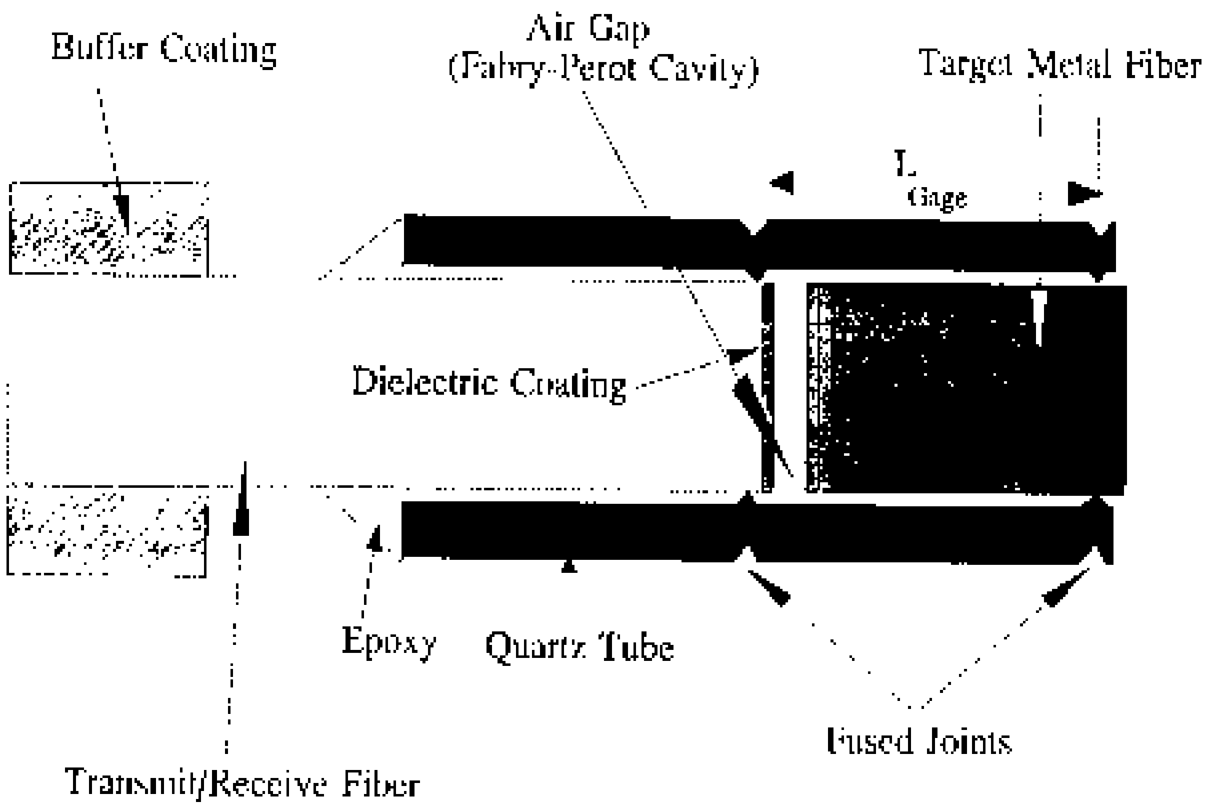

Figure 2-4 Temperature-Compensated Extrinsic Fabry-Perot Strain Sensor

Test Setup

As a first step in the project, fiber-optic gages were evaluated for strain measurements at room temperature. Both temperature-compensated and noncompensated gages were evaluated at static and low frequency dynamic strains. Initial tests results were not encouraging, since the sensors failed at temperatures above 150°F (66°C). The gage supplier changed the gage design to enable elevated temperature applications.

The fiber-optic sensor calibration was performed on a dog-bone-type steel (ASTM A182-F22 steel alloy) specimen. The material for the specimen was chosen to match the material usually used in boiler tube headers. The geometry of the specimen is shown in Figure 2-5.

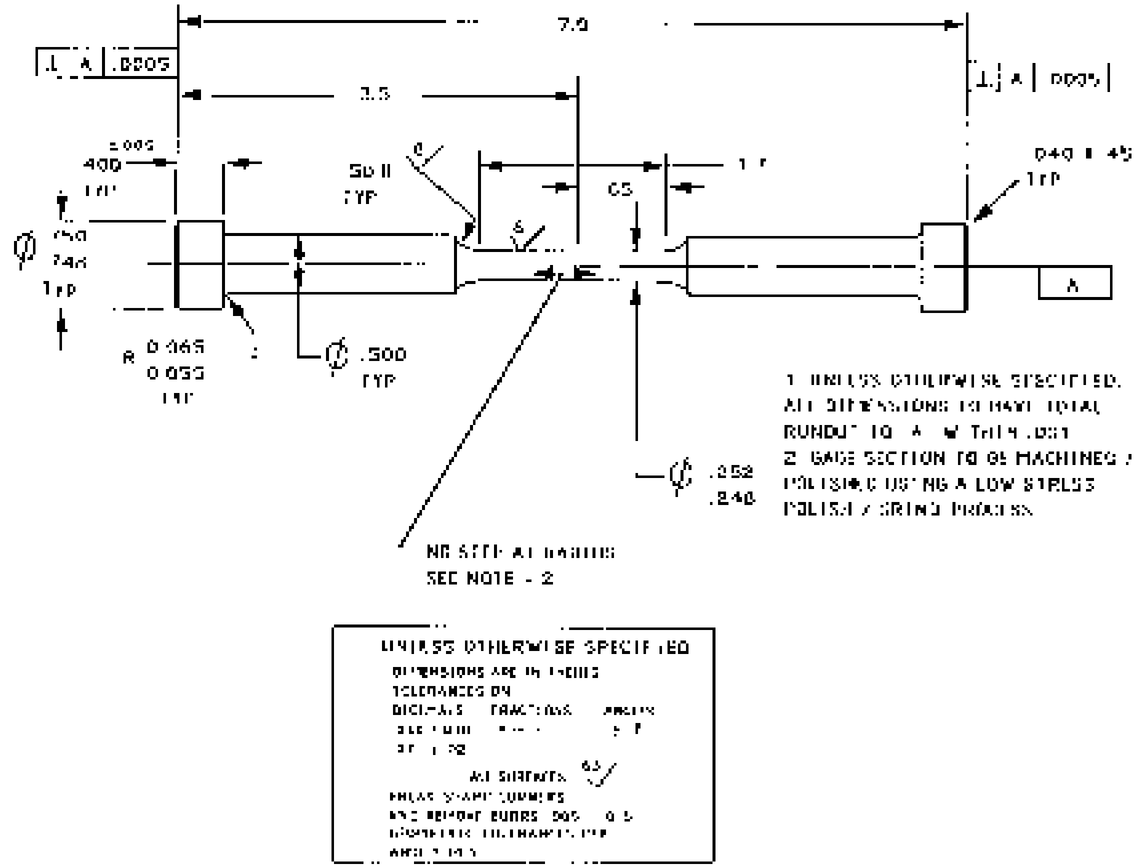

Figure 2-5 Geometry of Test Specimen

The surface of the specimen was cleaned with alcohol, and the fiber-optic strain gage was placed on the surface, and a piece of electric tape was used to hold the gage in place as shown in Figure 2-6. A thin line of adhesive was applied over the entire gage to ensure that the sensing region was covered. Curing time and method varied according to the adhesive used. Once the adhesive was fully cured, the electric tape was removed, and adhesive was applied to the rest of the fiber for protection.

A temperature-compensated fiber-optic strain gage and a noncompensated gage were mounted on the specimen using 5-min epoxy. The specimen was set up on an MTS machine, and a 0.5-in. (1.27 cm) gage length extensometer (MTS Model 632.13) was placed in between the two fiber-optic sensors as shown in Figure 2-7. Prior to installation, the extensometer was calibrated and zeroed prior to data acquisition. The fiber-optic sensors were zeroed prior to attachment of the test specimen.

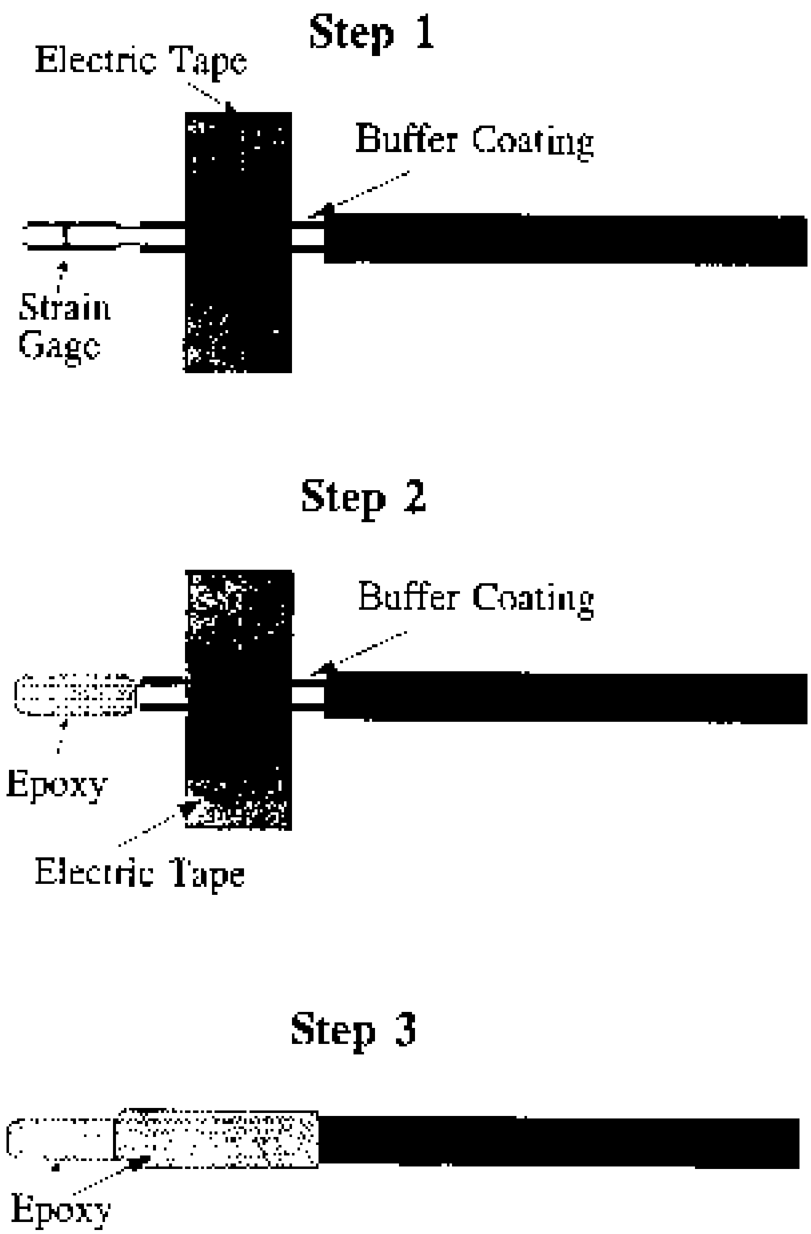

Figure 2-6 Sensor Installation

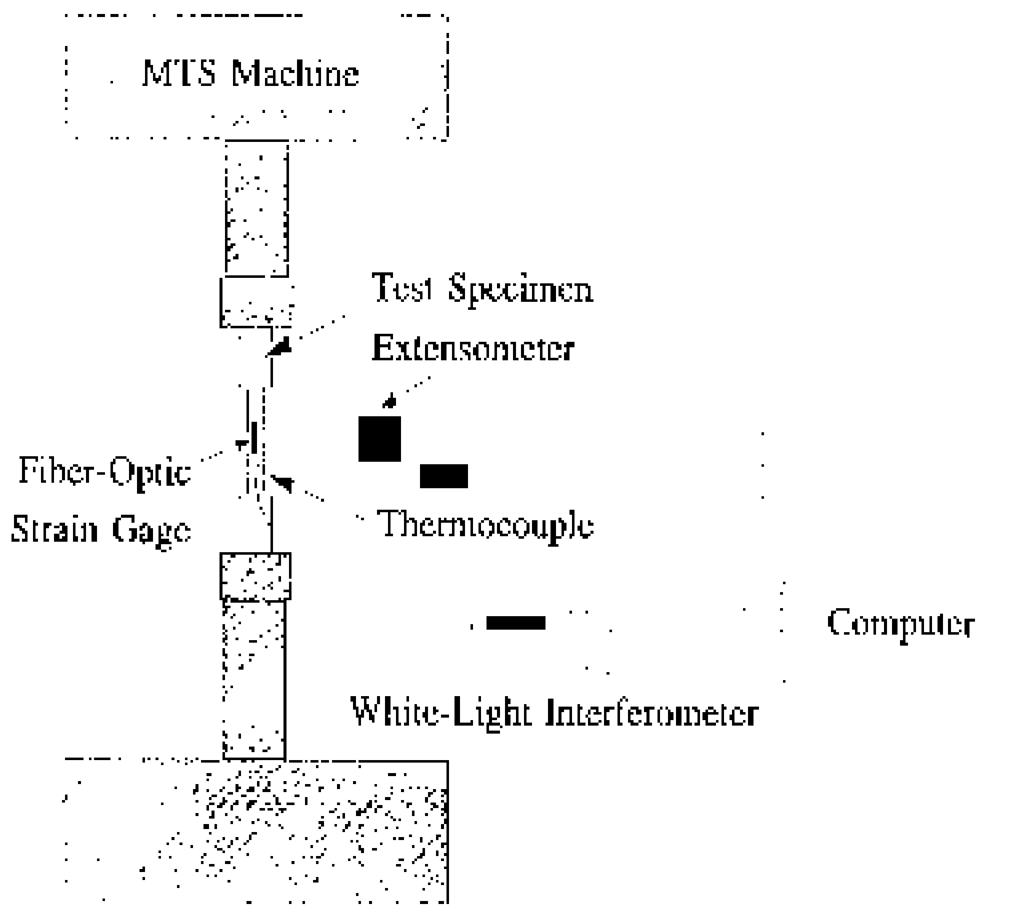

Figure 2-7 Calibration Setup

Figure 2-8 shows the entire experimental setup used for sensor calibration. The white-light interferometer and the data acquisition system are mounted on a rack placed close to the MTS machine. A close-up view of the virtual instrument created using the LabView software package is shown in Figure 2-9. Figure 2-10 shows the test specimen mounted on the MTS machine with the induction heater coil surrounding the specimen. The optical fiber leading to the Fabry-Perot sensor, the thermocouple used for monitoring the temperature, and the extensometer are also shown in Figure 2-10.

Figure 2-8 Photograph of Complete Experimental Setup

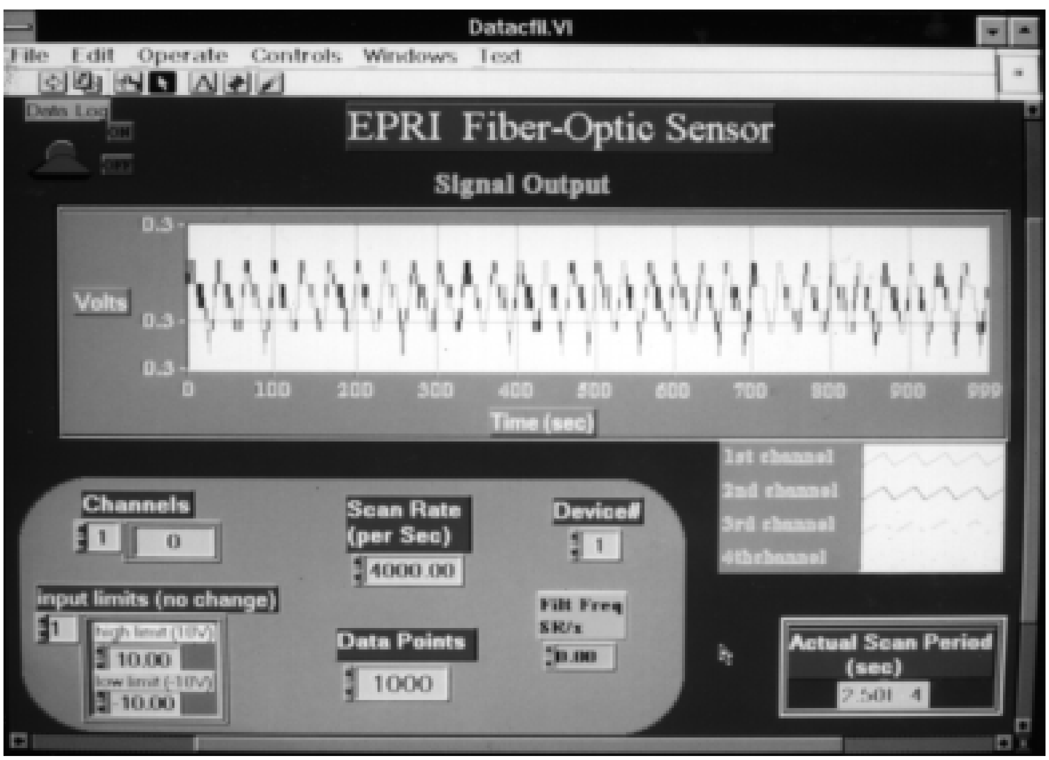

Figure 2-9 Close-up View of Computer Terminal

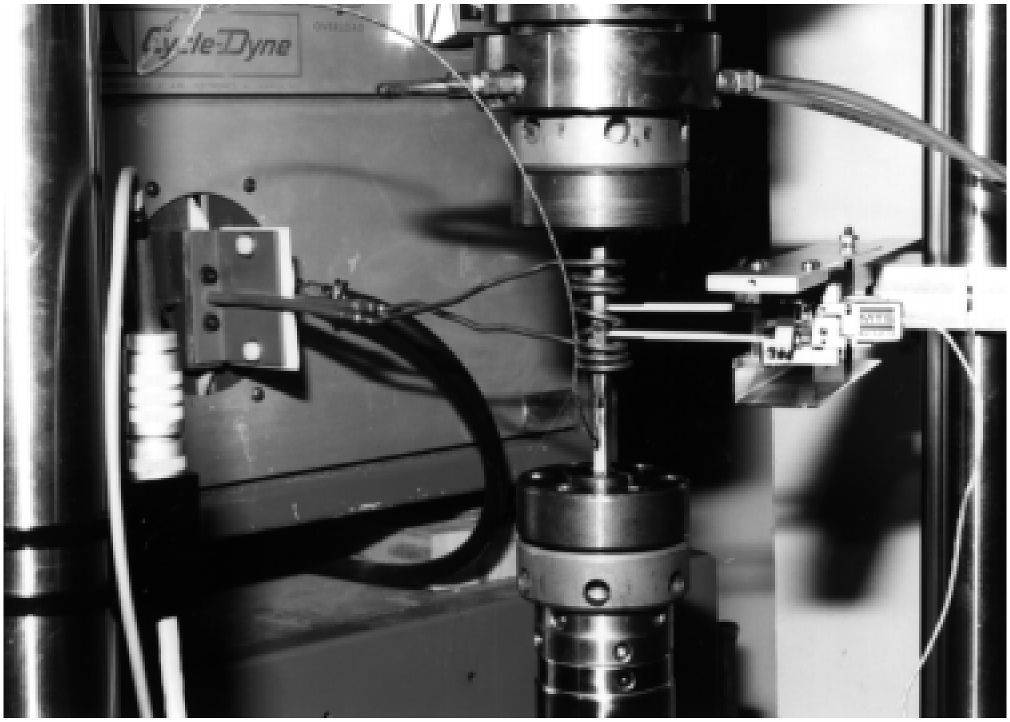

Figure 2-10 Test Specimen Mounted on MTS Machine

Gage Calibration

The specimen gages were calibrated at room temperature, moderate temperature, and for low-frequency dynamic use as described below.

Static Calibration at Room Temperature

Load was applied first in tension and then in compression to strain the specimen. Data from the two fiber-optic sensors were recorded for every 100 με read by the extensometer. The values read from the three sensors are tabulated in Table 2-1. As this table indicates, both fiber-optic sensors had an initial offset, and the strain variation did not correspond directly to the extensometer values. In order to see the trend, the fiber-optic sensors were offset, the noncompensated gage values were divided by 1.6, and the compensated gage values were divided by 3.1.

Figure 2-11 shows comparison plots for the fiber-optic sensor data and the corresponding extensometer data. The noncompensated gage range is ±1000 με with ±20 με accuracy, and the compensated gage range is ±2000 με with ±60 με accuracy. Figure 2-11 shows very good correlation between the extensometer values and the fiber-optic sensor values after multiplying by the calibration factor. The reason for the calibration factor change is explained later in this section.

Table 2-1
Values Obtained from Three Fiber-Optic Sensors

Extensometer Reading (με)	Noncompensated Gage (με)	Temperature-Compensated Gage (με)
0	-216	384
100	-60	694
200	102	1003
300	254	1282
400	410	1560
500	570	1820
400	450	1600
300	319	1288
200	142	947
100	-26	639
0	-232	312
-100	-414	-8
-200	-579	-302
-300	-733	-603
-400	-885	-895
-300	-761	-606
-200	-602	-276
-100	-435	18
0	-248	339

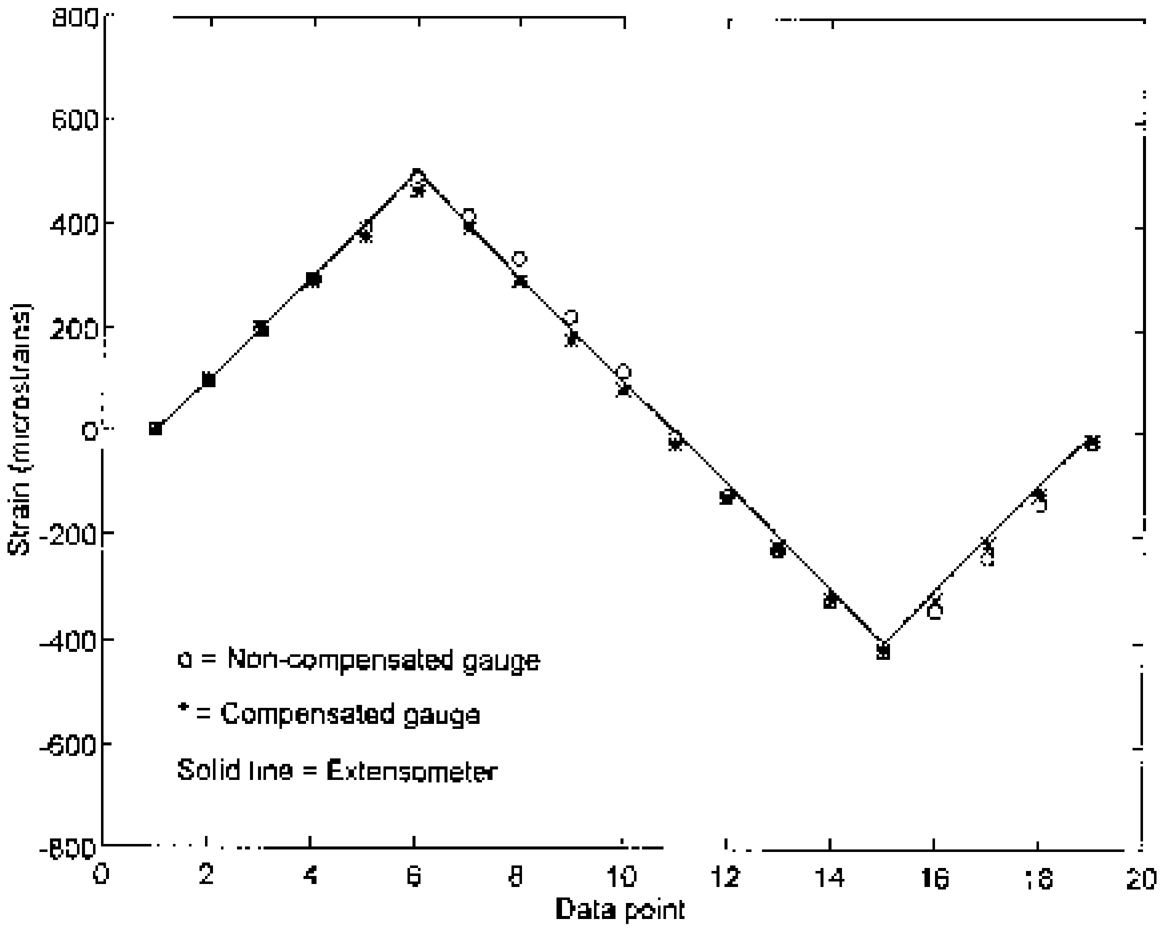

Figure 2-11 Strain Gage Data Comparison Plot for Three Sensor Types

Static Calibration at Moderate Temperature

In order to calibrate the gages at moderate temperatures above room temperature (up to 300°F [150°C]), a noncompensated gage was attached to the test specimen using a high-temperature epoxy (ECO BOND 104), good to 450°F (250°C). The epoxy was cured at 250°F (120°C) for 6 hr and further cured at room temperature for 12 hours. For this testing, the extensometer was replaced by an MTS high-temperature extensometer, good to 2000°F (1095°C). When the gage was hooked up to the white-light sensor, there was no signal, indicating failure. Suspecting that the 250°F (120°C) curing temperature might be the source of the failure, another attempt was made using a different epoxy (EPO-TEK 353ND), which is good to 360°F (185°C). In this case, the gages were cured at 150°F (66°C) for 1.5 hours. The gage performed well, and results agreed well with the extensometer value at room temperature (80°F [27°C]). When attempting to change the temperature to 100°F (38°C), the heating element overshot to 200°F (95°C) for a few seconds. During this time, the gage failed.

The thermal strain on the specimen is given by:

$$\varepsilon_T = [\delta L/L] = \alpha_{steel}\,\delta T \qquad (1)$$

where α is the thermal expansion coefficient of steel alloy used and δT is the change in temperature. This suggests that the thermal strain induced during the temperature rise to 200°F (95°C) is about 940 $\mu\varepsilon$. Therefore, it was suspected that the gage was strained beyond its 1000 $\mu\varepsilon$ limit. The gage failed even before any data was logged.

Next, a temperature-compensated gage ($\pm$2000 $\mu\varepsilon$) was attached to the specimen in a similar method using EPO-TEK 353 adhesive. This gage performed well at room temperature, and the temperature was increased at 10°F intervals. The calibration plot for this gage is shown in Figure 2-12. At 150°F (66°C), the temperature once again shot up to 200°F (95°C) accidently, and the gage failed. This was a puzzle, because the sudden temperature jump did not cause the strain to exceed the limit of the sensor. The gage was examined under the microscope, and a crack was noted on the surface of the epoxy. A close-up photograph of the failed gage is shown in Figure 2-13. It was not clear whether the crack extended to the gage or was limited to the epoxy.

In order to investigate the possibility of the crack extending to the gage, a similar test was conducted on a similar gage. The data shown in Figure 2-14 was acquired at 10°F intervals while the specimen was heated to 200°F (95°C). Initially, the gage showed reduced sensitivity, 0.75 times the value of the extensometer. At around 150°F (66°C), the sensitivity changed to 1.0 and remained close to this value until 200°F (95°C). The gage was allowed to cool down, and data was gathered once again at 10°F intervals. The calibration plot is shown in Figure 2-15. The calibration factor fluctuated between 1.0 and 1.10 until reaching 120°F (50°C). Below this temperature, the gage sensitivity changed once again to a different value, 1.5.

The gage was allowed to cool overnight and was then tested. The calibration factor had changed to 3.1. The explanation is that the gage started to fail around 150°F (66°C) during the warm-up cycle, when the sensitivity changed the first time. From that point on, it kept on failing until it reached the final 3.1 calibration factor. A crack similar to the previous gage was noticed when the gage was inspected under the microscope. Figure 2-16 illustrates the two gages and the cracks. Careful analysis revealed that the gages had failed at the fused joint of the transmit/receive fiber, which explains the difference in calibration factor throughout the entire calibration process.

A possible explanation for the scale factor discrepancy is the change in gage length due to glass tube fracture at the fused locations. Fiber-optic strain gages are manufactured by inserting two optical fibers from both ends of a small hollow glass tube as shown in Figure 2-17. The fibers are attached to the glass tube using arc fusion (or CO_2 laser), and the fused joints are potential failure sites. Excessive strain on the transmit/receive fiber caused all the gages to fail at this joint. When the fused joint fails, the gage length changes to the point where the fiber is attached to the glass tube, which, in this case, will be close to the end of the tube. At the end of the tube, the fibers are attached to the tube by the adhesive used for bonding the gage to the specimen.

The construction methods for the noncompensated gage and the compensated gage are illustrated in Figures 2-3 and 2-4. In the case of the noncompensated gage, the Fabry-Perot gap is placed at the center of the 10-mm-long glass tube, and the incoming fiber and the target fiber are fused on either side of the gap at a distance 2.25 mm from the center. The gage length is 4.5 mm. This could vary from gage to gage depending on the range of the sensor. If the soldered joint of the incoming fiber fails, the gage length becomes 7.25 mm as illustrated in Figure 2-4. Thus, the scale factor changes to 7.25/4.5, which equals 1.6. In the case of the compensated gage, the metal rod is attached to the tube at the end and the gage length is 2.9 mm. If the soldered joint of the incoming fiber fails, the gage length becomes 9 mm as illustrated in Figure 2-4. Thus, the scale factor changes to 9/2.9, which equals 3.2.

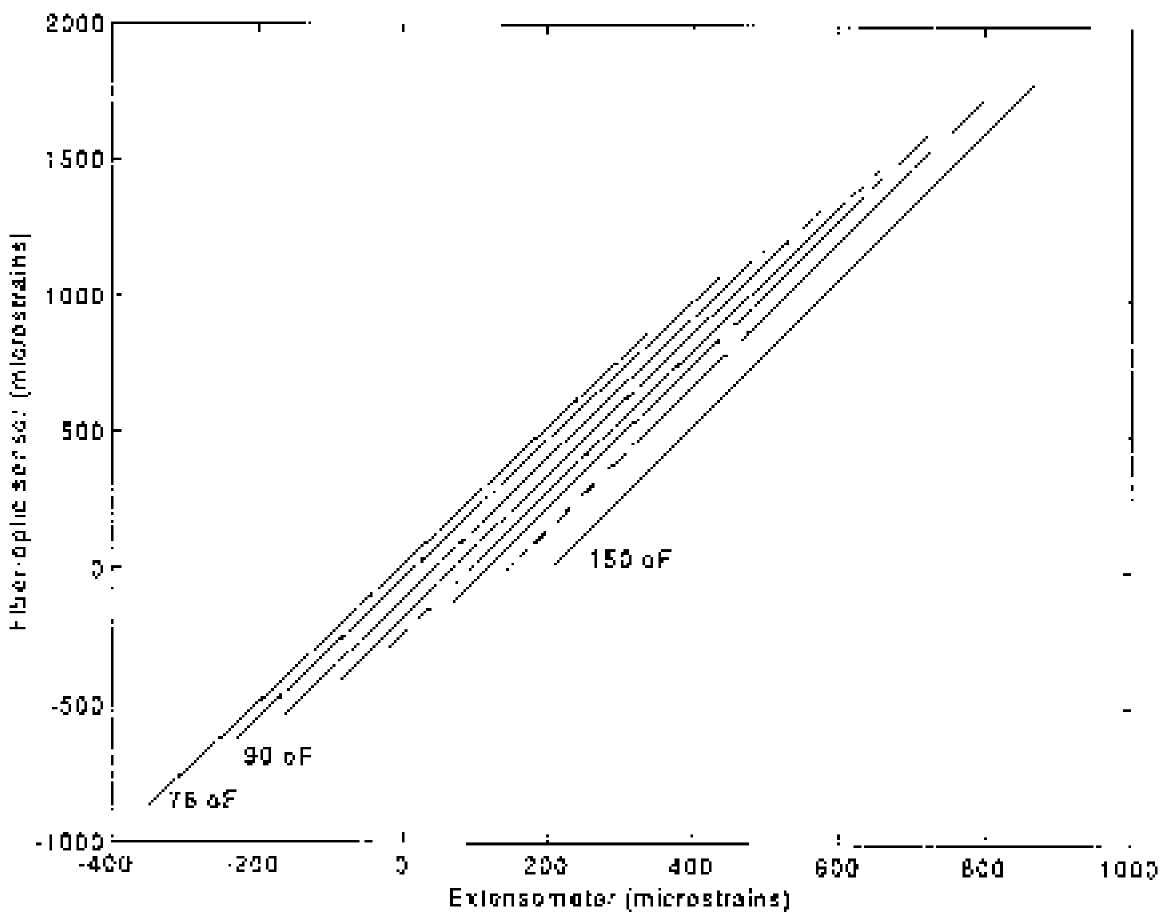

Figure 2-12 Calibration Plot for Temperature-Compensated Gage

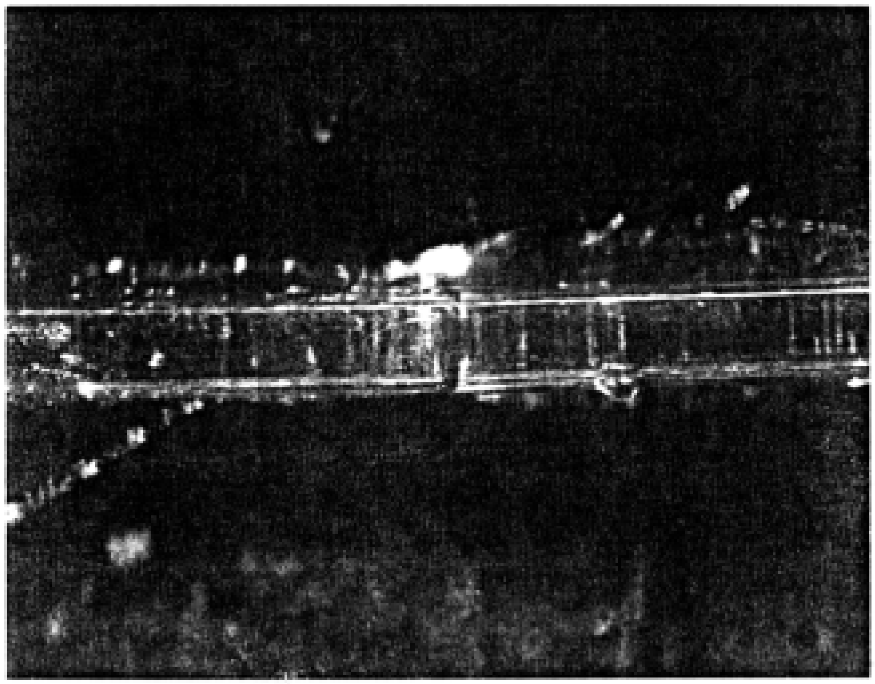

Figure 2-13 Close-up View of Failed Fiber-Optic Strain Gage

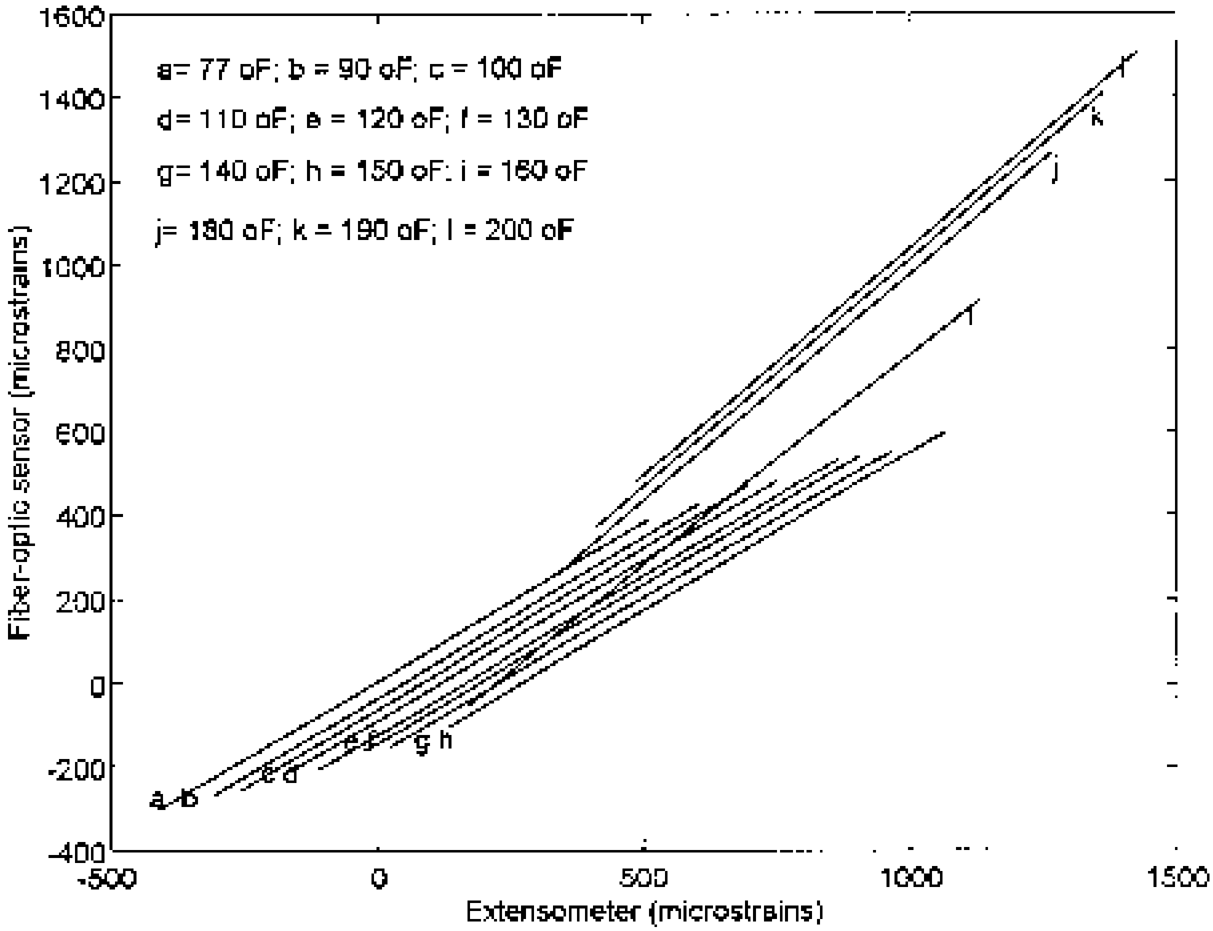

Figure 2-14 Calibration Data for Elevated Temperature Testing

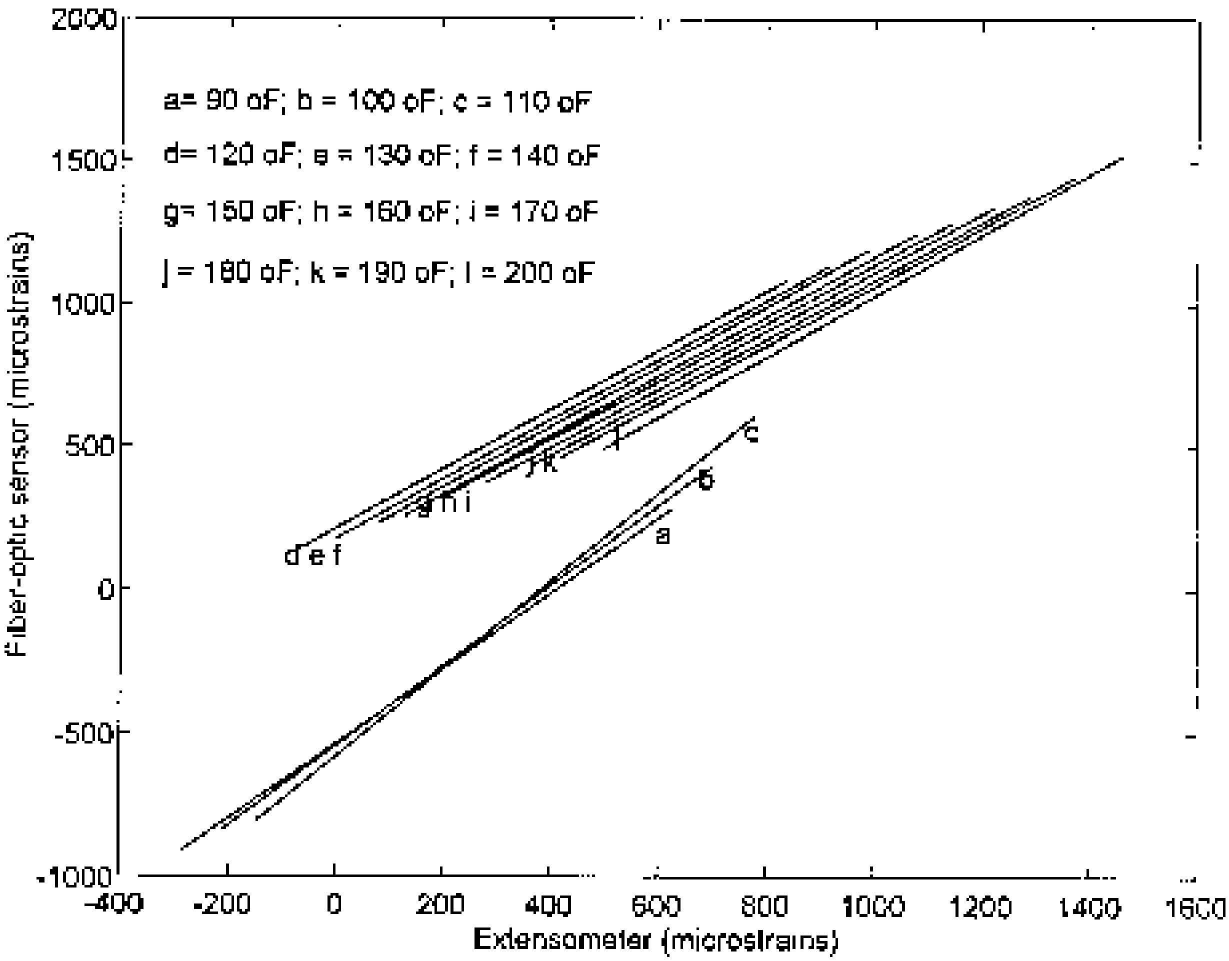

Figure 2-15 Calibration Data During Cooldown

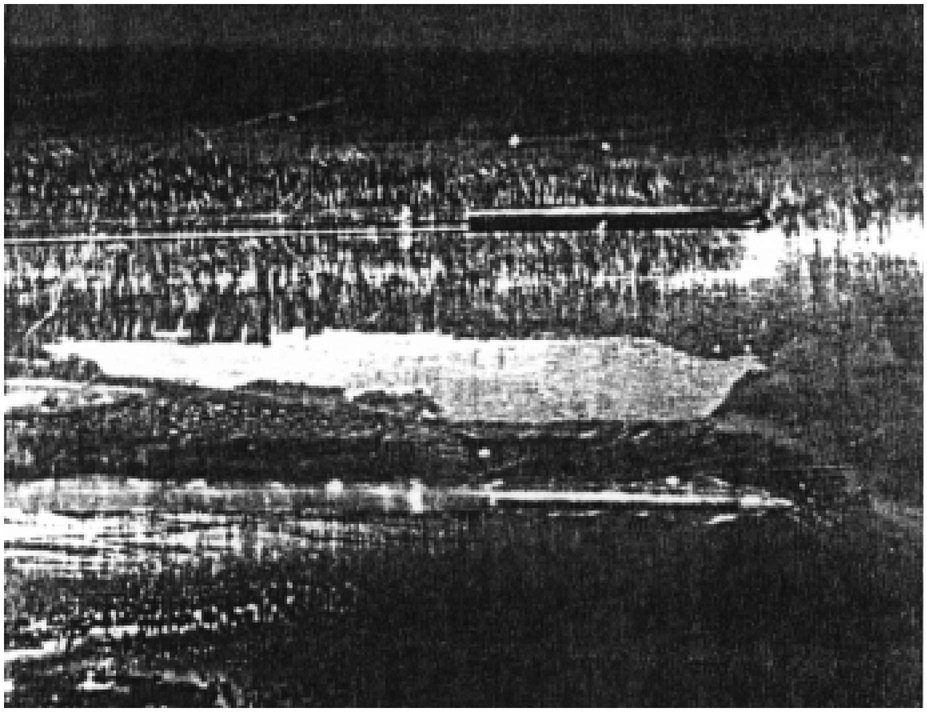

Figure 2-16 Photograph of Failed Gages

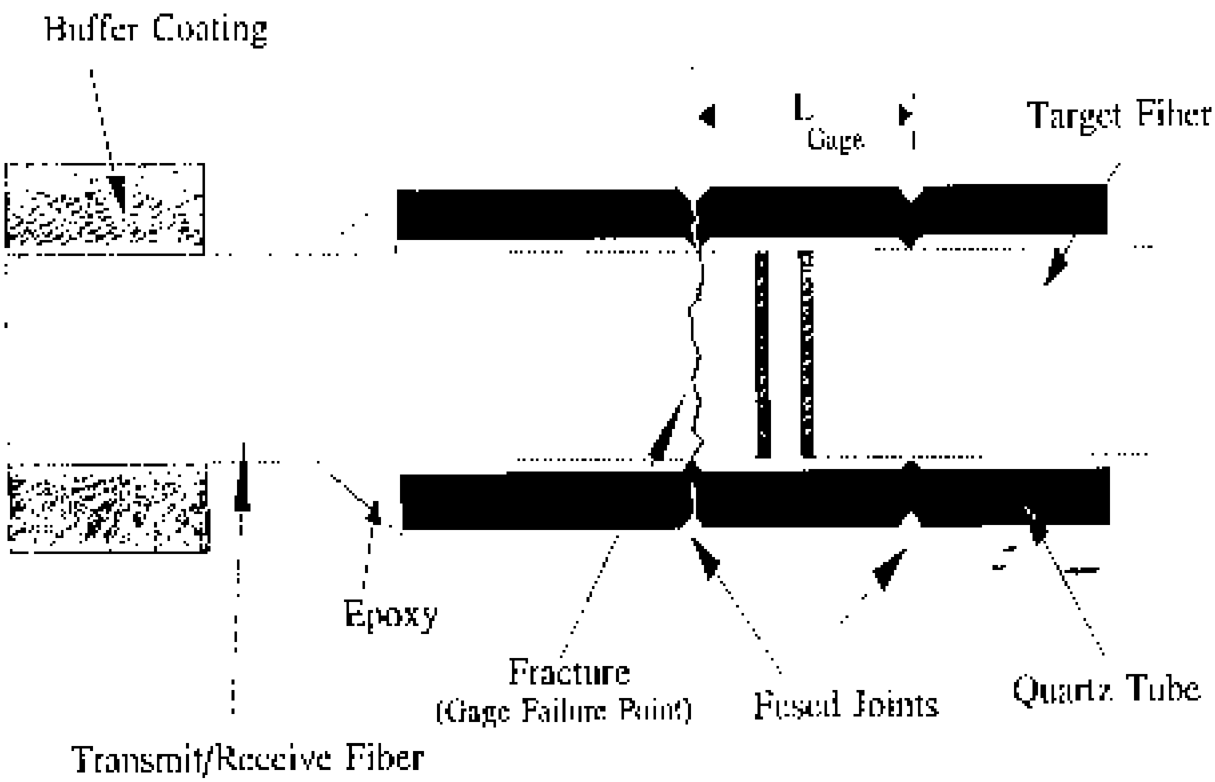

Figure 2-17 Schematic of a Failed Fabry-Perot Strain Gage

Low-Frequency Dynamic Calibration

A compensated fiber-optic strain gage was attached to the test specimen using MBond-200 strain gage adhesive. The test specimen was subjected to a very low

frequency cyclic load (0.1 Hz), and the corresponding data from the fiber-optic strain gage and the extensometer were recorded and are shown in Figure 2-18a. Figure 2-18b shows the calibration plot of the fiber-optic strain gage reading versus extensometer reading. The linear fit through the experimental data is represented by:

$$y = 1.04x + 0.02 \quad (2)$$

The test specimen was subjected to the 0.1-Hz cyclic load for 1 hour. The data were recorded once again and are shown in Figure 2-19a. The calibration plot is shown in Figure 2-19b. The linear fit through these points is represented by:

$$y = 1.05x - 0.01 \quad (3)$$

The two sets of data indicate that the calibration values of the gage did not change within the accuracy of the tests over the 1-hour period of 0.1-Hz cyclic loading (corresponds to about 360 cycles).

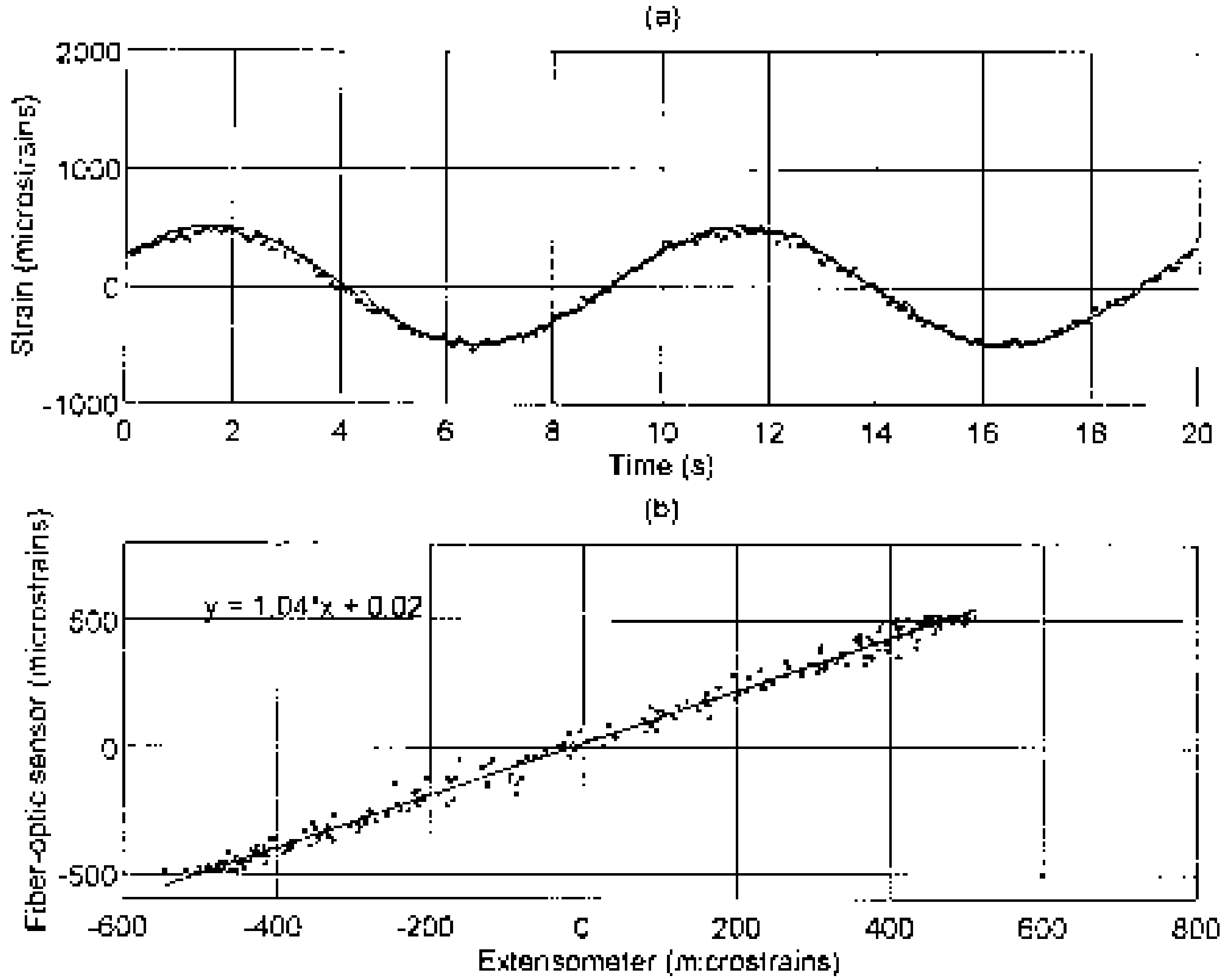

Figure 2-18 Data from Low-Frequency Dynamic Calibration
a) Strain data from fiber-optic sensor and extensometer
b) Dynamic calibration data

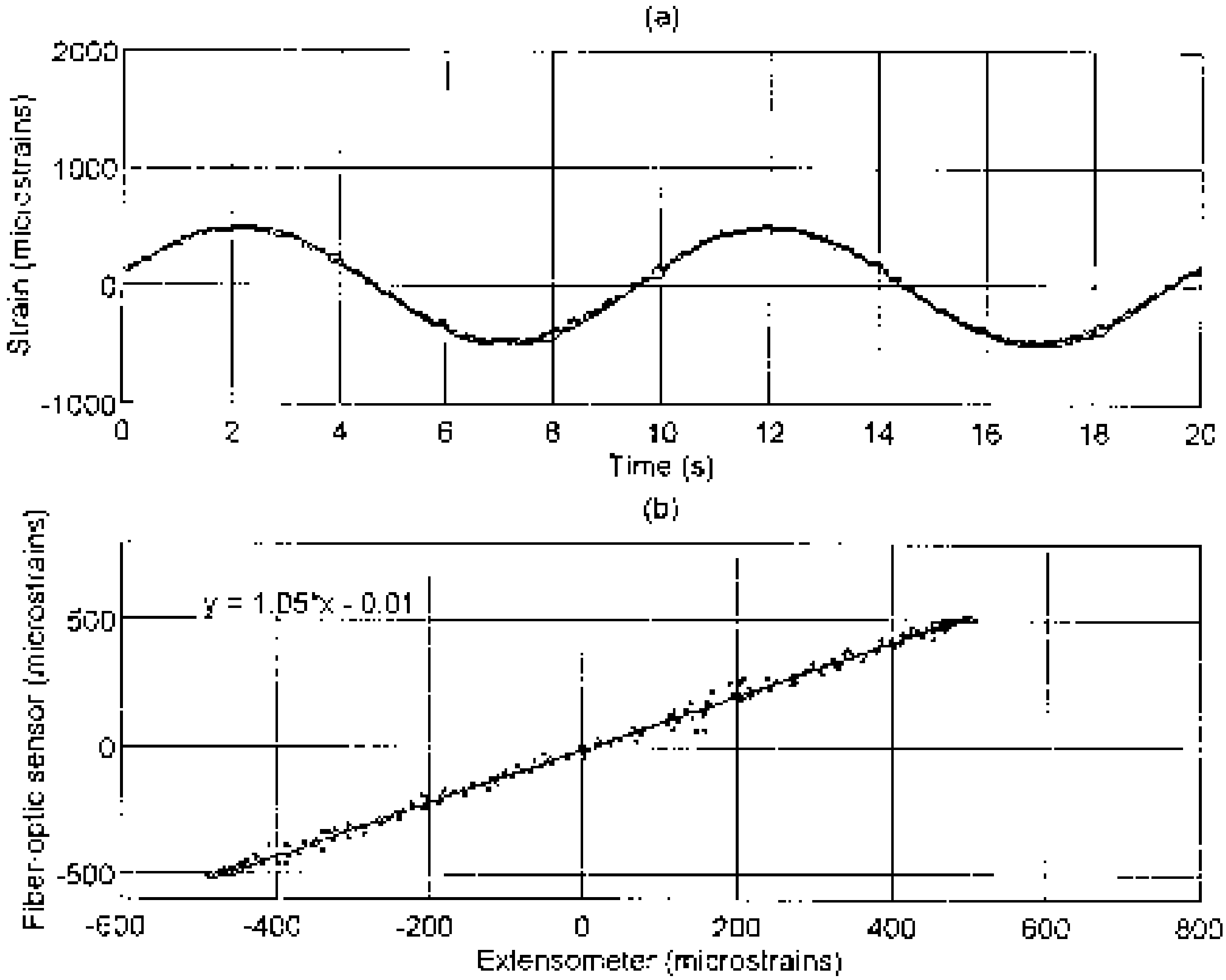

Figure 2-19 Data after 1 hr of 0.1-Hz Cyclic Loading
a) Strain data from fiber-optic sensor and extensometer
b) Dynamic calibration data

Temperature Measurement

To determine the ability of the gage to measure temperature, a temperature-compensated gage was evaluated. Figure 2-20 illustrates the setup used for temperature testing. A K-type thermocouple was attached to the test specimen next to the two gages and the test specimen was loaded on the MTS machine with the induction heater wrapped around the specimen. The specimen was heated at 10°F intervals from room temperature to 200°F (95°C), and the corresponding strain reading from the fiber-optic stain gage and the thermocouple were recorded simultaneously. At every instant, the specimen was maintained at temperature until thermal equilibrium was reached.

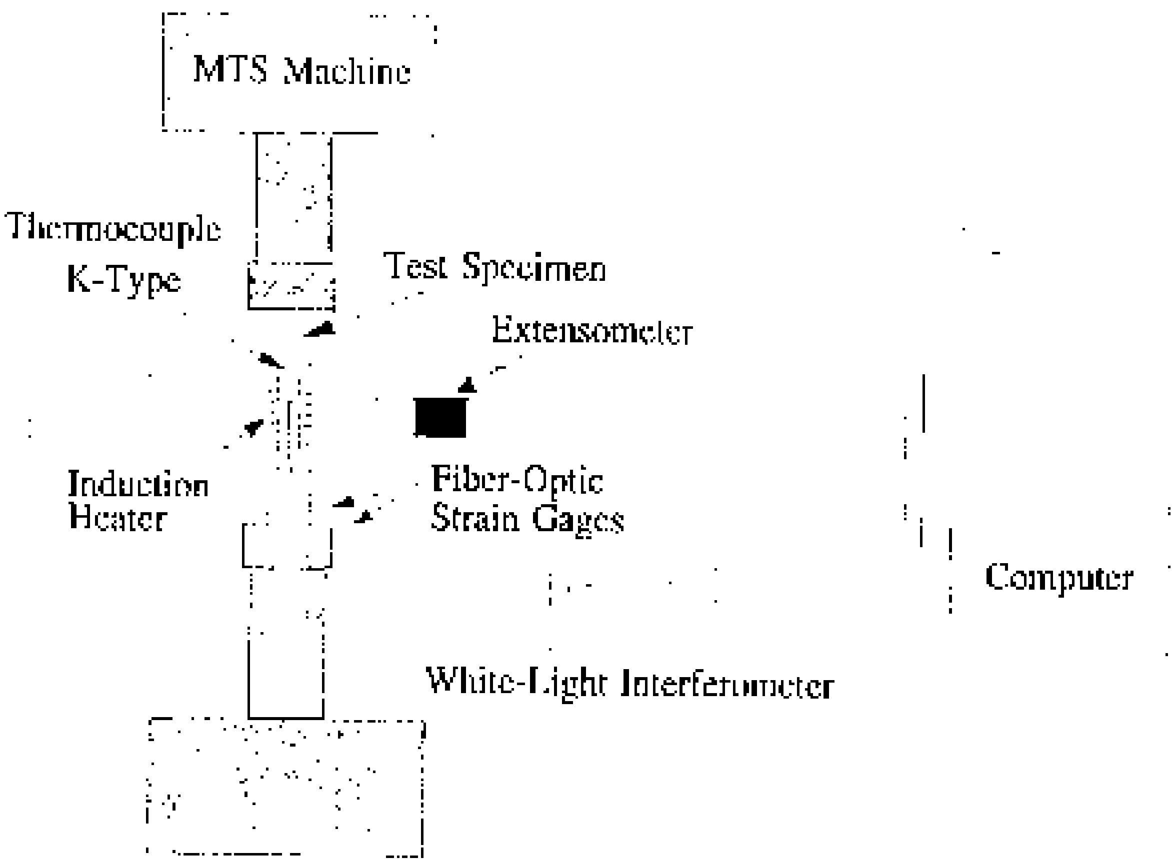

Figure 2-20 Setup Used for Temperature Testing

The temperature measurement was performed by making the Fabry-Perot air-gap length change due to thermal expansion of the glass tube and the target fiber. If the entire gage is made from quartz glass, then the temperature sensitivity of these gages would be very small and not useful at high temperatures. However, if the target fiber inside the gage is replaced by a metallic fiber (as in the case of the temperature-compensated gages), the sensors become very sensitive to temperature. The difference in thermal expansion coefficients between the glass tube and the metallic target fiber becomes the effective thermal expansion coefficient of the gage.

For example, if the thermal expansion coefficient of the glass microtubing and the metal target fiber are 3 με/°F and 7με/°F, respectively, then the effective thermal expansion of the gage is 5 με/°F. The main drawback of this approach is that most metals have a nonlinear thermal expansion with increasing temperature. Therefore, at high temperatures, the calibration plot may not remain linear and will require linearization. Alternatively, using a different type of glass for the microtubes may be a better approach, since glass materials tend to have linear thermal expansion coefficients for a larger temperature range.

The data gathered up to 200°F (95°C) shows promise for using these sensors as temperature sensors. Figure 2-21 presents a strain versus temperature plot; the temperature reading shown was obtained from the K-type thermocouple. The strain read by the fiber-optic sensor was negative, since the thermal growth of the fiber resulted in a reduced interferometer gap (equivalent to compression). The strain as a function of temperature is linear. The slope of the decreasing temperature plot is about 6% lower than the increasing temperature case. This may have been introduced by the induction heater inducing voltage on the thermocouple during the heating-up time. During the cooldown period, the induction heater was off.

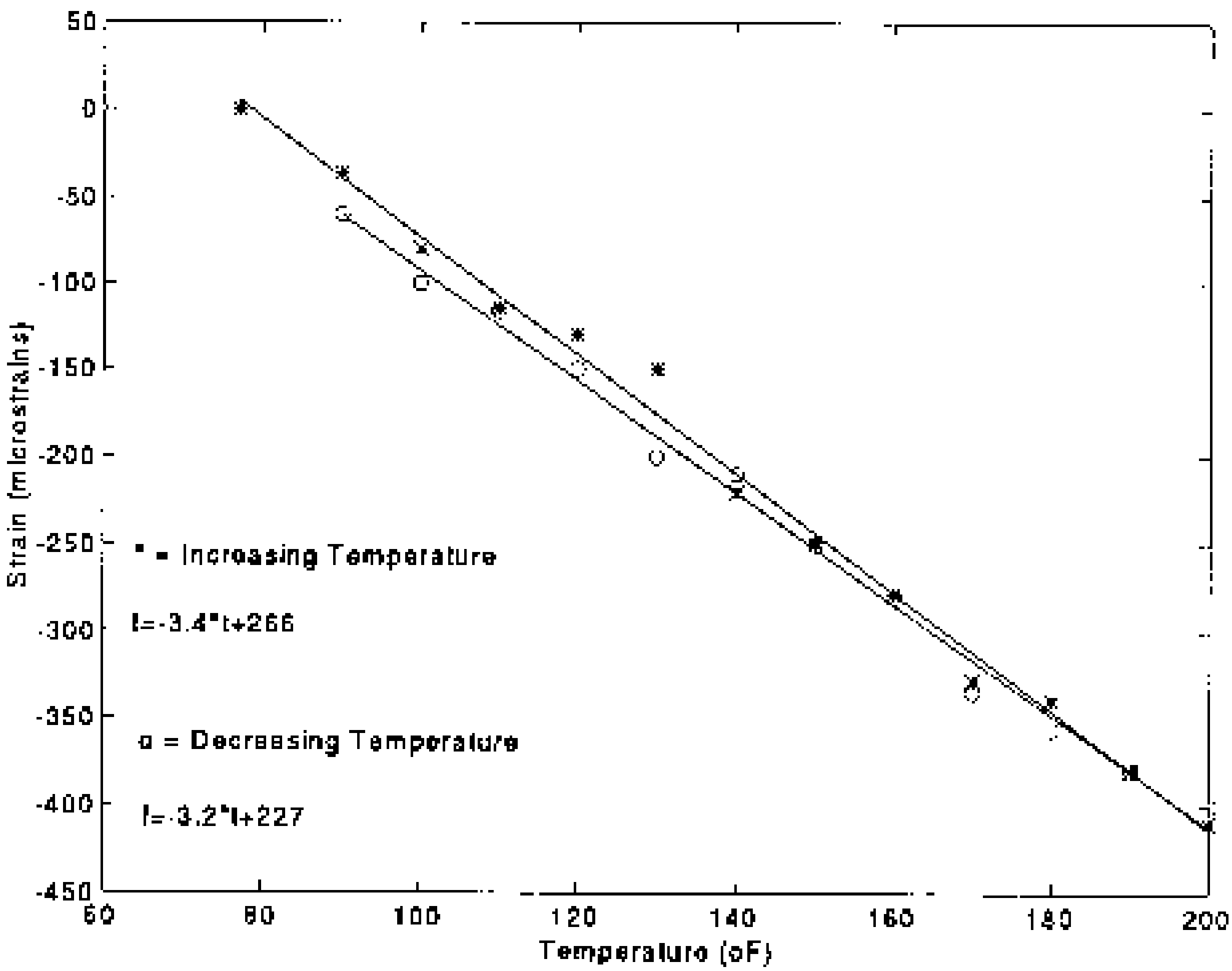

Figure 2-21 Plot of Strain versus Temperature

Discussion of Results

The fiber-optic sensors performed very well at room temperature but failed at slightly elevated temperatures. This was due mainly to failure of the fused joints. The gage design was modified to correct this problem. Also, the gages were rather fragile and needed to be ruggedized for practical applications (see Section 3 for more details on this). The temperature-compensated gages did not seem to fully compensate the thermal strain. This may be due to the fact that the specimen material and the target fiber material were not the same. Unless these are made from the same material, the gages are not effective for high-temperature applications.

As summarized in Table 2-2, the fiber-optic gages proved to be easier to use than the electrical strain (resistive) gage, since no bridge completion and balancing is involved.

Table 2-2
Comparison of Electrical Strain Gage and Fiber-Optic Gage

Characteristic	Electrical Strain Gage	Fiber-Optic Gage
Bonding (normal applications)	M-Bond 200 type adhesives work well. More rugged than a bare fiber gage.	GA 2 is a better candidate (requires more shear strength). Gages must be ruggedized.
Ease of use	Difficult bridge completion and balancing required.	No bridge balancing required.
Drift	Generally drifts over a period of time.	No visible evidence in a 24-hr test.
Thermal compensation	Required	Not required
Transverse strain compensation	Required	Not required

3

HIGH-TEMPERATURE APPLICATION EVALUATION

Evaluation of fiber-optic sensors in a high-temperature environment was the main focus of this project. This section documents these efforts, describing the various packaging and attachment methods investigated and the results of both laboratory testing and testing of the sensors in the field at a host utility.

Packaging and Attachment Methods

One goal of the project was to find a suitable method to attach fiber-optic sensors to high-temperature (up to 1000°F [538°C]) structures. The sensors had to withstand the hot and dirty environment of a power plant, be easy to attach, and long-lived. Therefore, it was decided to attach the sensors to a metallic shim that could be spot welded to the structure of interest for strain measurements. The schematic of the proposed spot weldable fiber-optic strain gage is shown in Figure 3-1.

The attachment of the glass fiber-optic sensor to a metal shim was a major challenge. Most strain gage epoxies are not suitable for temperatures higher than 600°F (315°C). Several different methods were investigated to attach the sensors to a steel metal shim (5- to 15-mil [0.13-0.38 mm] thick). These included:

- Casting small amounts of metal to encapsulate the glass fiber and the shim.
- Spraying molten metal (plasma spraying) to attach the sensors to the shim.
- Constructing extrinsic Fabry-Perot sensors directly on the shim.
- Using adhesives to attach the sensor to the shim.
- Metalizing (gold plating) the sensor and bracing it to the shim.

The details of each method are explained in the following subsections. In each case, the lessons learned are described and a path to full success detailed.

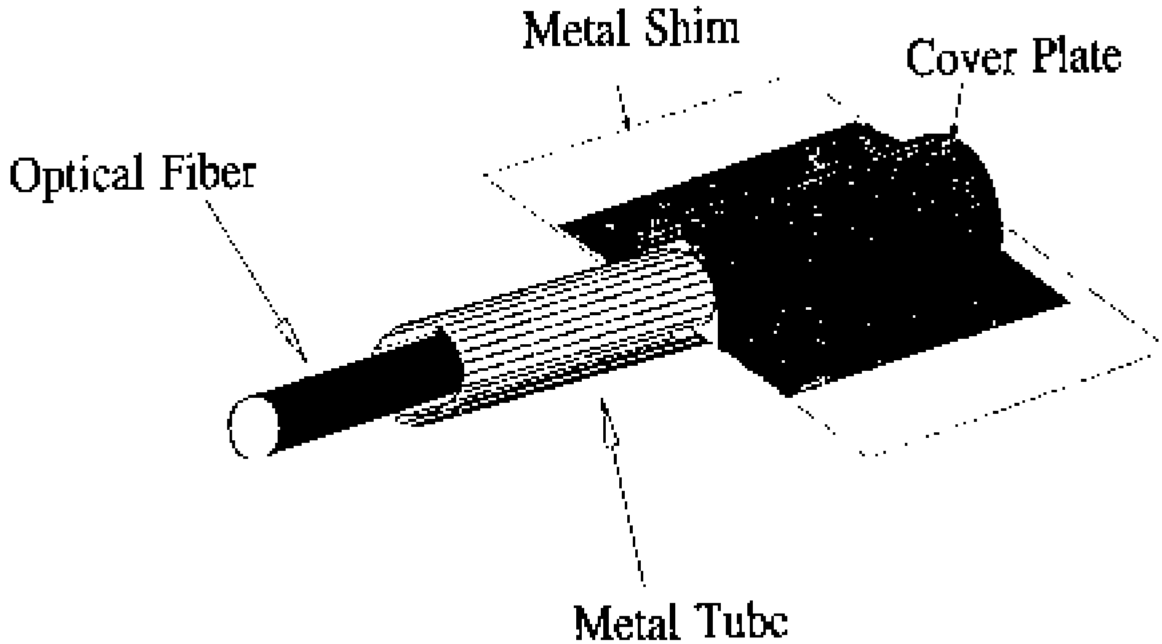

Figure 3-1 Schematic of the spot weldable fiber-optic strain gage.

Casting Process

This process involved casting a small amount of metal around both the optical fiber and a stainless steel metal tab (or shim). The metal tab allows the gage to be attached to the test object and also provides a strain transfer path from the test object to the gage. Figure 3-2 shows a sketch of the casting configuration. The material used to encapsulate the gage was selected after evaluating the physical properties of the gage and the operating temperature. The encapsulating material had to survive at the operating temperature of 1000°F (538°C), be nonreactive with the gage, not damage the gage during manufacture, and be as compatible as possible with the operating characteristics of the gage.

Some physical properties of the glass fiber were provided by the gage supplier and are listed in Table 3-1. From these properties, the glass was thought most likely to be a silica glass. Previous work demonstrated that aluminum could be successfully casted around glass [1], and aluminum-encapsulated gages have been tested up to 650°F (345°C). Because the operating temperature for the current application was 1000°F (538°C), close to the melting point of aluminum alloys, copper alloys were considered. The alloy chosen was CDA No. 93700, a castable bearing grade copper alloy. Its melting range, 1403 to 1705°F (761-929°C) TmSol to TmLiq is above the operating temperature. Shrinkage on freezing is low, thus minimizing the strain to the fiber-optic gage.

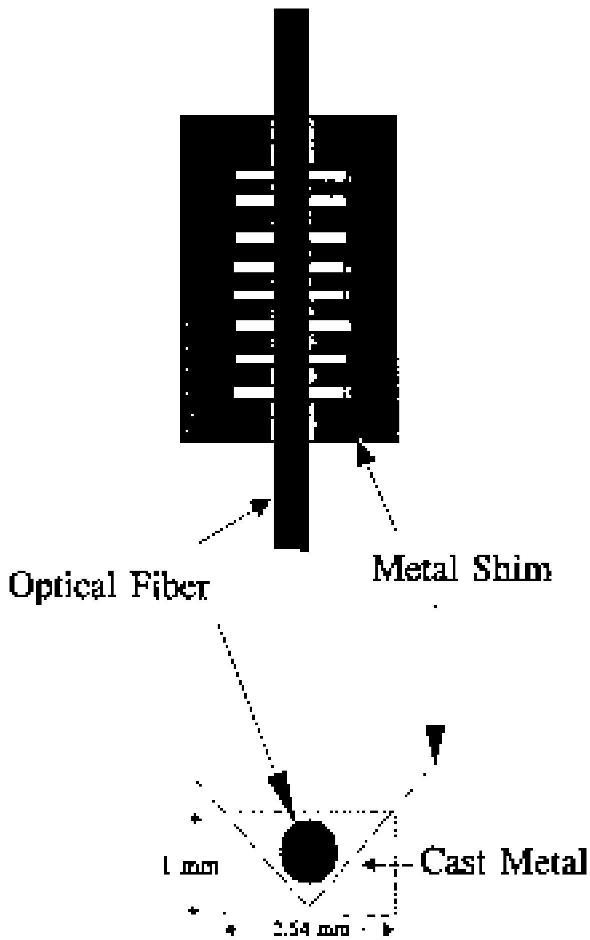

Figure 3-2 Configuration for Casting Process

Table 3-1
Physical Properties of Glass Fiber

Property	Metric	English
Modulus	71 GPa	10.29 msi
Poisson's Ratio	0.14	0.14
Thermal Expansion Coefficient	0.5/°C	2.77/°F

Small crucibles to melt the brass alloy and mold it to hold the fiber and the metal shim were made out of graphite. The casting environment needed to be inert to prevent oxidation. Therefore, an enclosure was built from plexiglass, which had inlets to fill the enclosure with argon to create an inert environment (see Figure 3-3). Heating elements and insulation were placed inside the enclosure so that the crucible could be heated to 2000°F (1095°C) to melt the brass alloy. Another similar heating unit was placed inside to preheat the mold to 1700°F (929°C). Thermocouples were installed to monitor the mold and crucible temperatures, along with controllers to accurately control the temperatures. A manipulator and gland seal were manufactured to move the crucible and pour the molten metal into the mold.

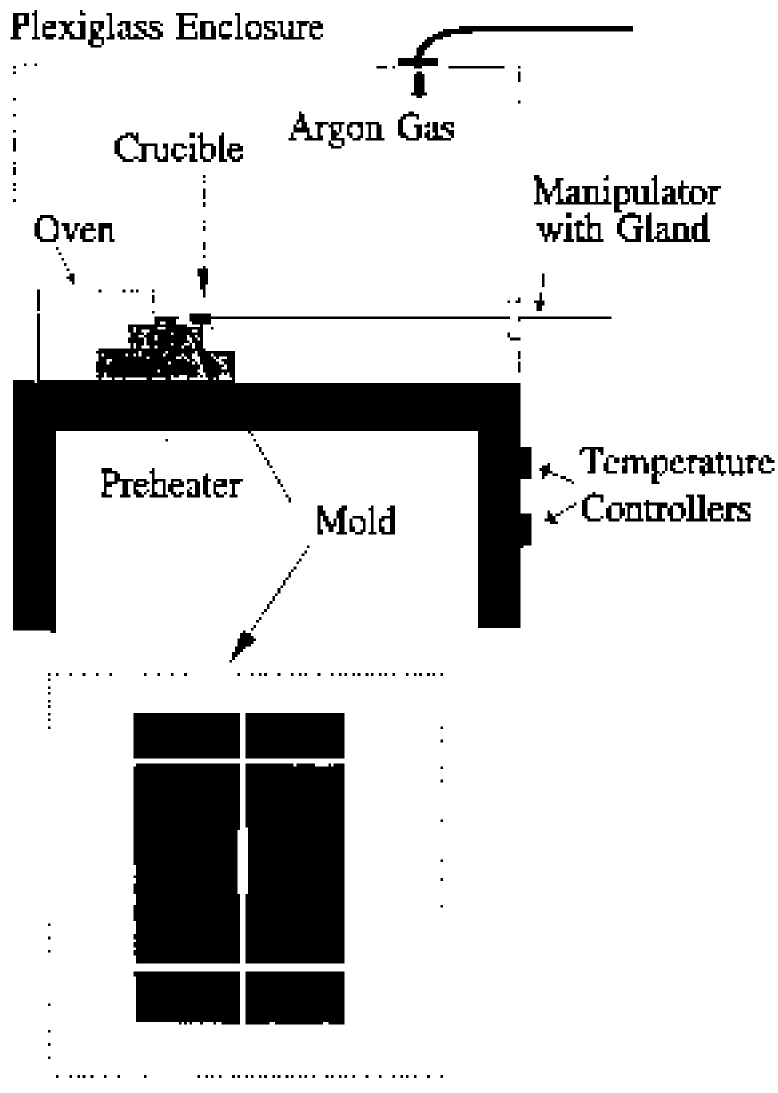

Figure 3-3 Casting Setup

A small length of optical fiber was placed on a thin metal shim as shown in Figure 3-2. The metal shim had several slots cut in it so that the liquid metal would flow around and entrap the fiber and the metal shim. The fiber and the metal shim were placed inside the mold, and a pour spout was placed directly above to allow the liquid metal to flow into the appropriate place. The mold was placed on a heating element. The brass alloy was placed inside the crucible, which was placed inside the oven using the manipulator. The amount of alloy placed in the cold crucible was about two times the amount needed to fill the mold. The casting enclosure was sealed and filled with argon, and the oven temperature raised to 2000°F (1095°C) and the mold temperature to 1700°F (929°C). Once the temperatures stabilized, the molten metal was removed from the oven and poured into the mold within 5 seconds. Then, the mold was allowed to cool, and the cast part was removed and inspected.

The small molding parameters made it difficult to obtain complete castings. Surface tensions were high compared to the weight of material, preventing complete filling of the cavity. Several trial runs with limited success led to the investigation of other methods.

Plasma Spray

Plasma spray offered the option of directly depositing the encapsulating material around the gage, avoiding problems with surface tension. As shown in Figure 3-4, a small piece of metal shim was bent around the 1/4-in. (0.6 cm) test specimen so that once the sensor was attached to the metal shim, it could be spot welded to the test specimen without placing excessive strain on the gage. For the trials, an optical fiber was placed on the top surface of the metal shim, and epoxy was used to hold the fiber in place, as shown in Figure 3-5. A mask was built to confine the encapsulating material to a small region around the fiber. The metal shim with the optical fiber was placed behind the mask during the plasma spray process as shown in Figure 3-6.

After a few trials, the appropriate number of spray coatings needed to provide at least five fiber thickness of material around was identified. Figure 3-7 shows a photograph of a fiber being encapsulated by nickel aluminide, a common bond coat used in the plasma spraying of turbine blades. Good results using this coating were obtained with a single fiber.

In a final effort, an actual gage was used on a metal tab as shown in Figure 3-8. The results are shown in Figure 3-9. Once again, the weak area in the gage assembly caused a failure, plus the heat caused the gage to curl as shown in Figure 3-9. The glass gage construction method needs to be improved prior to making any more attempts with this technique. The program doesn't have sufficient funds to completely investigate this method. However, since the plasma spray process showed success with bare fibers it is a technique worthwhile investigating in future programs.

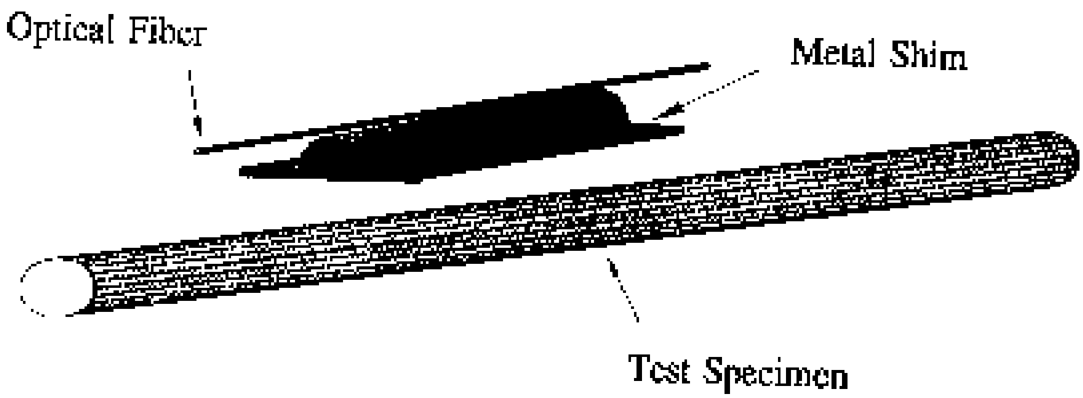

Figure 3-4 Strain Gage Configuration for Plasma Spraying

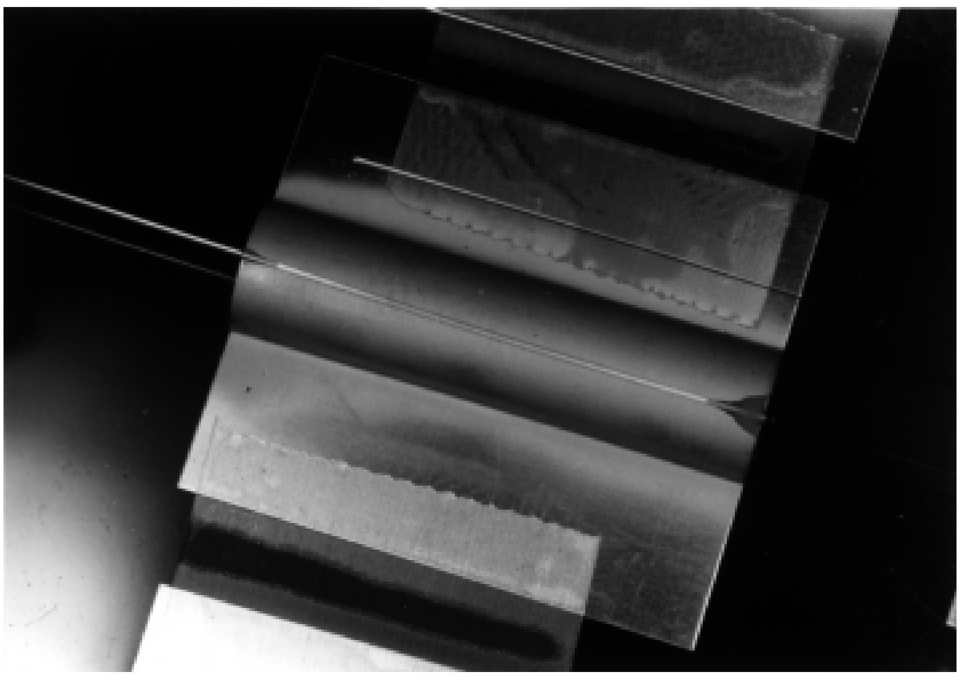

Figure 3-5 Optical Glass Fiber on Metal Tab with Epoxy Holding It in Place

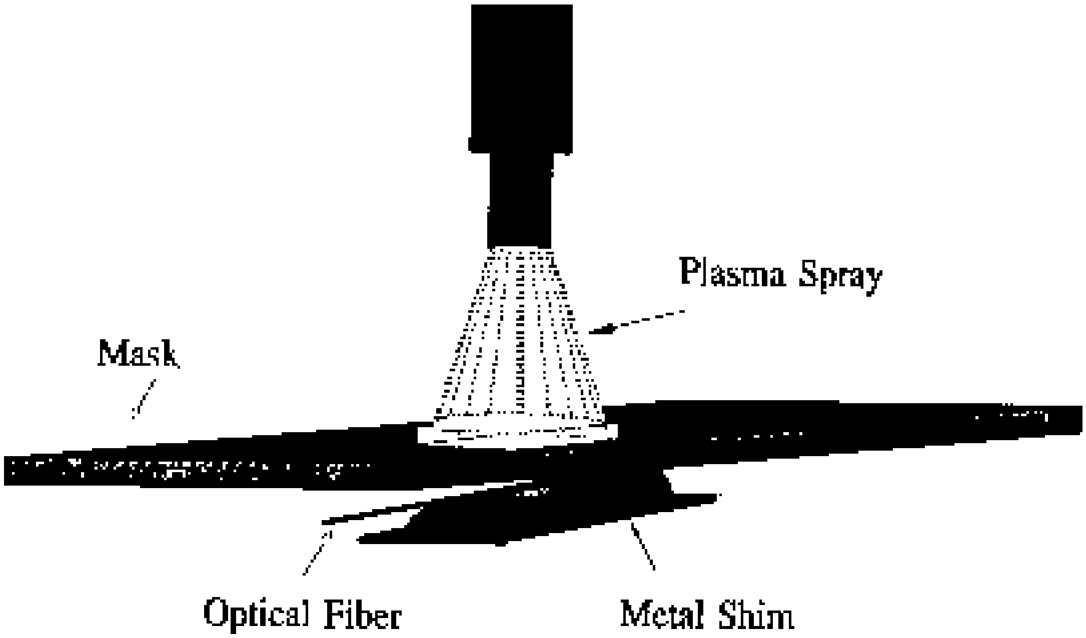

Figure 3-6 Plasma Spray Setup

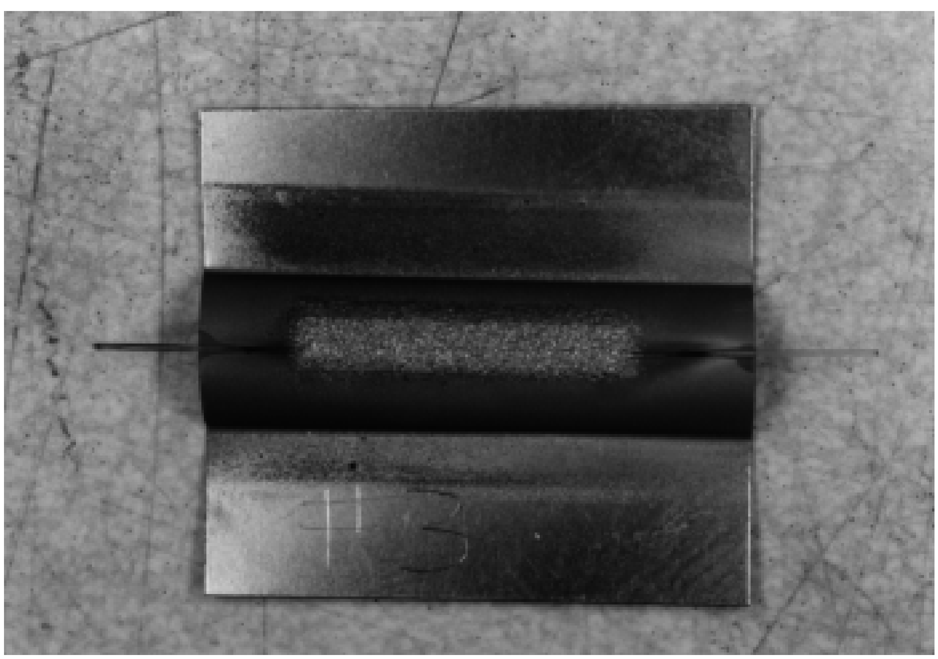

Figure 3-7 Piece of Optical Fiber Attached to Metal Shim by Plasma Spray Method

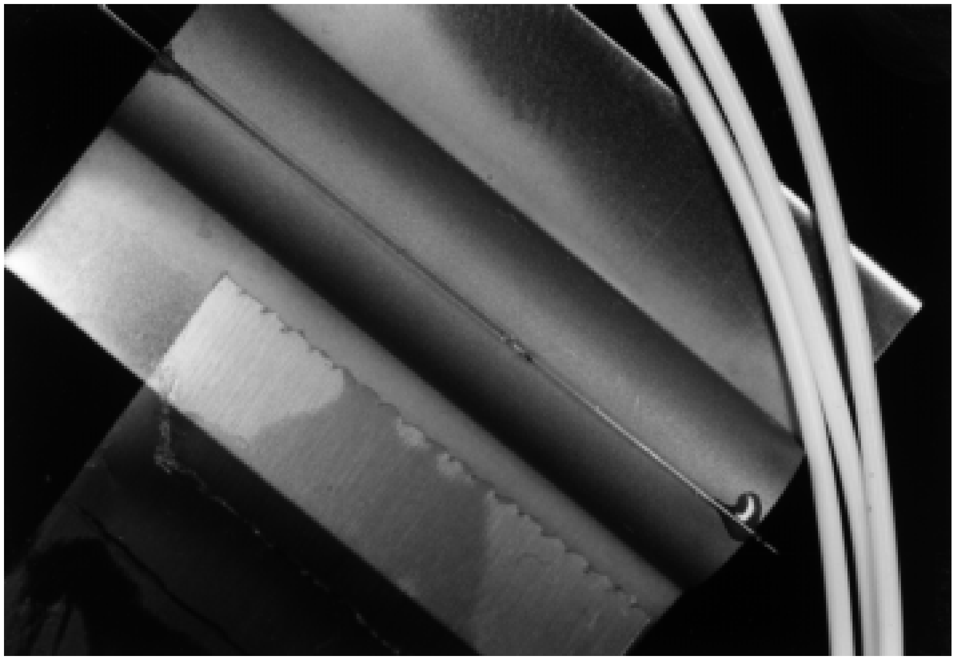

Figure 3-8 Fiber-Optic Strain Gage Held in Place on Metal Shim

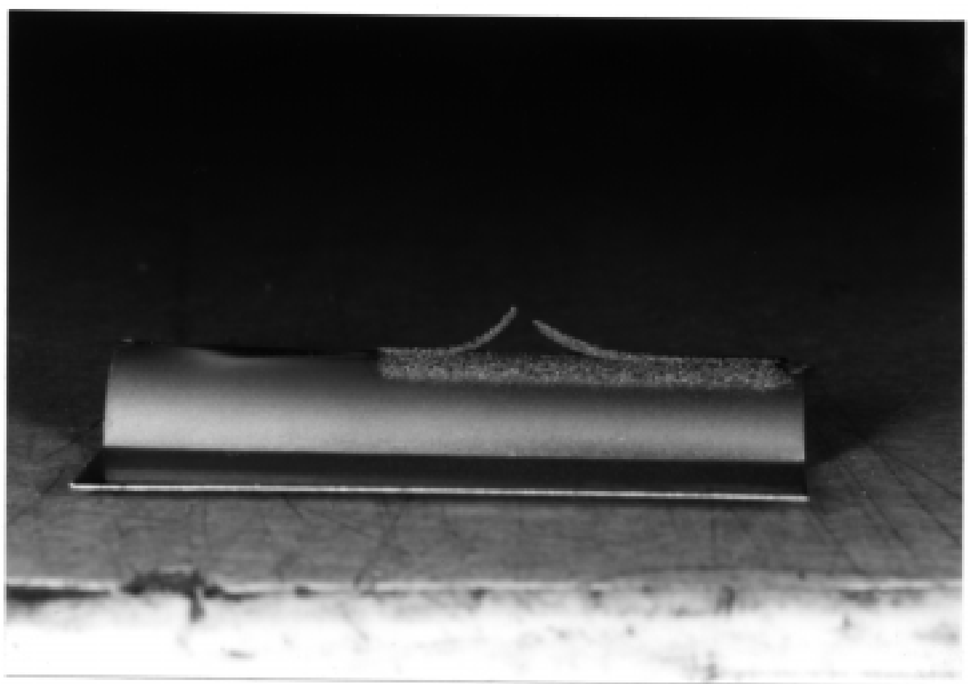

Figure 3-9 Results of Fiber-Optic Strain Gage

Metal Fabry-Perot Strain Gages

Creating Fabry-Perot sensors directly on the metal shim eliminated the need to attach the glass tube to the shim. The Fabry-Perot strain gages used in this study were constructed by inserting two optical fibers from both ends of a hollow glass tube as shown in Figure 2-3. The transmit/receive fiber and the target fiber, with the end face polished for reflection, were fused to the glass tube. Due to thermal stress, these gages generally failed at the fused joint of the transmit/receive fiber at elevated temperatures.

An alternative concept to build these sensors is illustrated in Figure 3-10. The logic behind this proposed design is that if the gages are attached to a metal shim which then will be spot welded to the structure of interest, why not create the sensors directly on the metal shim? As shown in Figure 3-10, a V-groove is made on the metal shim to house the optical fibers (transmit/receive fiber and target fiber). Based on this concept, a prototype gage was constructed using a polished metal rod as the target fiber and epoxy to hold it in place. This prototype was constructed using a single-mode fiber, so that the concept could be easily proved using the available laser interferometer optics. If this concept worked, then a Fabry-Perot sensor for the white-light interferometer would be built.

The prototype sensor was attached to a cantilever beam and subjected to an oscillatory strain. Typical data are shown in Figure 3-11. The optical fringes generated from the strain looked very clean and encouraging.

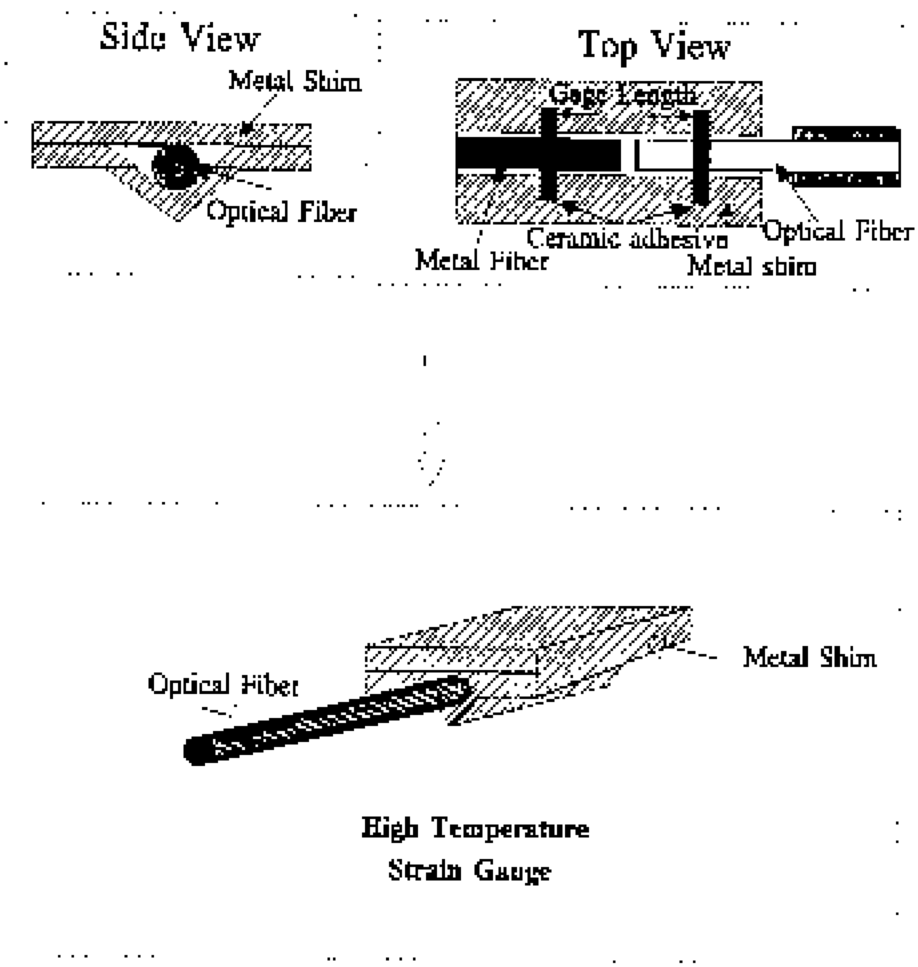

Figure 3-10 Alternative Concept for Constructing Fabry-Perot Sensors

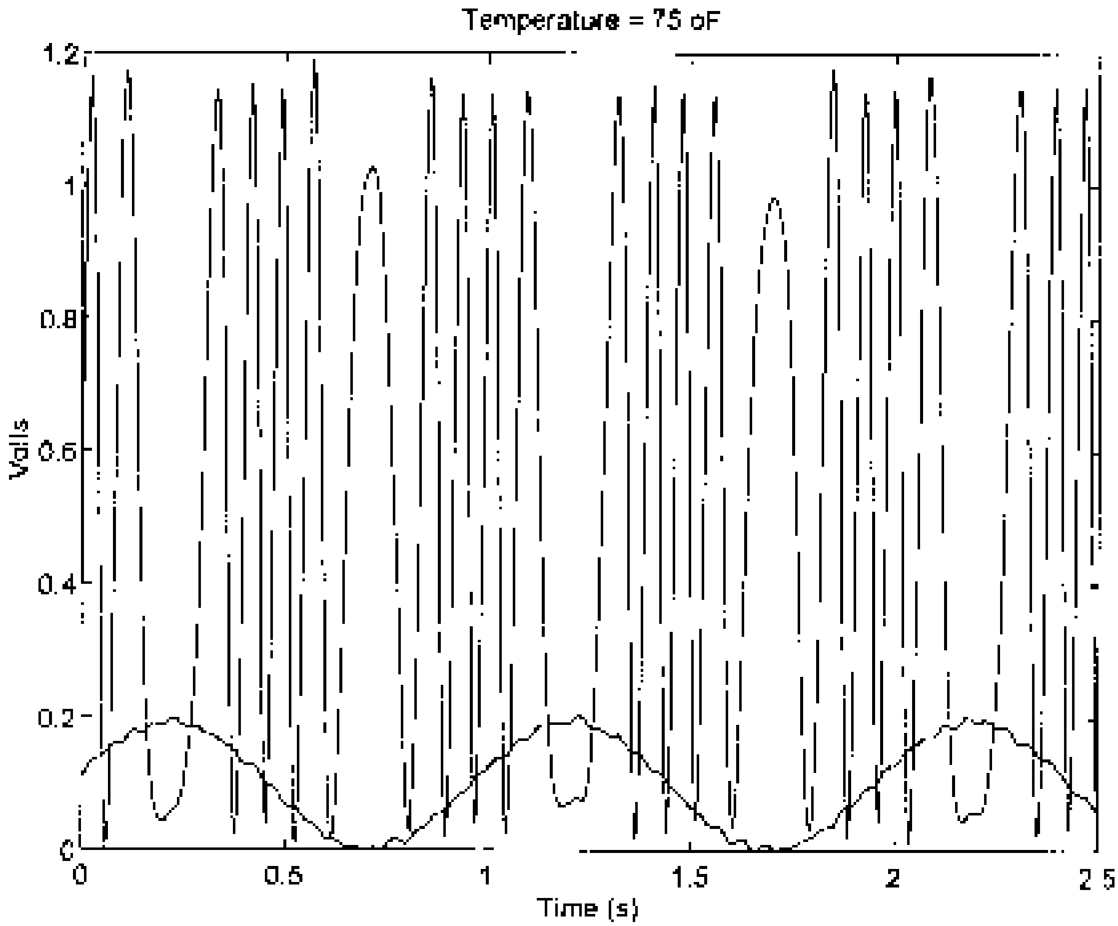

Figure 3-11 Fiber-Optic Sensor Output Illustrating Optical Fringe Movement Due to Sinusoidal Oscillation

A second prototype sensor was constructed as shown in Figure 3-12. In this prototype, the transmit/receive fiber and the target metal fiber were attached to the metal shim using a high-temperature ceramic adhesive. The central part of the gage was covered with a small piece of metal shim to prevent the fiber ends from vibrating and also to keep the air gap clean. This gage was attached to the test specimen and was subjected to a 1-Hz cyclic load. The specimen was heated at 100°F (38°C) intervals, and the data recorded are illustrated in Figure 3-13. The plots show the broadened optical fringes at the turning points. The time between two broadened optical fringes correspond to half a cycle period. The optical fringes recorded from the fiber-optic sensor remained clean until 300°F (150°C). At 400°F (205°C) and higher, the number of fringes for the same strain increased, and the fringe pattern looked very noisy. At 600°F (315°C), the data no longer looked valid. Therefore, the specimen was allowed to cool down, and data were acquired at 200°F (95°C) (see Figure 3-14). The data during the warm-up time and the cool down time at 200°F (95°C) look similar. The specimen was once again heated to 600°F (315°C). Then, data were acquired at 100°F interval from 600°F (315°C) to 1000°F (538°C) (see Figure 3-15). The strain sensitivity reduced again and became similar to the room temperature value. Figure 3-16 indicates the strain sensitivity of the gage at various temperatures.

An optical fringe corresponds to a half wavelength of displacement at the air gap. The expected number of optical fringes for the 0.5-in. (1.27 cm) gage length (distance between the ceramic adhesives) and 400 με is about 16. The observed value is 4, indicating the gage length to be smaller. The possible explanation is that the cover plate used in the central portion of the gage sandwiched the fibers tight between the bottom shim, thus altering the gage length (smaller than the distance between the ceramic adhesive joints). Once the temperature increased, the metal shims expanded, and the fibers became a loose fit. During this time, the gage length tried to change to the expected value. But, at the same time, the fiber was probably rubbing against the metal to cause noise in the signal. During the second warm-up time, the epoxy joints failed, and, once again, the central metal shim held the fibers in place to provide the signal. The specimen was removed and analyzed. It was found that the zerconium cement had lifted off the metal shim.

This method showed partial success. Further experimentation was not performed with this method, since construction of white-light gages did not seem short term. However, in the future , it is worth exploring this method further for constructing high-temperature fiber-optic strain gages.

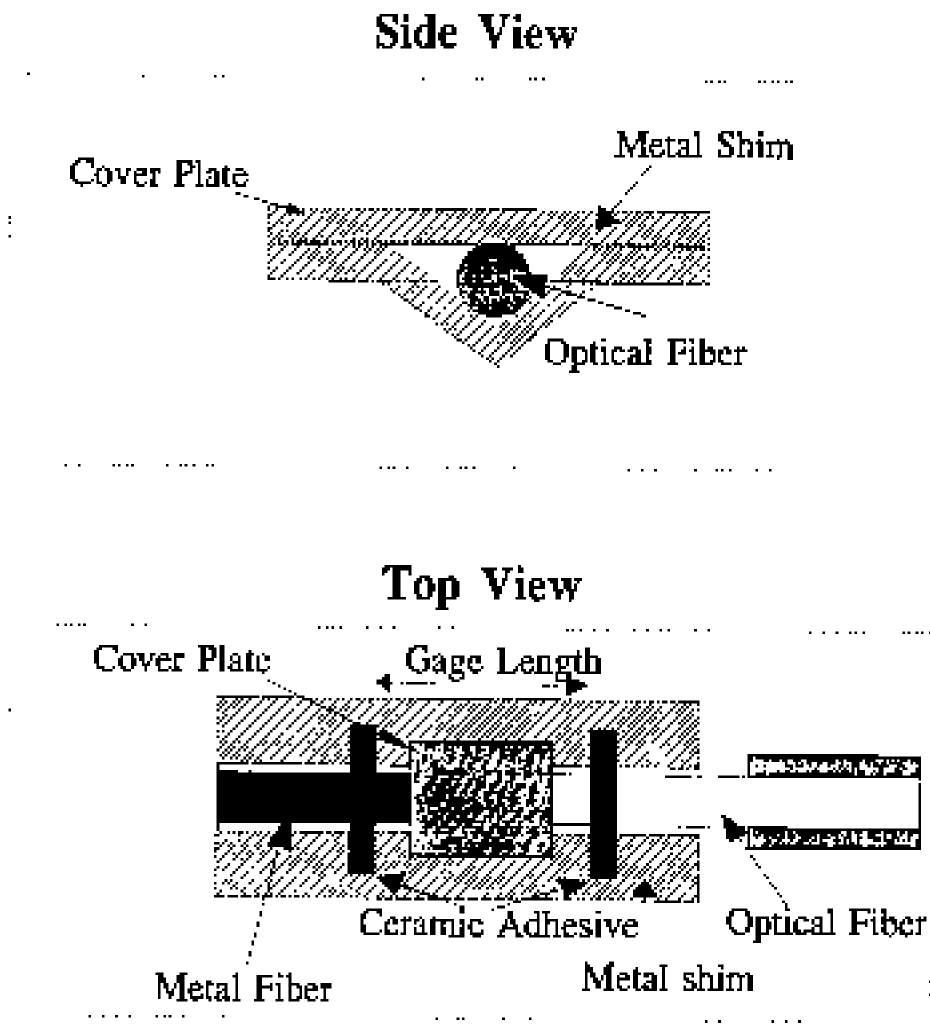

Figure 3-12 Metal Strain Gage

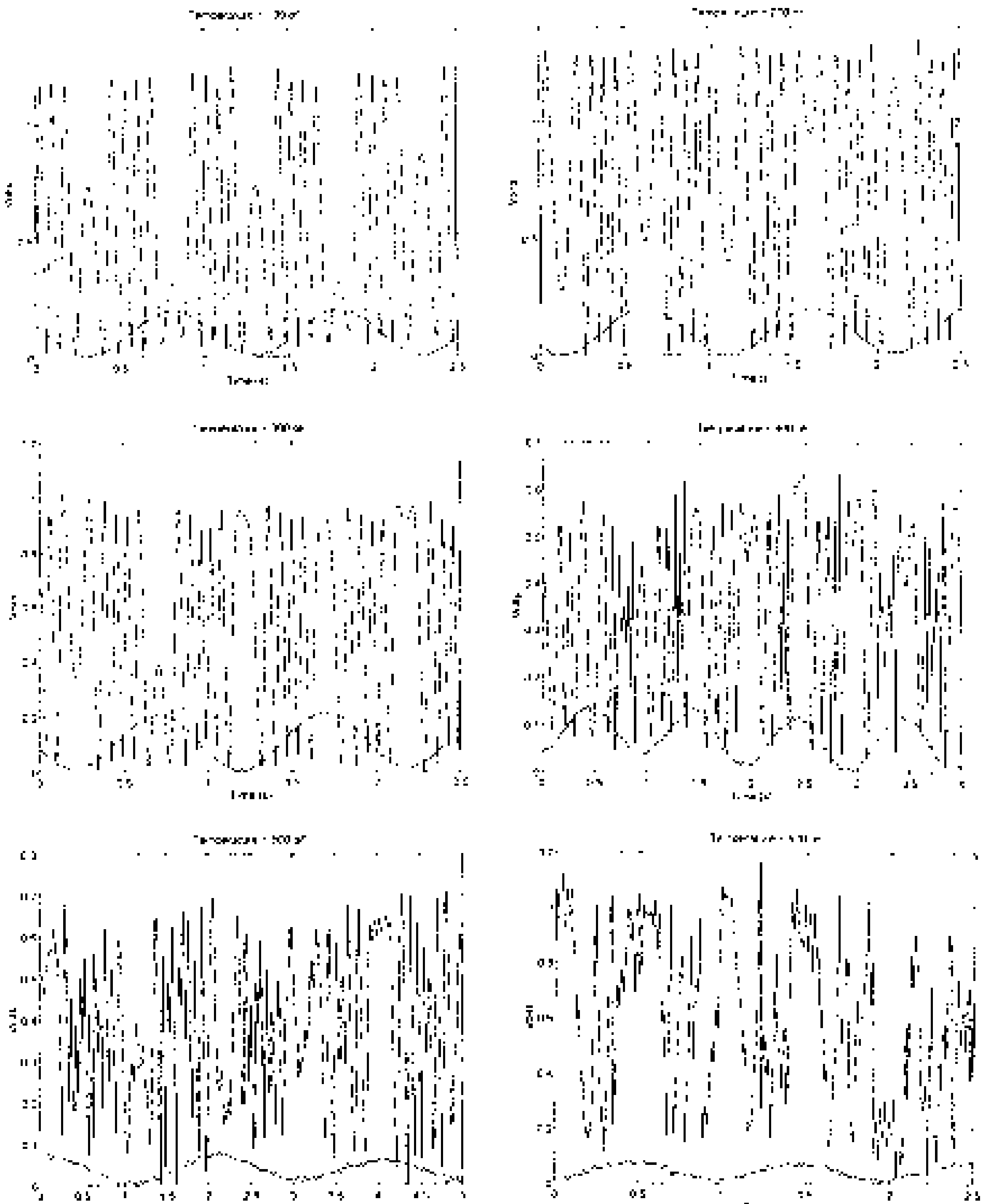

Figure 3-13 Data Acquired at 1-Hz Cyclic Load and at 100°F Temperature Intervals up to 600°F.

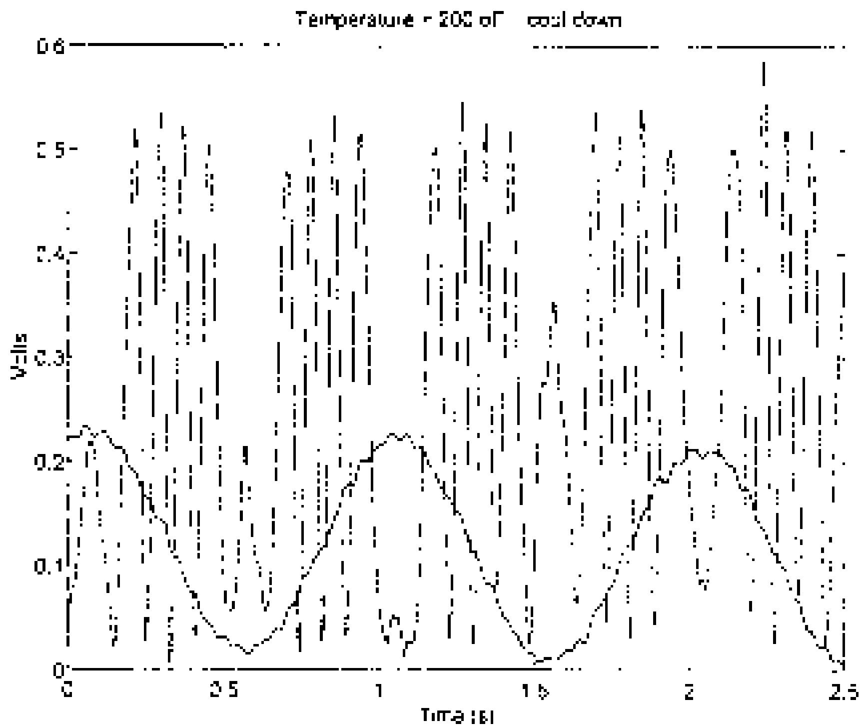

Figure 3-14 Data after cool down to 200°F

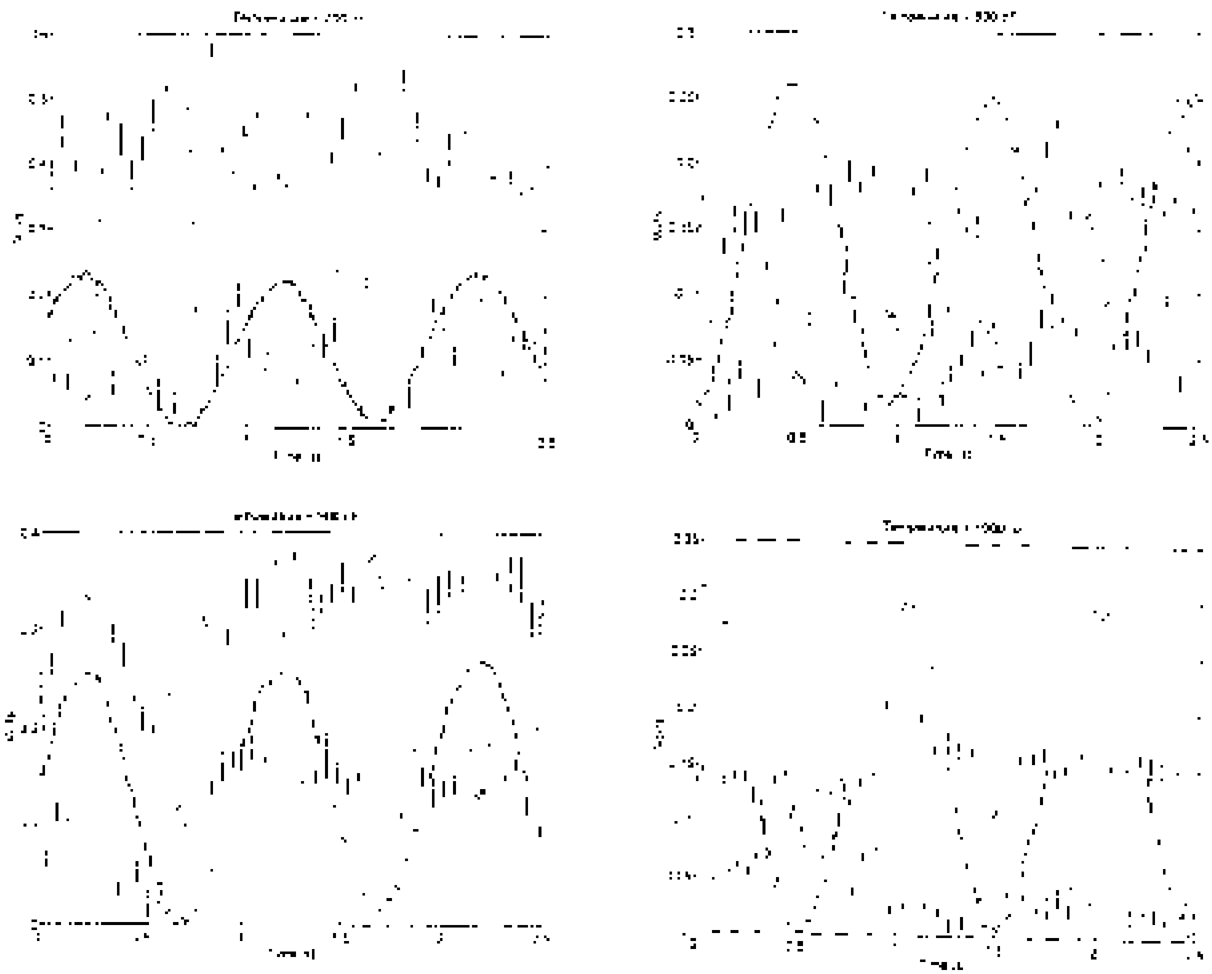

Figure 3-15 Data Acquired at 100°F Temperature Intervals After Reheating

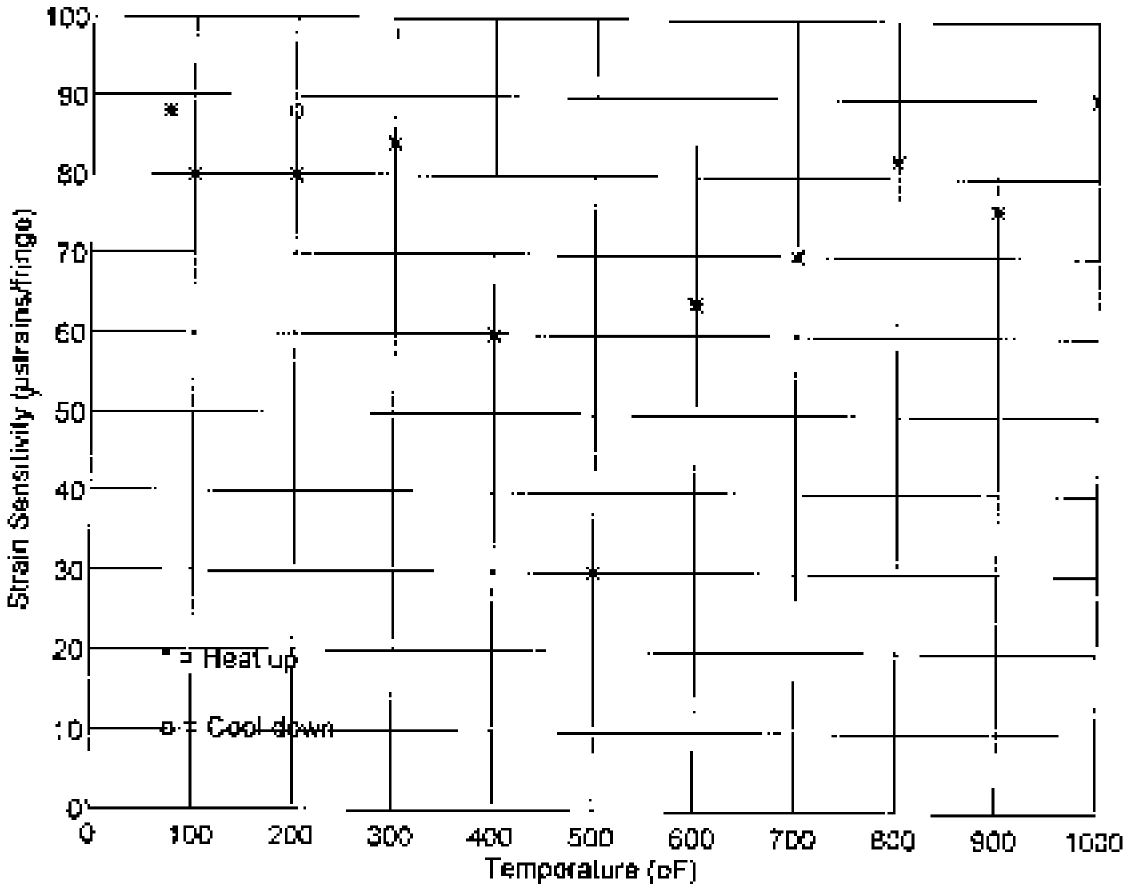

Figure 3-16 Strain Sensitivity of Gage at Various Temperatures

High-Temperature Adhesive

Using high-temperature adhesives to bond gages to the metal shim looked like a short term solution. In order to identify a suitable adhesive to attach the fibers to the metal shim, three different high-temperature adhesives (Duralco 4700, Sauereisen #8, and Aremco 571) were used in the testing. Of the three, Sauereisen #8 and Aremco 571 are ceramic adhesives, and Duralco 4700 is an organic adhesive. Table 3-2 summarizes the properties of each adhesive.

Three small pieces of optical fibers were attached to a steel specimen using the above-mentioned adhesives as shown in Figures 3-17 through 3-19 The specimen was heated up to 600°F (315°C) and allowed to cool down. Only Aremco 571 showed microcracking, as shown in Figure 3-20, and the other two remained intact. Next, the sample was reheated to 1000°F (538°C) and was allowed to cool. Sauereisen #8 started to lift off the specimen while heating up. Duralco 4700 remained unchanged up to 750°F (400°C), then it burned off, which was confirmed by microscope inspection, and the fiber had fallen out as shown in Figure 3-21. Microscope inspection showed the other two ceramic adhesives lifted off the metal surface, but both were very much attached to the optical fiber as shown in Figures 3-22 and 23. The Aremco 571 had fewer microcracks as compared to the Sauereisen #8.

Once again the result was not satisfactory. The only candidate that showed partial promise was Duralco 4700, that too was good only to 750°F (400°C).

Table 3-2
Properties of High-Temperature Adhesives

Property	Duralco 4700	Sauereisen #8	Aremco 571
Maximum service temperature (°F)	750	2600	3200
Coefficient of thermal expansion (/°F x 10^{-6})	36	2.6	7.0
Tensile strength (psi)	11,100	250	Not listed*

*Indicated as poor.

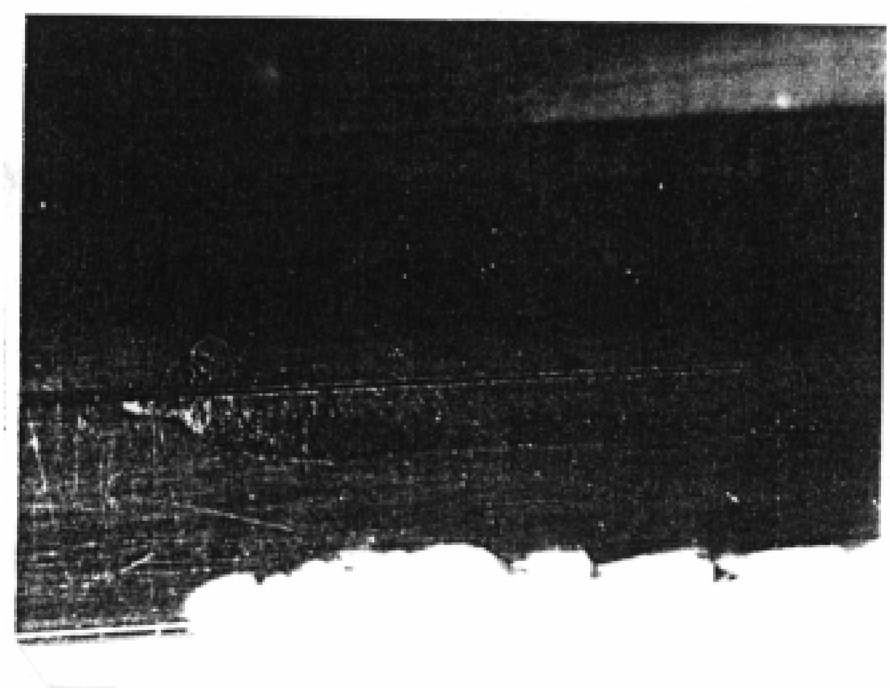

Figure 3-17 Optical Fiber Attached with Duralco 4700

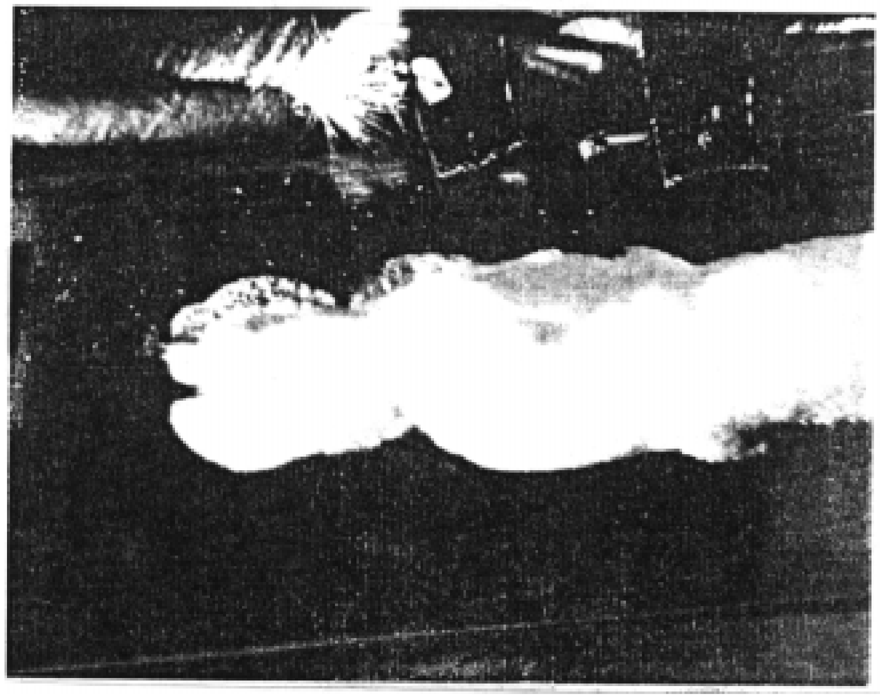

Figure 3-18 Optical Fiber Attached with Sauereisen #8

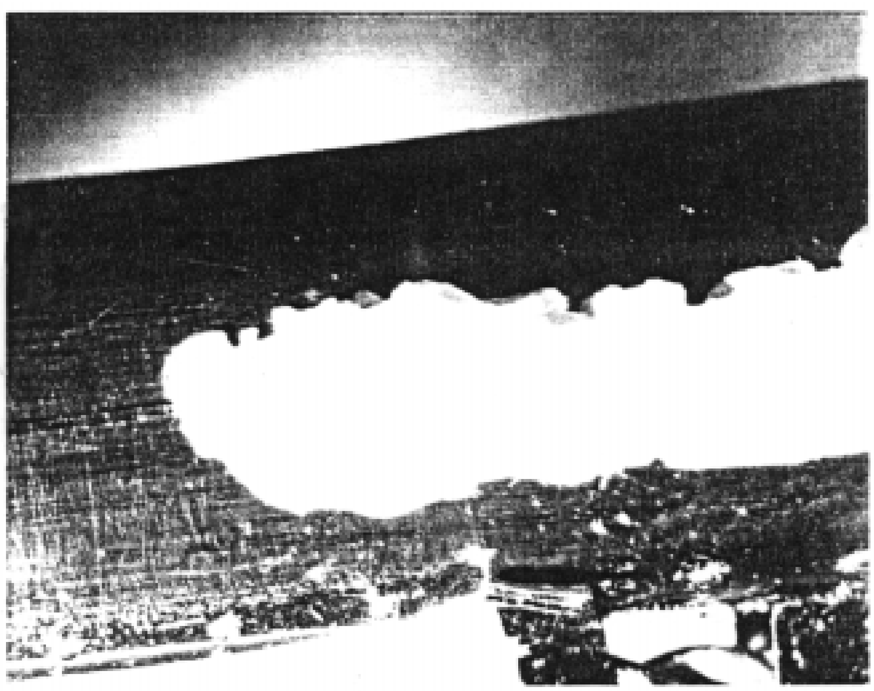

Figure 3-19 Optical Fiber Attached with Aremco 571

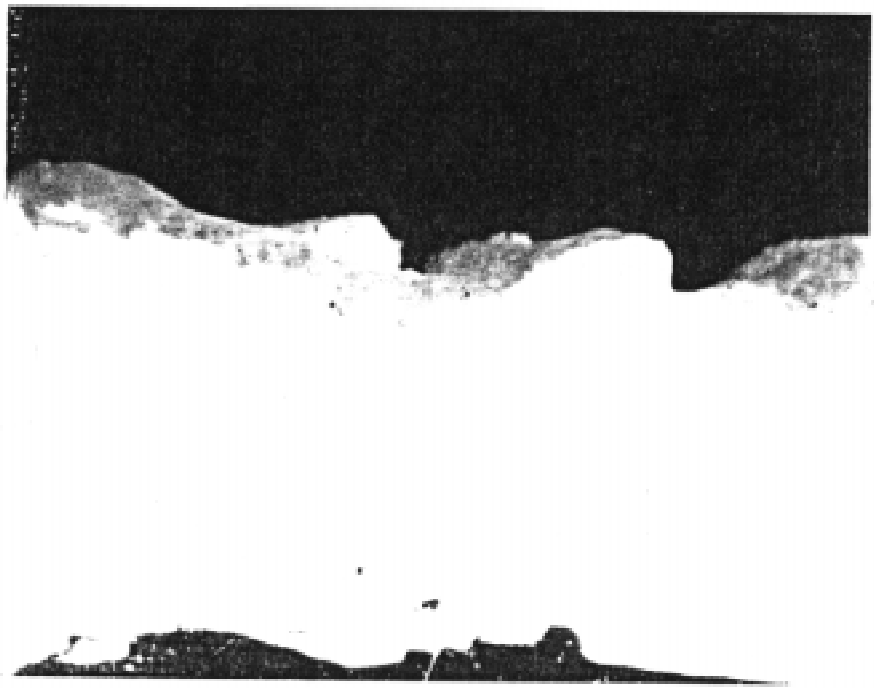

Figure 3-20 Aremco 571 after Heating to 600°F, Showed Microcracking

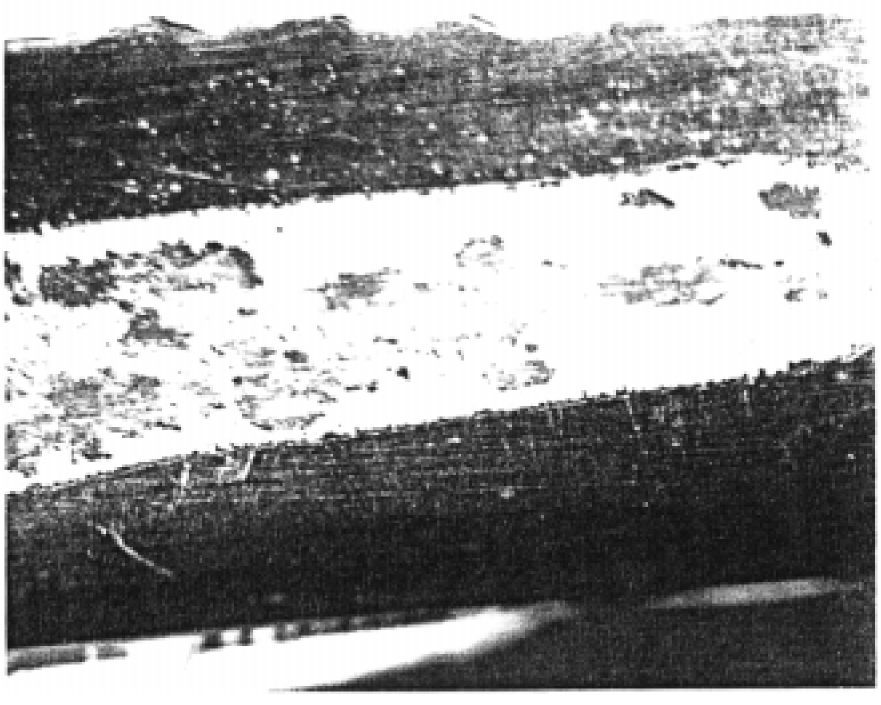

Figure 3-21 Optical Fiber after Duralco 4700 Burned Off

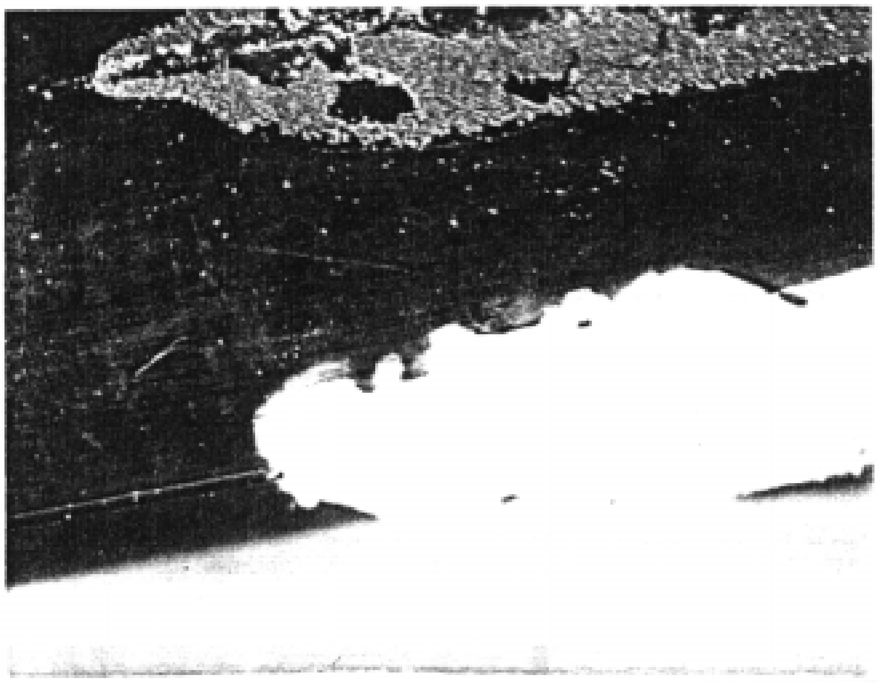

Figure 3-22 The Aremco 571 Ceramic Adhesive After Heating to 1000°F.

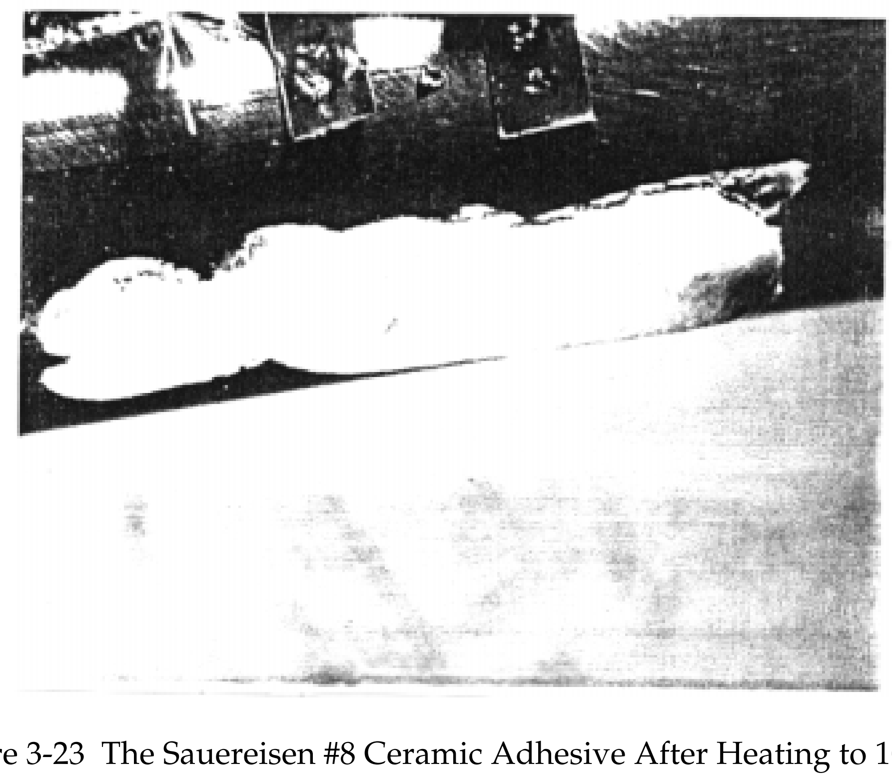

Figure 3-23 The Sauereisen #8 Ceramic Adhesive After Heating to 1000°F.

Metalizing Glass

Metalizing (gold plating) the optical fiber sensor and bracing it to a metal shim was another method that was investigated. Initially a piece of gold coated fiber was spot welded to a metal shim and this package was temperature cycled between room temperature and 1000°F (538°C) three times within a very short period of time. The fiber was still attached to the metal shim and did not show any debonding. This was very encouraging.

Most manufactures are equipped to gold coat the fibers during the fiber drawing process but not after it is manufactured. One of them (Fiberguide) offered to gold coat the sensors and brace them to the metal shim, on an experimental basis. Two Fabry-Perot gages were used in this process. Figure 3-24 shows a photograph of a fiber-optic sensor braced to a metal shim. Only one gage seemed to have a good signal. When the metal shim was heated to 1000°F (538°C) and cooled down it showed fair amount of (2000 με) compressive residual strain. After two or three cycles the gage broke.

This is a technique that has promise in the long term. The main reason for the limited success with this technique is the robustness of the glass gages. Once the glass gage construction method is improved and their robustness increases this technique should work well. The plating methods and the bracing technique also needs development.

Figure 3-24 Metalized fiber-optic strain gage braced to a metal shim

High-Temperature Strain Measurements - Laboratory Testing

The following subsections describe the laboratory testing portion of the project, which involved strain measurements at high temperatures above 600°F (315°C).

High-Temperature Tests

To understand the effects of temperature on unpackaged fiber-optic strain sensor, a noncompensated fiber-optic strain gage (improved version) was placed on a test specimen (not attached), and a J-type thermocouple was attached next to it. The test specimen was placed inside the induction heater coil on the MTS machine, and the temperature was increased from room temperature to 1000°F (538°C). The temperature was held at 1000°F (538°C) for a few seconds before cooling down to room temperature. Data from the thermocouple and the sensor were recorded simultaneously.

During the warm-up time when the induction coil was on, the J-type thermocouple read higher values compared to the K-type thermocouple used for the induction heater controller. This is probably due to the constituent material iron present in the J-type thermocouple. Both thermocouples read the same value during the cool down. Figure 3-25a shows the thermocouple data, with the corresponding sensor data is shown in Figure 3-25b. Data taken during the cool down were used to plot strain versus temperature for the fiber-optic sensor and is illustrated in Figure 3-25c. The solid line in this figure represents the linear fit through the data points. The temperature sensitivity of the strain gage is only 0.11 $\mu\varepsilon$/°F. This may be mostly due to the thermal expansion coefficient mismatch between the glass tube and the optical fiber used in the gage construction. It is a very small amount and can be compensated for in any measurements. As shown in the data plots, the fiber-optic sensor had no problem operating up to the target temperature of 1000°F (538°C). The temperature sensitivity of the fiber-optic strain gage is very small (0.11 $\mu\varepsilon$/°F).

As expected the fiber-optic sensors can easily operate at 1000°F (538°C), however the major hurdle is the attachment method to sense strain. The thermal strain on steel pipes at 1000°F (538°C)is of the order of 6000 $\mu\varepsilon$. This requires the range of the fiber-optic strain sensors to be 0 to 10,000 $\mu\varepsilon$. The current gages have a maximum range of $\pm$ 3000 $\mu\varepsilon$ which means a total measurement range of 0 to 6000 $\mu\varepsilon$ is possible, by making the gages with its signal peak placed at the extreme left (corresponding to 0 $\mu\varepsilon$). However the difficulty is when the gages are attached to a metal with an adhesive it sees a residual compressive strain anywhere from 100 to 2000 $\mu\varepsilon$. This means the peak of the optical signal has to set at the center so that the final gage can see the full range. This is only a short term problem. The gages were improved to $\pm$ 5000 $\mu\varepsilon$ later in the program.

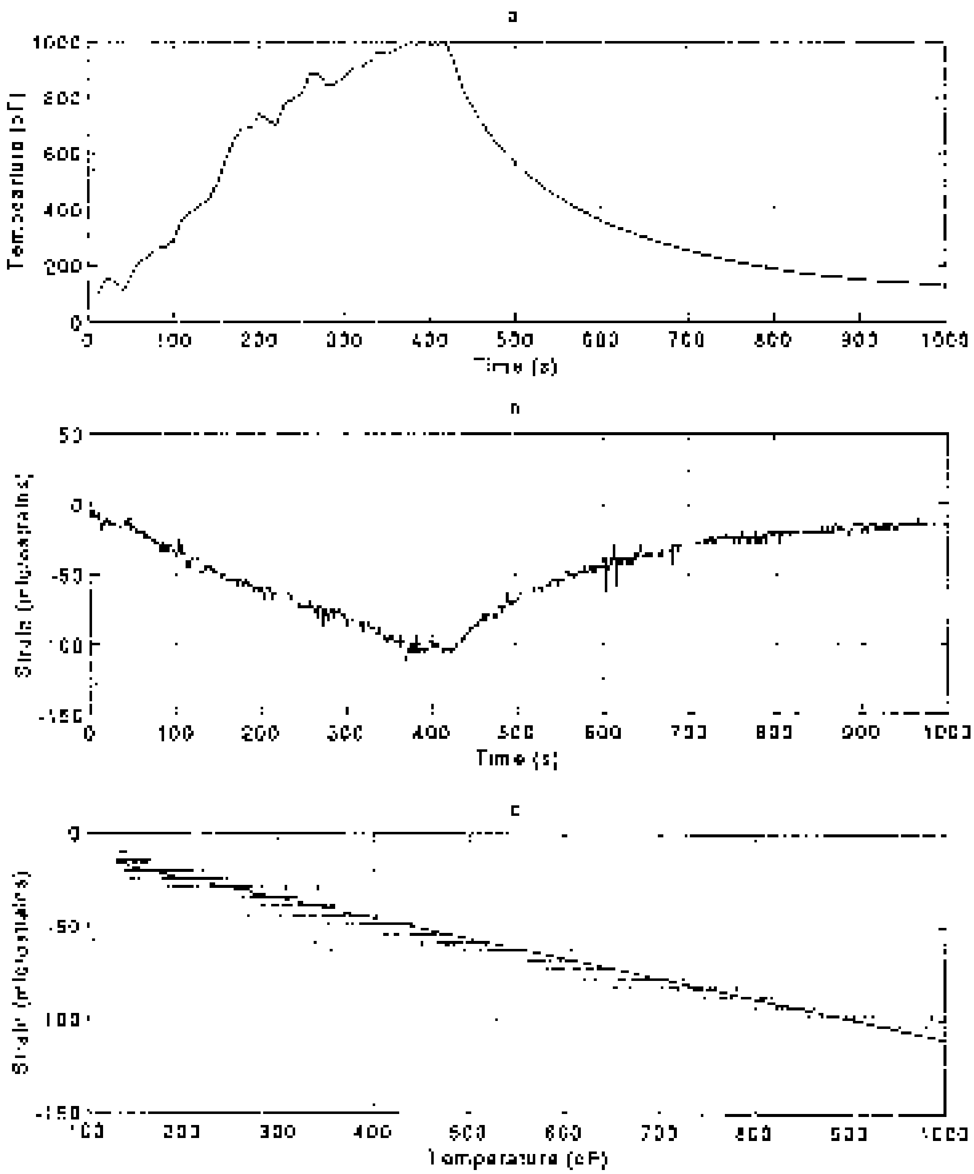

Figure 3-25 Thermocouple and Sensor Readings
a) J-type Thermocouple Reading b) Corresponding Fiber-Optic Strain Sensor Readings c) Plot of Strain versus Temperature during Cool down

High-Temperature Strain Measurements

Cotronics cement is the only candidate bonding agent identified thus far that could be used for strain gages applications above 600°F (315°C). The next step was to study the strain transfer characteristics of this adhesive and also the behavior of the strain gages when constrained. A fiber-optic strain gage was attached to a test specimen with the Cotronics cement. Sensor calibration was performed on a test specimen made out of

INVAR. This specimen material was chosen so that the thermal strain at the maximum temperature did not exceed the measurement range of the current strain gages. A fiber-optic strain gage (±3000 $\mu\varepsilon$) was mounted on a tension specimen using the Cotronics cement (rated for 650°F [345°C] for long term). Figure 3-26 shows a photograph of the specimen set up on an MTS machine. The high-temperature, 0.5-in (1.27 cm) gage length extensometer was placed at the same location as the fiber-optic strain gage but on the opposite side of the specimen.

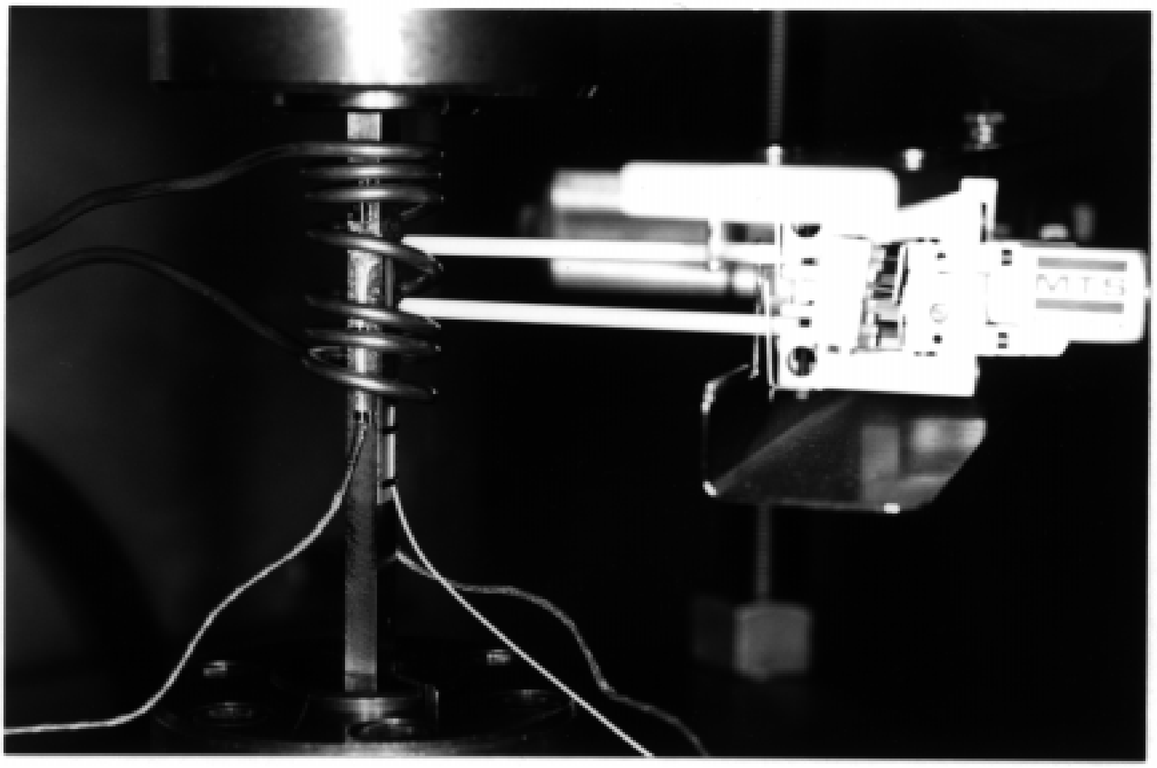

Figure 3-26 High Temperature Strain Measurement Setup

The extensometer was calibrated and zeroed prior to installation. The fiber-optic sensor was also zeroed prior to data acquisition. The test specimen was subjected to a 1-Hz cyclic strain at room temperature (75°F) [24°C], and the corresponding data from the extensometer, and the strain gage were acquired simultaneously. Figure 3-27a indicates the strain values measured using the two strain gages. The fiber-optic sensor output needed to be calibrated (error in actual gage length). Figure 3-27b shows the calibration plot, and the linear fit through the data points is represented by

$$fb = (0.23) \times ex - 0.09 \qquad (1)$$

where fb and ex correspond to the fiber-optic sensor data and the extensometer data, respectively.

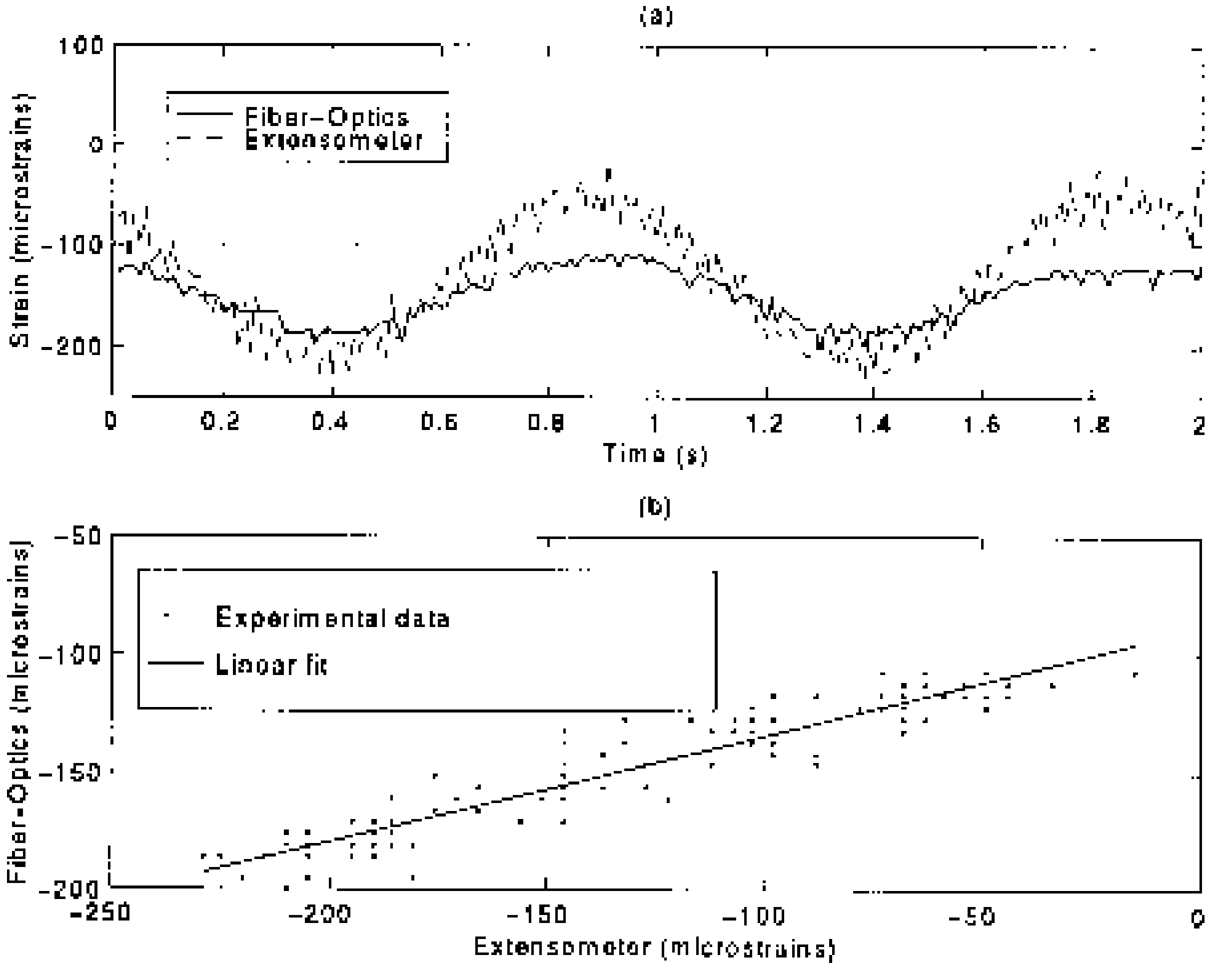

Figure 3-27 a) Strain Values Measured Using the Fiber-Optic Strain Gage and the Extensometer b) The calibration plot

The specimen temperature was raised to 550°F (290°C) over a 200-second time interval, and a cyclic load was applied. The specimen was then allowed to cool down to near room temperature, and the cyclic load was applied. Figures 3-28 a and b indicates the temperature reading from the thermocouple and the corresponding extensometer and fiber-optic sensor output, respectively, when the temperature of the specimen was raised from near room temperature to 550°F (290°C) . Here again, the J-type thermocouple read about 100°F more when the induction heater was on, compared to the reference K-type thermocouple. This is probably due to excess voltage induced by the induction heater. Although the temperature reading shown in Figure 3-28a is from 200 to 700°F (95°C to 370°C), the actual temperature reading from the K-type thermocouple was from 100 to 550°F (38 to 290°C). The calibration during the warm up and cool down process are fb = (0.33) X ex - 0.08 (2)

fb = (0.27) X ex + 0.06

The slope of these calibrations are more than the previous value. One explanation for this discrepancy is that the tension specimen was twisting within the set up during mechanical straining. The calibrations obtained during the cyclic loading at 550°F (290°C) and 133°F (56°C) (after cool down) are

fb = (0.22) X ex + 0.03 (3)

fb = (0.21) X ex - 0.06

respectively. The values are in good agreement with the previous cyclic loading value.

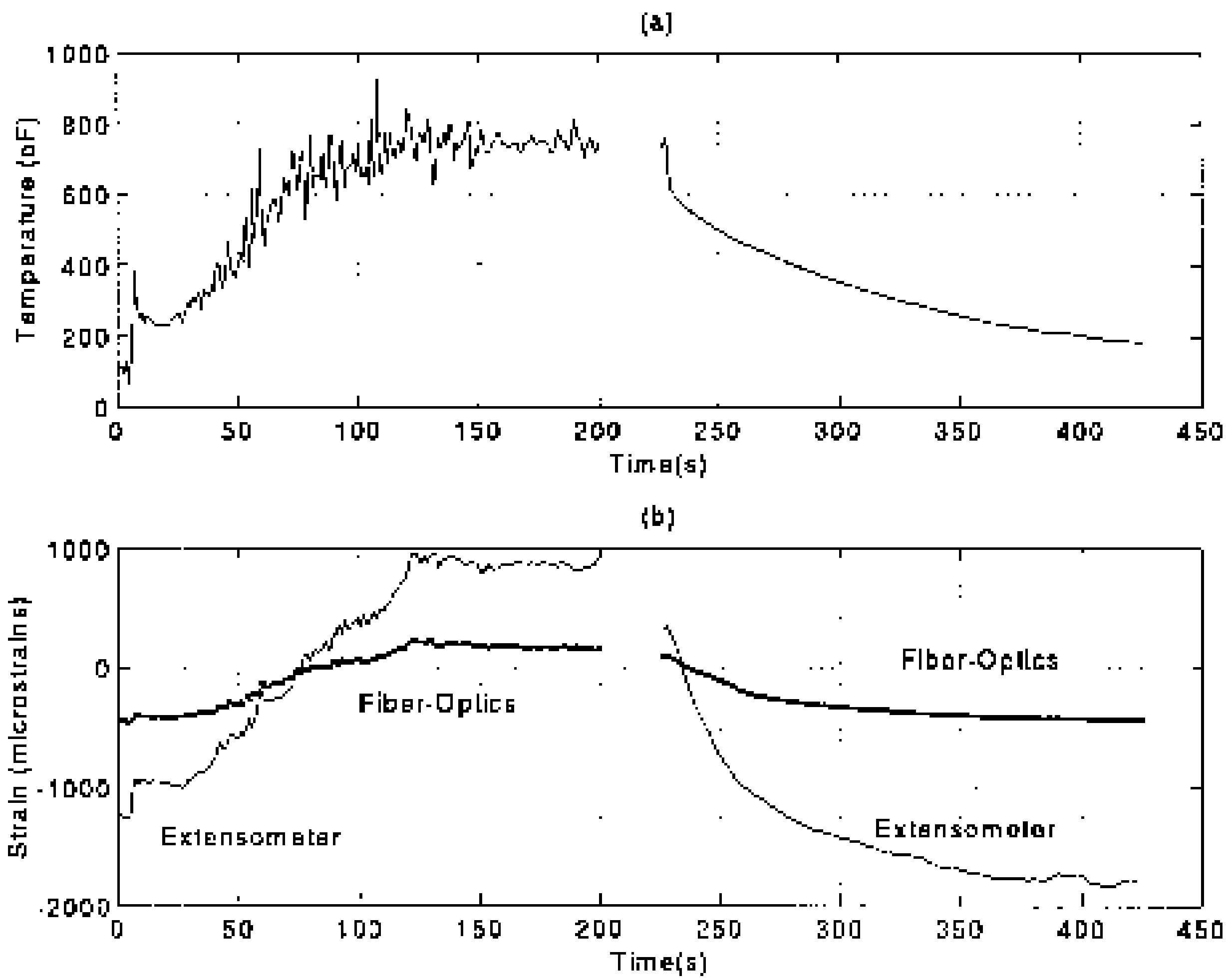

Figure 3-28 a) Thermocouple Reading b) Fiber-Optic Sensor and Extensometer Readings

Strain Measurement at Temperatures above 650°F (345°C): A Ceramic Coat Bonding Agent

A fourth adhesive, Sermetel 588 (by Sermatech), which has metal oxides mixed into a ceramic slurry, was tried. As before, a piece of fiber was attached to a metal using Sermetel 588. After air curing the adhesive, it was oven cured at 150°F (66°C) for 30 minutes and then cured again at 600°F (315°C). The sample was heated up to 1000°F (538°C) and was allowed to cool down. Microscope inspection of the sample showed no adhesive cracking or debonding.

Based on the above results, Sermetel 588 was chosen to bond the sensor to a test specimen to make strain measurements at high temperatures. Initially, a ±3000 με fiber-optic strain gage was attached to a test specimen using Sermetel 588. After the initial cure at 150°F (66°C), the test specimen was placed in the high-temperature test rig. The specimen was heated up to 600°F (315°C), and the adhesive was allowed to cure for 30 minutes. Once the adhesive was fully cured, the specimen was allowed to cool down. The sensor showed a 2000 με compressive strain after cure, which provided a larger measurement range for the fiber-optic sensor.

A ±3000 με fiber-optic strain gage was attached to a steel specimen using Sermetel 588 and tested up to 1000°F (538°C). The sensor survived the temperature and the attachment cement did not show any cracking or debonding. As mentioned earlier, this cement is the ideal candidate for strain gage packaging. However, more testing is needed to fully characterize the physical properties of the ceramic coat. Figure 3-29 shows the thermal strain sensed by the high-temperature extensometer and the strain gage. The sensor data matches the extensometer reading at higher temperatures (400 to 1000°F) (205-538°C), but shows deviation at lower values (less than 200°F [93°C]). Since the gage range was not sufficient to measure the total strain, the fiber-optic sensor saturated off around 4200 με. The 4200 με was achievable because the gage showed a substantial amount of residual strain during the curing stage of the ceramic coat.

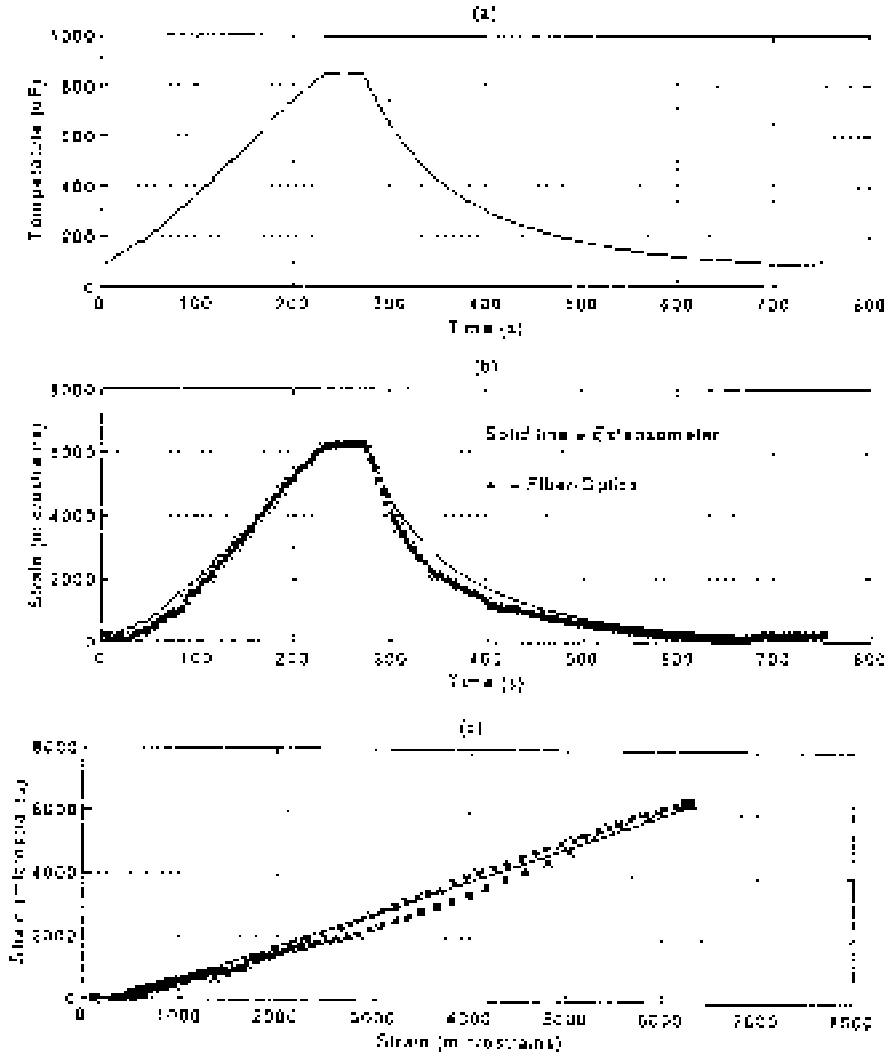

Figure 3-29 Thermal strain sensed by the extensometer and the fiber-optic strain gage (attached with Sermetel 588)

High-Temperature Strain Measurements - Host Utility Testing

Two fiber-optic strain gages packaged for high-temperature testing were installed on a main steam line at TVA's Kingston Power Plant. The main purpose of this testing was to study the feasibility of installing these sensors in a power plant application. It also provided information regarding the long-term durability of these sensors in a power plant environment.

With the help of TVA and EPRI Instrumentation and Control (I&C) Center staff, the main steam line on Kingston Unit 5 was identified as the component for sensor installation. Two application tasks for this installation were identified: 1) strain measurement on the main steam line, and 2) temperature measurement inside a thermowell on a cold reheat line. Specifications for the steam line pipe are as follows:

- Outer pipe diameter: 17 in. (43 cm)
- Inner pipe diameter: 12 in. (30 cm)
- Pipe wall thickness: 2.5 in. (6 cm)
- Operating temperature: 1050°F. (566°C)
- Operating pressure: 1830 lb/in.
- Material: Steel Alloy A155-52T PQ I 2.25% Cr 7 1% Mo.

Two spot-weldable strain gages were constructed in the laboratory. Figure 3-30 illustrates the gage bonded to a stainless steel shim with the ceramic coat. These gages were calibrated in the laboratory by placing them in an oven. Figure 3-31 shows the calibration curve for one of the gages and the nonlinear response. One reason for this behavior could be the thermal expansion characteristics of the ceramic coat used to adhere the gages to the metal shim. The manufacturer's data sheet indicated that the mean thermal expansion coefficient for this ceramic coat is 5×10^{-6} and 8.7×10^{-6} for the first cycle and temperature exposure for the second cycle. The thermal expansion versus temperature plot from the manufacturer's data sheet is shown in Figure 3-32. As this plot indicates, the heating and cooling are not the same. Further, thermal expansion below 200°F is very nonlinear, but, from 200 to 1000°F (95 to 538°C), is very linear. This could partly explain the nonlinearity in the gage calibration under 200°F (95°C) and the hysteresis. Further work is needed to characterize the ceramic coat.

In December 1994, the two gages were spot welded on the main steam line in the longitudinal direction. During this period, the insulation of the steam pipes was being replaced, and this short window was the opportunity to install the gages. Figure 3-33 illustrates a gage after attachment to the pipe, and Figure 3-34 illustrates a protective cover placed over the gages. The lead-in section of the fiber had a stainless-steel tubing around it. As shown in the photographs, the tube was bent to bring the fibers out of the insulation area. Once the gages were installed, the pipe was covered with 10 in. (25.4 cm) of insulation. The optical fibers (terminated with ST-type couplers) were tied to a support bar close to this location. Two fiber-optic extension cables (roughly 50-ft [15 m] long) were used to connect the gages to the sensor demodulator. This arrangement is illustrated in Figures 3-35 and 3-36.

The two gages were nulled prior to their installation on the steam line. A small amount of residual strain was noticed after the spot welding. The sensors were left in place for about two to three weeks, until the unit was started.

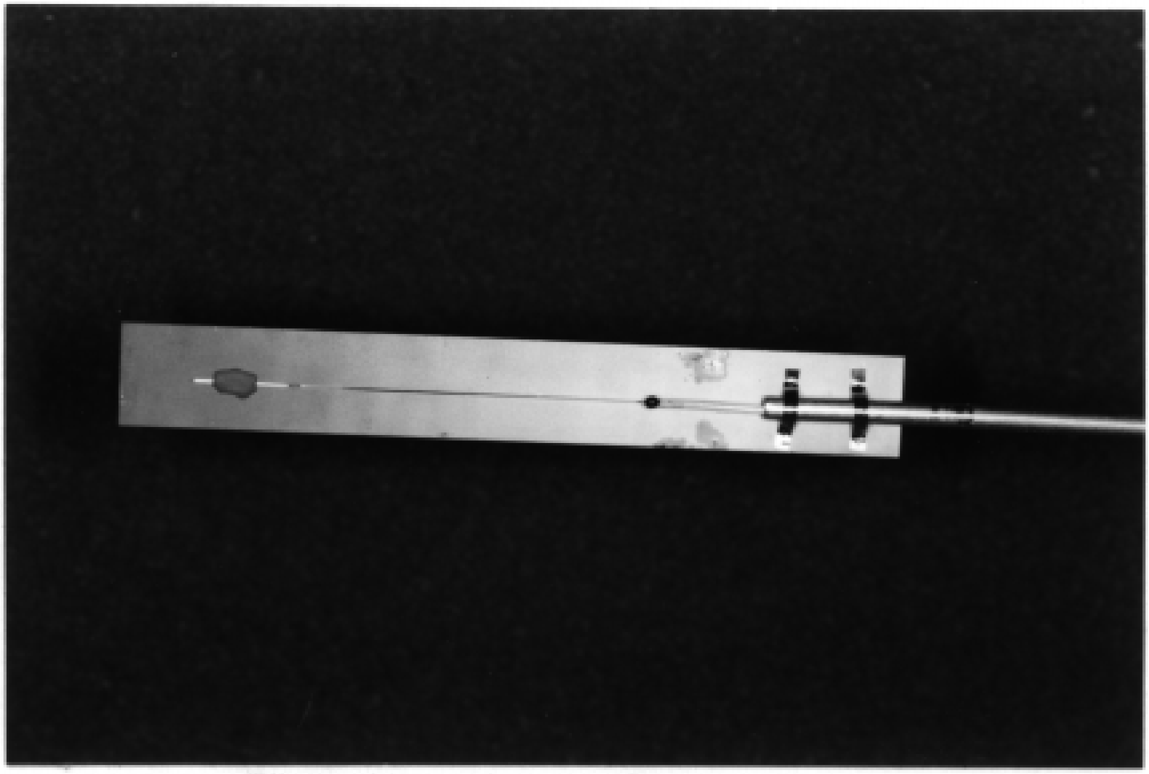

Figure 3-30 Gage Bonded to Stainless Steel Shim with Sermetel 588 (ceramic coat).

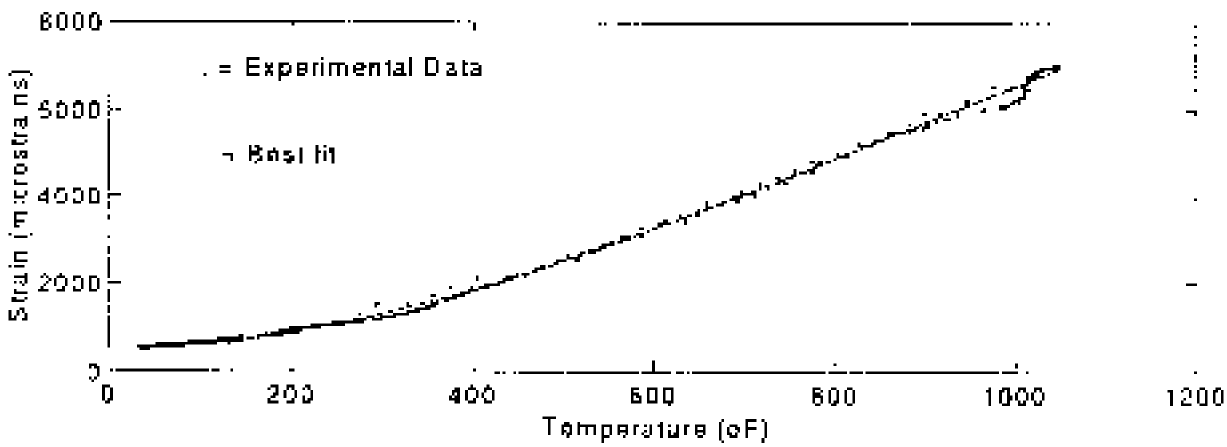

Figure 3-31 Calibration Curve for the High-Temperature Gage
(attached with Sermetel 588)

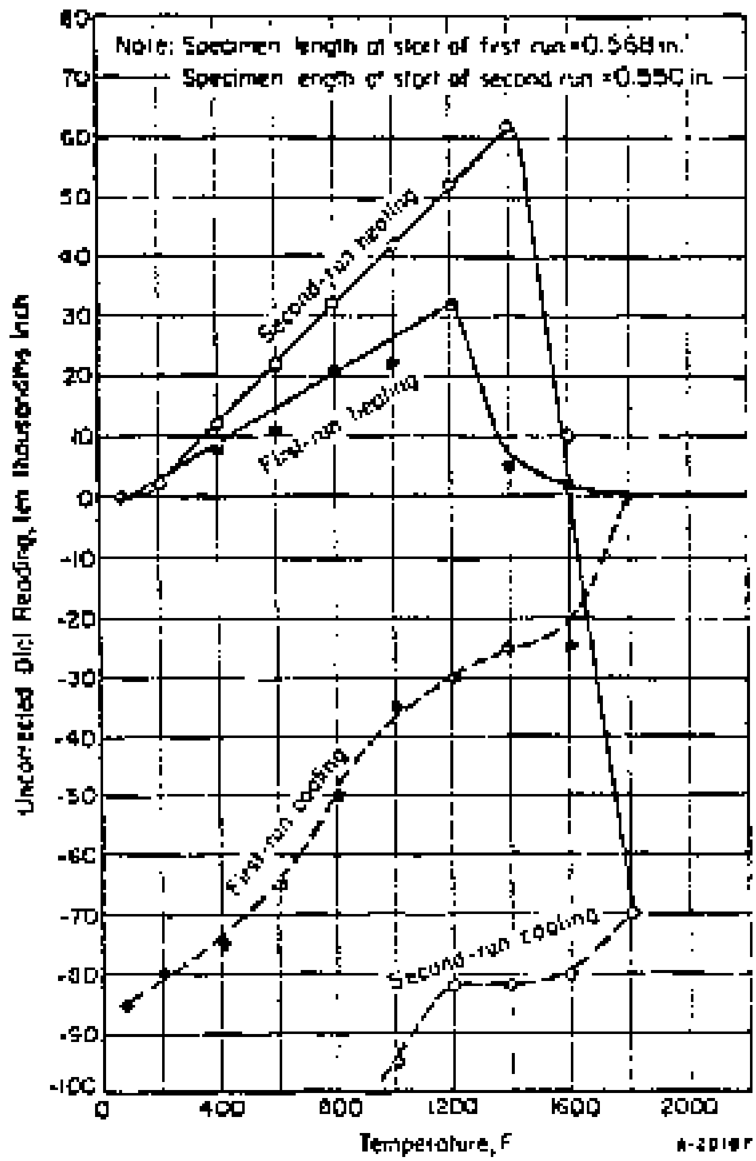

THERMAL EXPANSION OF P-1 CEMENT

Mean Thermal Expansion

First Cycle:

70 - 1200°F.......... 5.0 x 10^{-6} in./in./°F

1200 - 1800°F.......... Shrinkage

1800 - 70°F............ 8.5 x 10^{-6}

Second Cycle:

70 - 1400 °F.........6.7 x 10^{-6}

1400 - 1800°F ....Shrinkage

1800 - 70°F........... 7.8 x 10^{-6}

Figure 3-32 Thermal Expansion versus Temperature Plot for Sermetel 588 (manufacture's data).

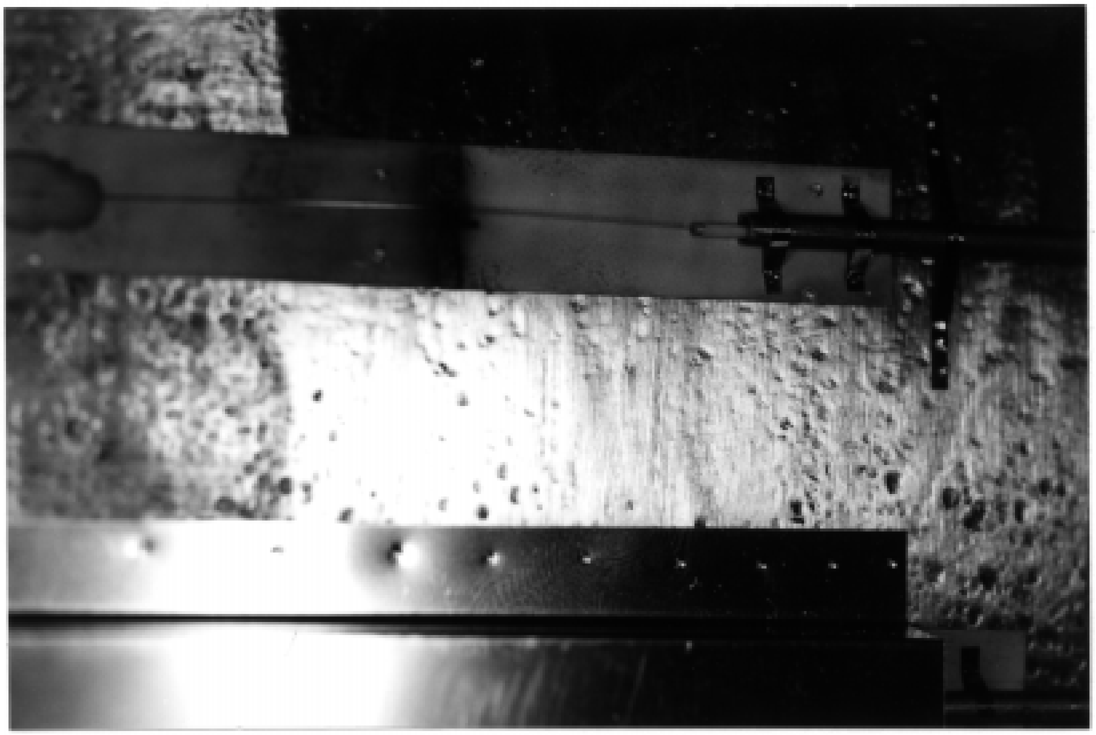

Figure 3-33 Fiber-Optic Strain Gage after Attachment to Steam Pipe

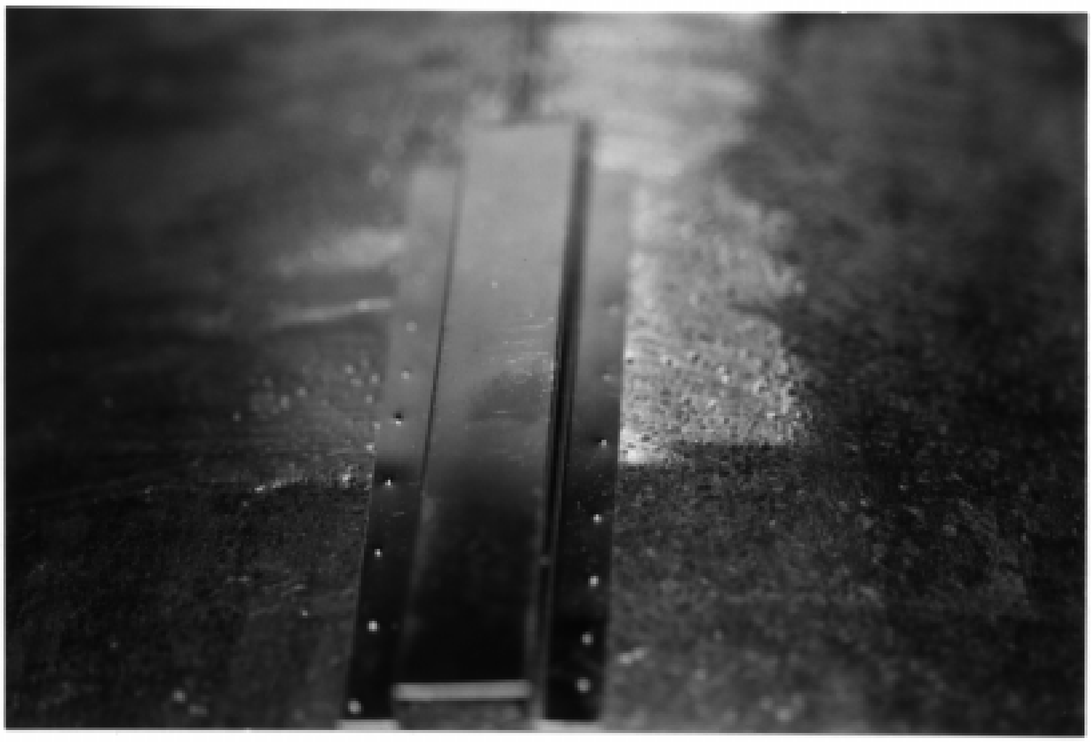

Figure 3-34 Protective Cover Placed over Gages

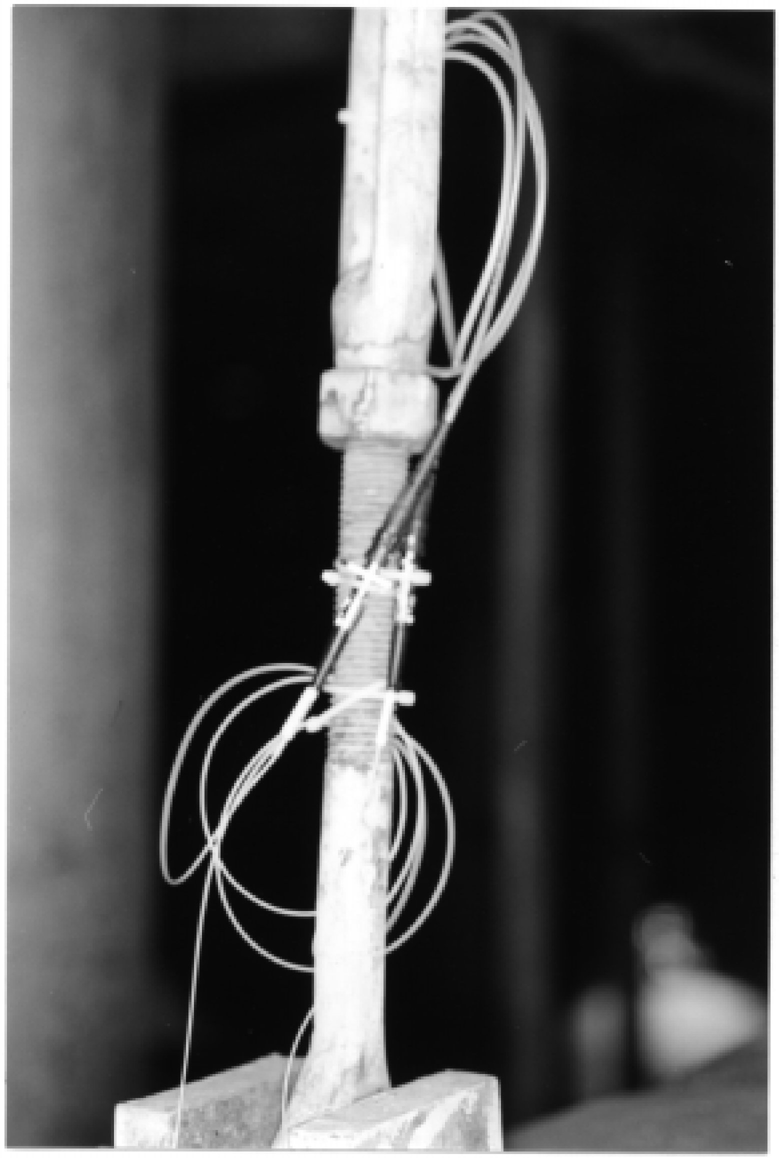

Figure 3-35 Fiber-Optic Extension Cables Connecting Gages to Sensor Demodulator: View 1

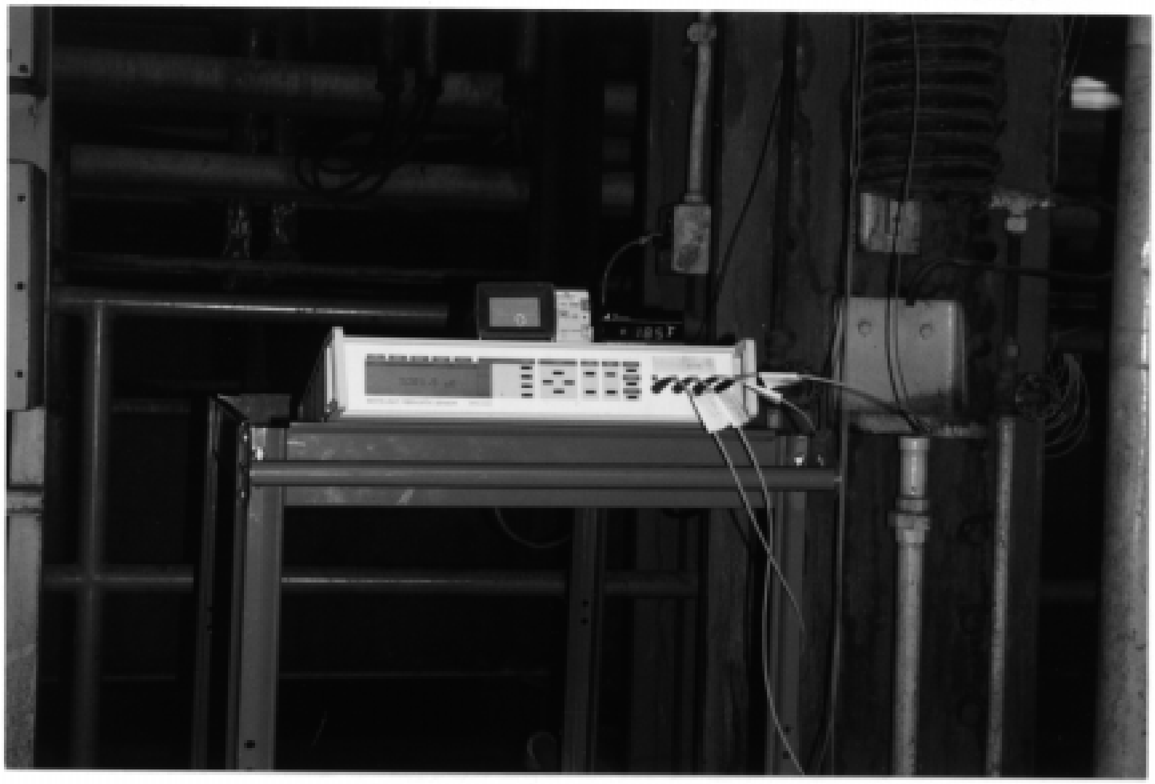

Figure 3-36 Fiber-Optic Extension Cables Connecting Gages to Sensor Demodulator: View 2

Transient Data

On January 6th, 1995, the unit was started, and data acquisition began just after midnight. Steam was passed slowly through the pipes, and the system was allowed to warm up. Data was gathered from the two gages during this period. The two gages were initially shifted by about 200 με, and the reason for this is not known. However, prior to data acquisition, the two gages were nulled. Data were gathered until the turbine was rolled and power generated at full load. More data were gathered beyond this during steady state for another 2 to 3 hours.

A thermocouple reading from the thermowell sensors is the only reference information available. This information was received from two locations: the control room and the diagnostic center.

The fiber-optic strain gages were mounted in the axial direction on the steam pipe. Thus it is reasonable to assume that most of the strain seen by the gages was due to thermal expansion. Using the calibration value obtained during the laboratory calibration for the stainless steel shim, the fiber-optic strain value was converted to temperature value. This conversion is shown in Figure 3-37. It is evident from Figure 3-

37 that the fiber-optic sensor data lags the estimated strain data during the initial warm-up period and slowly catches up to the final steady-state value at about 1000°F (538°C). By the time the generator was producing maximum load, the fiber-optic sensor data matched well with the data estimated from the power plant temperature sensors. The initial lag for the fiber-optic data is probably due to the fact that these gages were mounted on the outer surface of the steam pipe and it took a while for the metal to heat up to the equilibrium temperature. Where as the temperature sensors were in the steam path and were meauring the steam temperature directly.

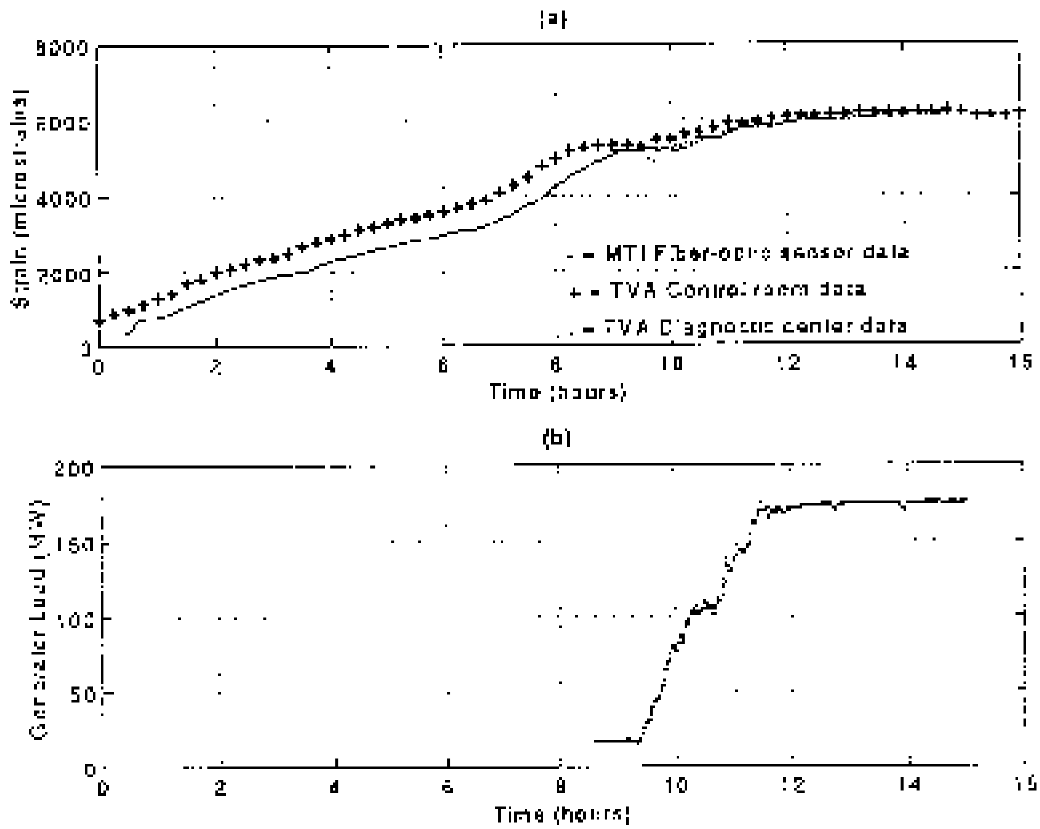

Figure 3-37 Host utility test data.
a) Strain data from the fiber-optic sensor and the corresponding values from the temperature sensor b) The generator load data during the same time period.

Long-Term Data

The gages were left on the main steam line for about two months. On March 6, 1995, the gages were connected back to the instrumentation for data acquisition. Unfortunately, the gages were not working. All connections were checked. One noticeable mistake was made in tying the lead-in fiber cables with the ST connectors to the support wire that also became very hot after the pipes became hot. Typically, the connectors are rated for only 150°F (66°C). However, this was not the problem, since once the connectors were removed and the gages were butt coupled to the sensor unit, there was still no signal. It was determined that the gages had failed. Since they were buried under 10 in. (25 cm) of insulation, there was no way to inspect them.

Discussion of Results

The metal arc spray method seemed to work well with the bare fibers. However, the Fabry-Perot gages did not survive this process. With improvements to the Fabry-Perot gage construction, the method should work. Sermetel 588, a ceramic coat, seems to be a good candidate for high-temperature attachment and was therefore selected as the candidate to attach the fiber-optic sensors. However, in the long run, the metal arc spray method needs to be studied for encapsulating gages because it can survive much higher temperatures. Also, Sermetel 588 has nonlinear thermal properties and unusual thermal expansion behavior beyond 1200°F (650°C).

The gages performed very well up to the operating temperature of the steam pipe (1050°F [566°C]). However, they did not survive the long-term testing, and the reason for this is not known. A lack of funding under this project prevented further work, but a similar task was performed under EPRI project WO3462-01. In this project, the thermal expansion of a stainless steel rod was used to measure temperature and the gages survived the long-term testing. However, the temperature of this test was only 650°F (345°C). Although it is not the same environment, it did prove that the gages have the potential to survive long term at high temperatures. In order to derive more conclusive results, further testing is needed to characterize the gages.

4

DISTRIBUTED SENSING EVALUATION

Along with the high-temperature application evaluation, the feasibility of multiplexing white-light Fabry-Perot sensors was also studied during this project. In practice many gages are needed to estimate the health of the structure. Having the capability to multiplex several gages using commercially available fiber-optic multiplexers (or switches) is very important in lowering the over all system cost.

As shown in Figure 4-1, fiber-optic sensors can be multiplexed in series or in parallel to obtain information from several sensing locations. Both methods have their merits and limitations. Series multiplexing may appear attractive because it uses only one optical fiber to carry information to and from the sensors. However, if one gage fails, the sensors beyond this point will not provide information. On the other hand, if the sensors are multiplexed in parallel, all gages except the failed one would provide information. The trade-off for parallel multiplexing is that every sensor needs a lead-in optical fiber to transport information to the electrooptics. For the high-temperature application of interest here, this requires that the lead-in fibers be ruggedized to survive the environment. Therefore, the optical fibers have to be placed inside an armed cable. In general, several (20 to 30) optical fibers can be placed inside one of these cables. For this reason, the size of the cable does not change whether a single optical fiber for a lead-in cable (series multiplexing) or 20 fibers (parallel multiplexing) are used.

The sensing type selected for this application allowed parallel multiplexing to be implemented with ease. In order to prove the concept of measuring strain at multiple locations, a commercial 1 X 2 fiber-optic switch (DiCon Fiber Optics Inc.) was selected. This component was an off-the-shelf multimode fiber-optic switch used in the communications industry.

The experimental arrangement used to evaluate sensor multiplexing is shown in Figure 4-2. A fiber-optic strain gage was attached to a test specimen placed inside an induction heater coil so that the specimen would experience thermal strain as the specimen was heated. As shown in the figure, an extensometer was placed next to the strain gage. A second fiber-optic strain gage was mounted on a cantilever beam along with an electrical strain gage. The two fiber-optic strain gages were connected to the 1 X 2 fiber-optic switch, which was connected to the white-light interferometer. LabView software was used to drive the switch and, at the same time, acquire data. The fiber-optic switch was operated at 2 Hz, and the scan rate for the data acquisition was also set at 2 Hz.

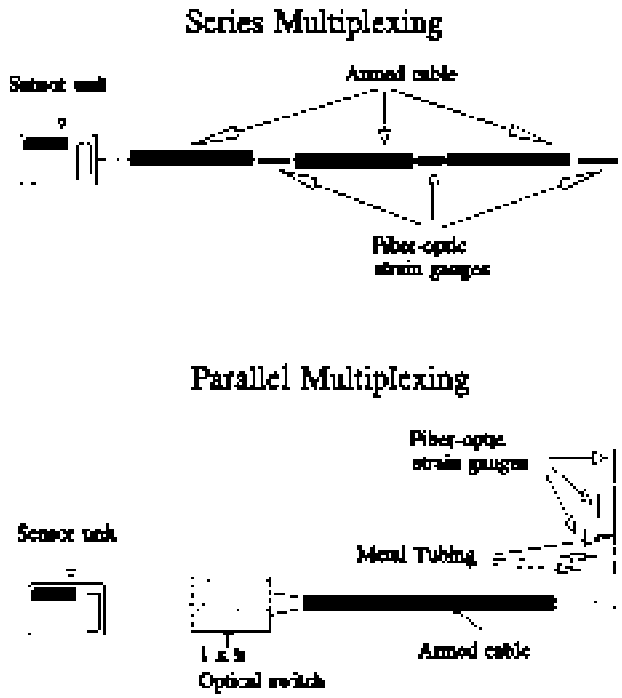

Figure 4-1 Schematic of fiber-optic sensor multiplexing schemes

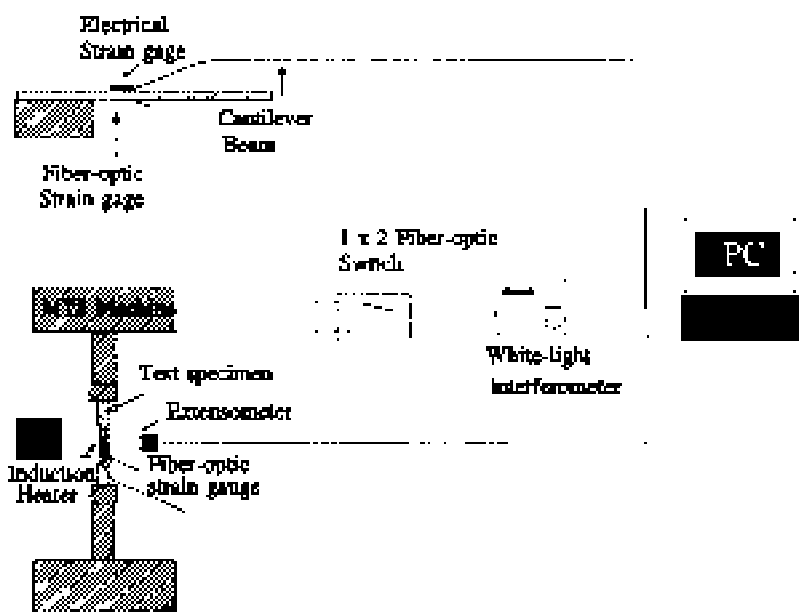

Figure 4-2 Experimental setup for sensor multuplexing

The first strain gage measured thermal strain as the specimen was heated to 100°F (38°C) and allowed to cool down. The second gage measured the mechanical strain of the cantilever beam subjected to arbitrary strain. The electrical strain gage and the extensometer measured the mechanical strain of the cantilever beam and the thermal strain of the test specimen, respectively.

Figure 4-3 shows the front panel of the data acquisition system. The output data from the extensometer, electrical strain gage, and the fiber-optic strain gages are represented by a solid line, a solid line with plus (+) symbols, and circles, respectively. During data acquisition, the optical switch toggled between the two fiber-optic gages.

As shown in Figure 4-3, data from the fiber-optic matched well with data from the electrical strain gage. In addition, the fiber-optic gage measurement of thermal strain showed a higher value than the extensometer. The reason for this discrepancy is that the two fiber-optic strain gages used in the experiment were not identical and had different gage lengths. The sensor unit would allow only one gage length to be inserted at a given time. Therefore, the gage factor (or calibration factor) was inserted into the data after the fact.

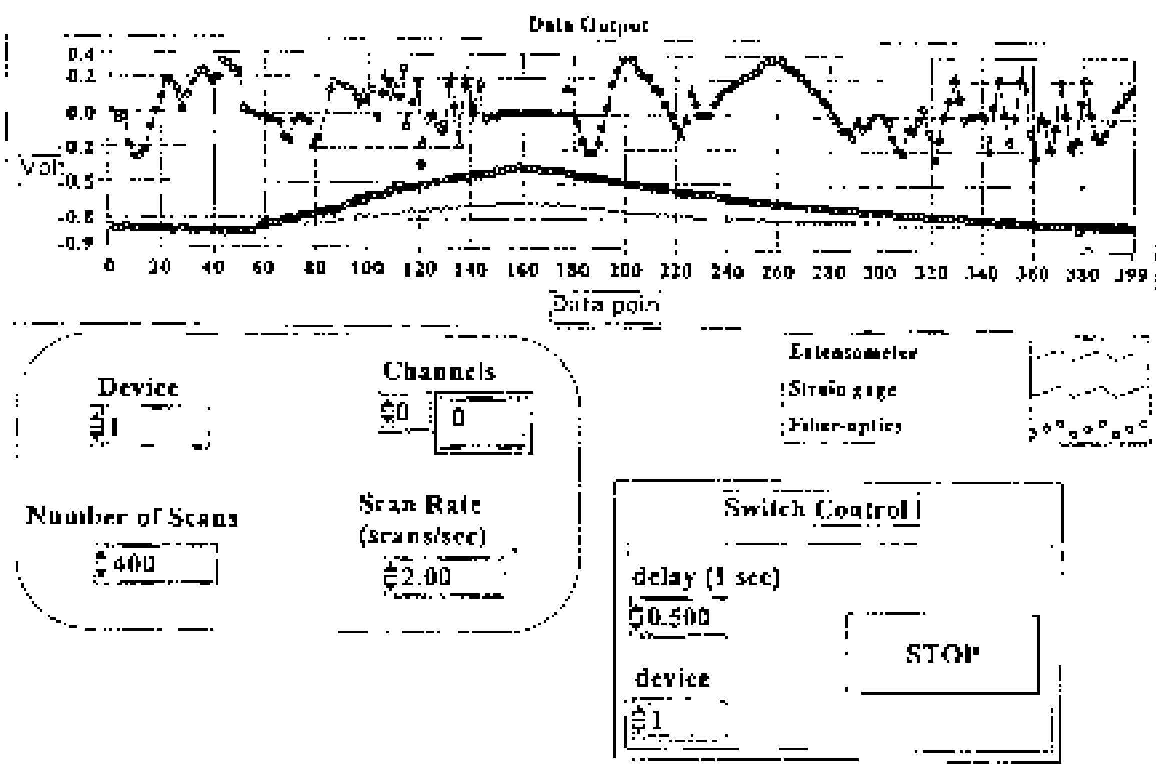

Figure 4-3 Front Panel of Data Acquisiiton System

Figure 4-4 illustrates the cumulative signal and the separated signals generated during the experiment. As these plots indicate, the fiber-optic sensor data matches well with the electrical strain gage signal and the extensometer signal. It is also evident in these plots that the fiber-optic sensor occasionally picks up an erroneous data value caused by noise in the system. The noise introduced during switching is one reason that faster switching between the two fiber-optic sensors is not possible.

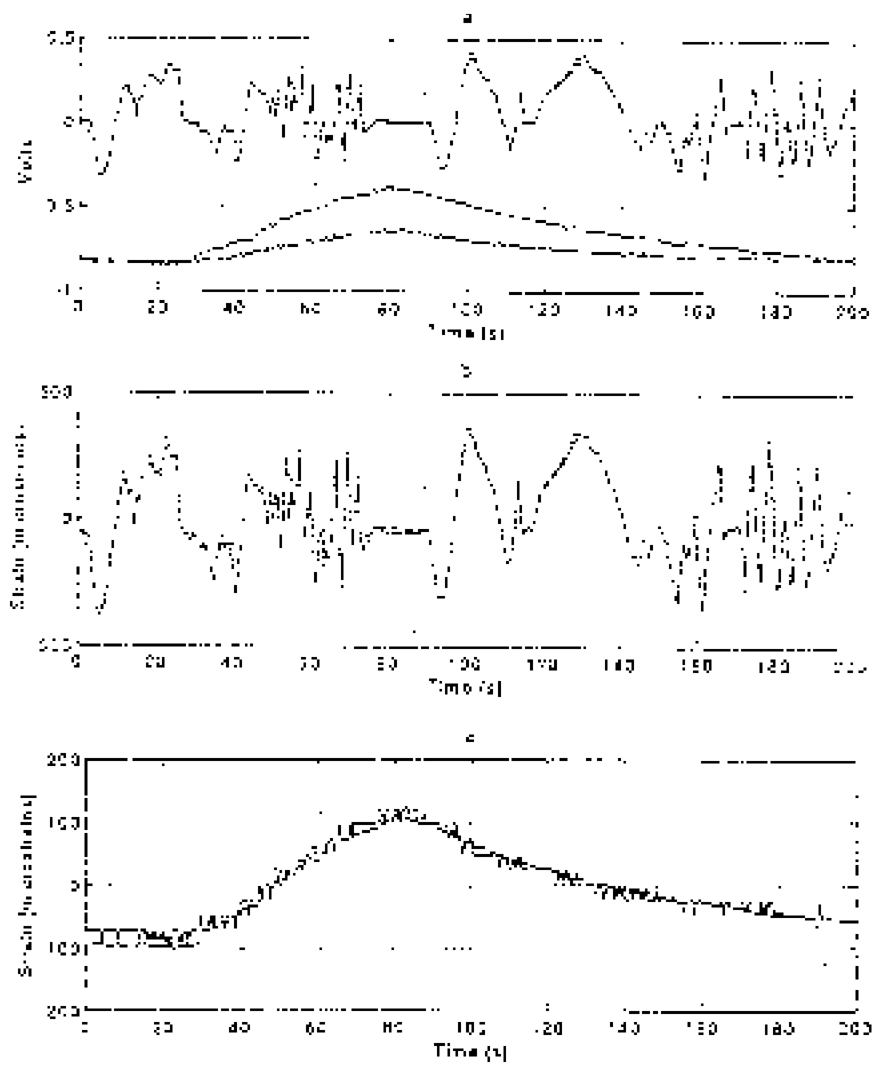

Figure 4-4 Cumulative Signal and Separated Signals
a. Cumulative data from four sensors
b. Processed data for the cantilever beam sensors
c. Processed data for the thermal strain specimen
(dots represent the fiber-optic sensor data)

As this work demonstrates, fiber-optic strain gages can be multiplexed easily using off-the-shelf fiber-optic switches. One of the problems associated with this scheme is the noise introduced by the switch itself. The optical switches mechanically displace to align the two fibers, which is accomplished by a solenoid. To minimize the noise, the device must be operated slowly, which, in this case, was 2 Hz. Therefore, the switches can limit the speed of operation. The other issue is the cost per channel. Typically, a 1 X 2 switch costs $300, a 1 X 3 costs $900, and a 1X 4 costs $2000. Higher channel switches are rather expensive and can significantly increase the price per channel. An alternative scheme to multiplex these sensors is explained below.

Using a 2 X 2 closed-circuit device (CCD) array instead of the 1-D array currently used in the white-light interferometer system would increase the number of input channels. In this case, the optics would be modified to accommodate several sensor inputs and to produce the correlated signals on the 2-D CCD array. The signals can then be processed and separated out to read data from each of the sensors. This approach would provide a passive optical switch which is more desirable for the intended application.

Cumulative Signal and Separated Signals a. Cumulative data from four sensors b. Processed data for the cantilever beam sensors c. Processed data for the thermal strain specimen (dots represent the fiber-optic sensor data)

5

CONCLUSIONS AND RECOMMENDATIONS

The conclusions that can be drawn from the feasibility study are summarized below.

- The work conducted under this project demonstrated that Fabry-Perot fiber-optic strain sensors can withstand temperatures up to 1000°F (538°C). The sensor demodulation based on white-light interferometric technique appears to have the necessary qualities to produce a viable fiber-optic sensor system for long term structural health monitoring. Since the extrinsic Fabry-Perot strain gages are sensitive only to axial strain, the data interpretation is straight-forward. The thermal and mechanical strain on a structure can be seperated. Further, these sensors can be easily attached to structures and can also be multiplexed using off-the-shelf fiber-optic switches.
- At the beginning of the study, the laser-welded joints in the earlier configurations of the extrinsic Fabry-Perot gages failed at higher strains and temperatures. This weakness was overcome when the gage supplier modified the gages with a decoupled configuration, which relieved the strain on the lead-in fiber.
- Gage calibration is an area that needs improvement. Almost all the fiber-optic gages used in the study needed calibration since the gage length supplied by the manufacturer was inaccurate. However, once the calibration is done it does not require any additional field calibration.

To pursue development of these sensors for high-temperature environments, recommendations for future work include:

- Complete characterization of strain gages -
- Long-term testing - The fiber-optic gages have to be subjected longterm testing in the laboratory to estimate fatigue and creep.
- Rossett construction - In most applications the strain needs to be measured in two orthogonal directions. Therefore, fiber-optic strain gages in the form of rossetts (similar to resistive gages) have to be constructed.
- Stress analysis - This program showed the feasiblity of using fiber-optic strain gages at high temperatures. However, no work was performed to utilize these gages to estimate structural stress. The end user is interested using these sensors to estimate structural stresses, creep, fatigue etc. Therefore, further work needs to be done to correlate strain sensor data with theoretical predictions, and incorporate data into programs such as EPRI's Creep Fatigue Pro.

- Multiplexing using a 2-D array - Alternate mutiplexing schemes have to be identified and implemented so that many gages can be read on a single unit. The multiplexing schemes should allow many gages to be read at faster rate (250 to 500 Hz).

6

REFERENCES

1. "*Handbook on Experimental Mechanics*." Society for Experimental Mechanics, Prentice-Hall, Inc., Englewood Cliffs, NJ, 1987.

2. Butter, C. D. and G. B. Hocker. "Fiber-Optics Strain Gauge." *Applied Optics* 17, 1978, pp. 2867-2869.

3. Culshaw, B. and J. Dakin. "*Optical Fiber Sensors: Volumes I and II*." Artec House Inc., Norwood, MA, 1990.

4. Udd, E. "*Fiber-Optic Sensors: An Introduction to Engineers and Scientists*." John Wiley and Sons, NY, 1990.

5. Sirkis, J. S. and H. W. Haslach, Jr. "Interferometric Strain Measurement by Arbitrarily Configured, Surface-Mounted Optical Fibers." *Journal Lightwave Technology*, LT-8, 1990, pp. 1497-1503.

6. Murphy, K. A., M. F. Gunther, A. M. Vengsarkar, and R. O. Claus. "Quadrature Phase Shifted, Extrinsic Fabry-Perot Optical Fiber Sensors." *Optical Letters* 16, 1991, pp. 273-275.

7. Lee, C. E., J. J. Alcoz, Y. Yeh, W. N. Gibler, R. A. Atkins, and H. F. Taylor. "Optical Fiber Fabry-Perot Sensors for Smart Structures." *Smart Materials Structures*, 1992, pp. 123-127.

8. Weiss, J. "Fiber-Optic Strain Gauge." *Journal of Lightwave Technology*, Vol. 7, 1989, pp. 1308-1318.

9. Morey, W. W., J. R. Dunphy, and G. Meltz. "Multiplexing Fiber Bragg Grating Sensors." *Fiber and Integrated Optics*, Vol. 10, 1992, pp. 351-360.

10. Belleville, C. and G. Duplain. "White-Light Interferometric Multimode Fiber-Optic Strain Sensor." *Optical Letters*, Vol. 18, 1993, pp. 78-80.

11. Measures, R. M. "Advances Toward Fiber Optic Based Smart Structures." *Optical Engineering*, Vol. 31, 1992, pp. 34-47.